Vienna VLBI Software
Version 2.2

User manual

Edited by Matthias Madzak
Sigrid Böhm
Hana Krásná
Lucia Plank
David Mayer

VIENNA UNIVERSITY OF TECHNOLOGY
DEPARTMENT FOR GEODESY AND GEOINFORMATION
RESEARCH GROUP ADVANCED GEODESY

User manual of the Vienna VLBI Software VieVS Version 2.2

May 2014

Please send comments on this document or the Software to:

David Mayer		
Department of Geodesy and Geoinformation	Phone:	+43 1 58801 12860
Vienna University of Technology	E-mail:	david.mayer@tuwien.ac.at
Gußhausstraße 27-29		
1040 Vienna		
Austria		

Vienna VLBI Software
Version 2.2

Research Group Advanced Geodesy/VLBI, Department of Geodesy and Geoinformation, Vienna University of Technology

J. Böhm, S. Böhm, A. Hellerschmied, A. Hofmeister, H. Krásná, M. Madzak, D. Mayer

Important External Contributors:

Hacettepe University, Ankara, Turkey
K. Teke

GeoForschungsZentrum Potsdam, Germany
T. Nilsson, B. Soja, M. Karbon

Chinese Academy of Sciences, Shanghai, China
J. Sun

University of Tasmania, Hobart, Australia
J. McCallum, S. Shabala, L. Plank

Main Astronomical Observatory Kiew, Ukraine
V. Choliy

Contents

Chapter 1

Introduction

1.1 How to use this document

This document provides a brief overview of the VieVS software. If you are new to VieVS and just want to get sessions analyzed you can use the exercises (Chapter 5) provided, where you can follow the work flow step by step. If you want more details about the Software you can go to Chapter 3 (User Guide).

An introduction into Very Long Baseline Interferometry (VLBI) can be found in the fundamentals chapter (Chapter 2).

We also provided a short Matlab crashcourse, which can be found in Chapter 6 (If you are new to Matlab you should consider using one of the many excellent Matlab tutorials on the web, e.g. at `http://www.maths.dundee.ac.uk/~ftp/na-reports/MatlabNotes.pdf` or a very complete one at `http://www.mathworks.de/help/pdf_doc/matlab/getstart.pdf`).

1.2 Get VieVS

To download VieVS, please visit *http://vievs.geo.tuwien.ac.at/* to get more information. We ask all our external users to send us a letter describing the purpose they would like to use VieVS for. You will get a username and password once you are registered which let's you access *vievs.hg.tuwien.ac.at* using sftp.

1.3 Start

Once you downloaded VieVS move the whole directory to the desired destination and start Matlab. After Matalb is started make the *VieVS/WORK/* directory to your Current Folder in Matlab. Typing *vievs* in the Command Window starts the interface of VieVS.

Chapter 2

Fundamentals

This chapter was originally taken from G. Xu (ed.), *Sciences of Geodesy - II*, DOI: 10.1007/978-3-642-28000-9_7, ©Springer-Verlag Berlin Heidelberg 2013, by Harald Schuh and Johannes Böhm

Very Long Baseline Interferometry is a microwave-based space geodetic technique that measures the difference in arrival times of signals from a radio source by cross correlation. Most commonly the observed radio sources are extragalactic objects but beacons from satellites have also been used. VLBI plays a unique role in the practical realization and maintenance of the International Celestial Reference Frame (ICRF) and contributes significantly to the International Terrestrial Reference Frame (ITRF), in particular for its scale. It is the only technique that provides the full set of Earth orientation parameters, which are indispensable for positioning and navigation on Earth and in space. In addition VLBI allows access to valuable information concerning interactions within the Earth system. In particular, direct measurements of nutation parameters and of the Earth rotation angle ($UT1 - UTC$) are uniquely provided by VLBI. Furthermore, several other geodynamic, atmospheric, and astronomical parameters can be derived from the long history of VLBI measurements starting in the late 1970's. In 1999, the International Association of Geodesy (IAG) accepted the International VLBI Service for Geodesy and Astrometry (IVS) as an official IAG Service and the IVS was also approved as a Service of the International Astronomical Union (IAU). Since then, the coordination of worldwide VLBI observation and analysis has improved significantly, leading to valuable results for the wider scientific community. Since 2005, the IVS has been working on a new VLBI system in terms of hardware, software, and operational procedures, known as VLBI2010. The IVS recommended a review of all current VLBI systems and processes from antennas to analysis and outlined the path to the next-generation system with unprecedented new capabilities envisaged: 1 mm position and 0.1 mm/yr velocity accuracy on global scales, continuous measurements to obtain uninterrupted time series of station positions and Earth orientation parameters, and a turnaround time from the observations to initial geodetic results of less than 24 hours. This new system will be realized in the coming years.

2.1 Introduction

2.1.1 Geometric principle

The geometric principle of Very Long Baseline Interferometry (VLBI) is simple and straightforward. The radiation from extragalactic radio sources arrives on Earth as plane wavefronts. This is different from nearby Earth satellites such as those of the Global Navigation Satellite

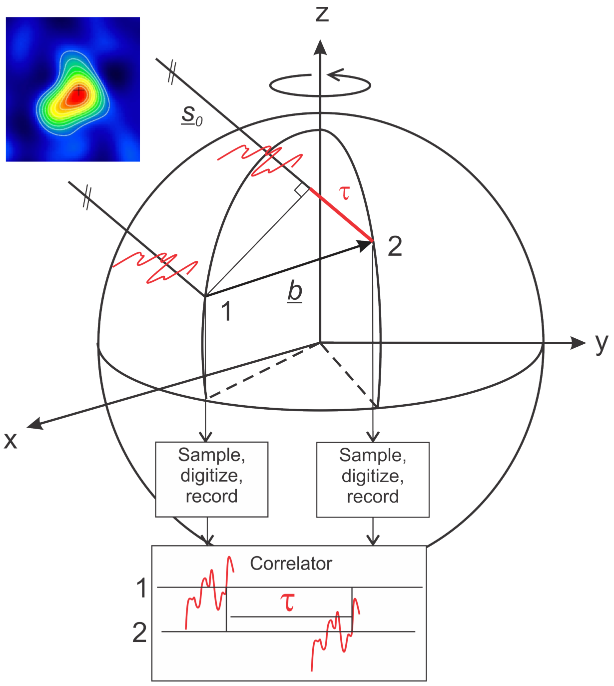

Figure 2.1: Geometric VLBI model

Systems (GNSS) where the finite distance to the emitter produces parallactic angles. The basic triangle for the determination of the baseline vector reduces to a rectangular one providing a direct relation between the baseline vector $\boldsymbol{b}$ and the direction to the radio source $\boldsymbol{s_0}$ (Campbell, 2000). The scalar product τ represents the observed delay between the reception times t_1 and t_2 at stations 1 and 2 (see Fig. 2.1, Eq. 2.1) with the sign convention $\tau = t_2 - t_1$ and the velocity of light c.

$$\tau = -\frac{\boldsymbol{b} \cdot \boldsymbol{s_0}}{c} = t_2 - t_1 \tag{2.1}$$

The delay τ is time-dependent, and the largest contribution to its variation is due to the fact that the interferometer is fixed to the Earth's surface and thus follows its diurnal rotation with respect to the celestial reference system that is realized by positions of radio sources. The geodetic VLBI concept uses two or more radio telescopes to observe numerous extragalactic radio sources distributed across the skies, mostly quasars or radio galaxies. In geodetic VLBI since the end of the 1970's the observations are done within S-band (2.3 GHz) and X-band (8.4 GHz)[1], and the data are recorded and time-tagged using very stable and precise time signals obtained from hydrogen masers. These data are then sent to particular correlation centers for cross-correlation to generate so-called fringes and to obtain the group delay observable τ which is relevant for geodetic and astrometric applications. From these delays, the baseline lengths b and other geodetic parameters can be derived nowadays with sub-centimeter accuracy. The VLBI technique measures very accurately the angle between the Earth-fixed baseline vector $\boldsymbol{b}$ and the space-fixed radio sources $\boldsymbol{s_0}$ which have to be transformed into a common system for the evaluation of Eq. 2.1 by parameter estimation techniques. Thus, even the most subtle changes in the baseline lengths and in the angles between the reference systems can be detected, and the main geodynamic phenomena such as Earth orientation parameters can be monitored

[1] A change of the frequency setup, e.g. observing on a frequency band between 2 and 14 GHz, is envisaged for the next VLBI generation, VLBI2010 (Petrachenko, 2009)

with unprecedented accuracy (Schuh, 2000). However, *'... if we leave the Euclidean geometry in empty space and return to the real world with curved space, flickering quasars, billowing atmospheres, wobbling axes, and drifting continents, we have to delve into layers of complexity, fortunately not only as a chore but also as an opportunity to gain a wealth of new knowledge about our system Earth.' (Campbell, 2000)* More details about the complexity of VLBI are provided in the next sections.

2.1.2 History and technological developments

In this section we give a summary of the early history of geodetic VLBI and of the VLBI technique. The interested reader may find further details on the history in Sovers *et al.* (1998), Campbell (2000), and Kellermann & Moran (2001), and the references therein. For details on technology, we refer to the textbooks by Thompson *et al.* (1986) and Takahashi *et al.* (2000), and the references therein. Very Long Baseline Interferometry is an outgrowth of radio interferometry with cable-connected elements designed to overcome the limited resolution of single dish radio telescopes (Cohen *et al.*, 1968). However, to reveal the structure of extremely compact radio sources, the resolving power of Connected Element Radio Interferometers (CERI) was insufficient, even at higher frequencies (Campbell, 2000). The advent in the late 1960s of high-speed tape recorders and high-stability atomic frequency/time standards made possible the construction of phase-coherent, Michelson-type interferometers whose elements required no physical connection between them and hence could be spaced arbitrarily far apart. In 1967, several groups working independently in Canada and the United States developed and successfully operated two-station interferometers (Bare *et al.* 1967; Broten *et al.* 1967; Moran *et al.* 1967; Brown *et al.* 1968). Signals received at each station were down-converted in frequency, time-tagged, and recorded on tape for subsequent playback at a correlator center, where the common signal received from a radio source at two (or more) antennas was detected by cross-correlation and integration although the signal itself is by far weaker than the background noise. This technique eliminated the need for a real-time phase-stable connection between radio telescopes. Potential geophysical applications of geodetic VLBI were recognized early (Gold 1967; Shapiro & Knight 1970). The first experiments that were explicitly aimed at achieving geodetic accuracy on long baselines were conducted by the Haystack/MIT group on the 845 km baseline between the Haystack Observatory in Northern Massachusetts and the National Radio Astronomy Observatory of Green Bank, West Virginia, U.S.A. (Hinteregger *et al.*, 1972). Since that time the station position precision improved dramatically from a few meters to the current level of one centimeter or even better. A major factor in the improved precision was made possible by equipment improvements such as wider spanned and recorded bandwidths, dual-frequency observations, lower system temperatures, and phase calibration. As an example the first geodetic observations used the MkI system (Whitney *et al.*, 1976) which could record only 0.72 Mbits/second, whereas modern systems allow to record at 1024 Mbits/second or even more. Other factors included improvements in observing strategies, analysis methods, and modeling of physical processes. The key to the high group delay precision of 1 ns (30 cm) attained in these experiments was the invention of the so-called bandwidth synthesis technique (Rogers, 1970), which helped to overcome the limitations of tape recording equipment in terms of recordable bandwidth (Campbell, 2000). A milestone was reached when the first significant estimates of the length change on the transatlantic baseline Haystack Onsala (Sweden) were announced. A baseline rate of 17 mm/yr with a statistical standard deviation of ± 2 mm/yr derived from 31 experiments between September 1980 and August 1984 was published by Herring *et al.* (1986). However, they reported that the systematic error could be as large as 10 mm/year. In comparison, Fig.2.2 indicates session-wise baseline length estimates from 1984 to 2011 between the stations Wettzell (Germany) and Westford (Massachusetts, U.S.A.) determined by the VLBI

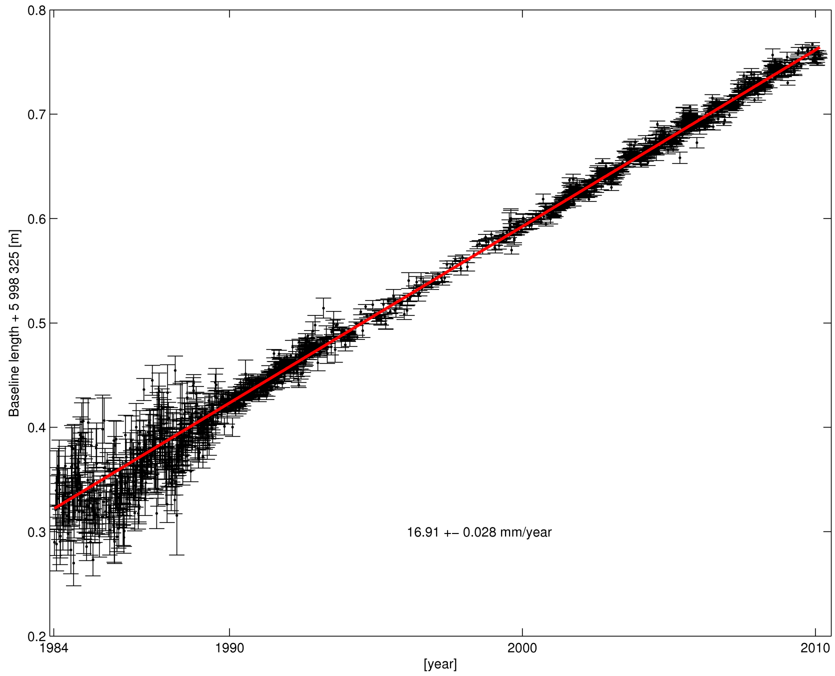

Figure 2.2: Session-wise baseline length estimates between Wettzell (Germany) and Westford (U.S.A.) from 1984 to 2011 as determined by the VLBI group at TU Wien with the Vienna VLBI Software VieVS (Böhm *et al.*, 2011). The estimated slope is 16.91 ±0.03 mm/year (plot by courtesy of Hana Spicakova).

group at TU Wien, Vienna, Austria. Clearly visible is the continuously improving accuracy, in particular during the first decade of the time series, and the seasonal variation of the length estimates, which is either due to modeling deficiencies (e.g., of troposphere delays), due to unmodeled loading effects (e.g., atmosphere or hydrology loading), or a combination of both of them.

2.1.3 Data Aquisition

Geodetic VLBI is an active observing technique which needs to control the radio telescopes and steer them to various positions on the sky in a predefined observing schedule; thus, scheduling is a very important part of VLBI. The package SKED (Vandenberg, 1999) developed at NASA Goddard Space Flight Center is widely used within the geodetic community to generate the observing plans for the radio telescopes. At any instant, different subsets of antennas will be observing different sources. (All observations to one source at a time form a so-called 'scan'.) The integration time varies from antenna to antenna to reach the required signal-to-noise-ratio (SNR) (Petrov *et al.*, 2009). The elevation mask is usually set to 5° but any obstacles or mountains have to be considered if they prevent observations at low elevation angles. There are various optimization criteria in SKED, but 'sky-coverage' is mostly selected. This strategy aims at filling large holes in the sky over the stations, which is important for the estimation of troposphere delays. More information about scheduling strategies can be found in Vandenberg (1999) or Petrov *et al.* (2009). The incoming signal first arrives at the primary paraboloidal dish of the radio telescope, then at the hyperboloidal subreflector, and finally it enters the feedhorn (see Fig.2.3 for an example of a Cassegrain antenna). The signal goes directly to the feed from

Figure 2.3: New skyline at site Wettzell with the 'old' VLBI radio telescope (20 m) at the right side and the new twin radio telescopes (13.2 m) in the background (by courtesy of Alexander Neidhardt, picture taken in 2011)

the paraboloidal reflector in the case of prime focus antennas. Then, the signals are amplified before they are heterodyned from radio frequency to intermediate frequencies of several hundred MHz, and finally down-converted to baseband frequencies (simultaneously in multiple frequency sub-bands or channels), where the signal is band-limited to a width of a few MHz, sampled and digitized (Sovers *et al.*, 1998). The system temperatures typically range from 20 to 100 K for S- and X-band. Finally, the signals are formatted and recorded on magnetic disks (or on tapes in the early years). Nowadays, data from shorter sessions can also be transferred to the correlators via high-speed broadband communication links. However, the majority of electronic transfer of the raw VLBI data is still asynchronous, i.e., the transfer is started during or after the observation but then needs more time than the actual observation (termed e-transfer). Only in a few experimental sessions, as e.g. described by Sekido *et al.* (2008), the transmission was carried out in real-time (termed e-VLBI).

VLBI radio telescopes need to have large collecting areas as well as high sampling and recording rates because the signal flux density is in the order of 1 Jansky (1 Jy = $10^{-26}\mathrm{Wm}^{-2}\mathrm{Hz}^{-1}$) or even lower. On the other hand the structure of the antennas has to be sufficiently stable to allow slewing between widely separated sources within a few minutes or faster (Sovers *et al.*, 1998). (See Section 2.2.5 for more information on antenna deformation.) Phase shifts caused by the instrumentation have to be calibrated to take full advantage of the precision of current frequency standards (e.g., hydrogen masers stable to 10^{-14} at 50 minutes or better). Otherwise, those phase shifts can corrupt the estimated phase and group delay of the incoming signal. The technique of phase calibration (Rogers, 1975) compensates for the instrumental phase errors by generating a signal of known phase, injecting this signal into the front end of the VLBI signal path, and examining the phase after the signal has traversed the instrumentation. This calibration signal is embedded in the broadband VLBI data stream as a set of low-level monochromatic tones along with the signal of the radio source (Sovers *et al.*, 1998). Those tones are used at a later stage by the post-correlation software. Furthermore, the length variations in the cables from the clocks to the antennas (called cable delays) have to be corrected properly. In the next step, the signals recorded at the antennas are combined pair-wise producing an interference pattern. These installations are called correlators, and they are presently run world-wide, e.g. in the U.S.A. (Haystack Observatory, Westford; U.S. Naval Observatory, Washington D.C.), in

Germany (Max Planck Institute for Radio Astronomy, Bonn), and Japan (National Institute of Information and Communications Technology, Kashima). They are made up of special hardware that is used to determine the difference in arrival times at the two stations by comparing the recorded bit streams. If $V_1(t)$ and $V_2(t)$ are the antenna voltages as functions of time t, T is the averaging interval, and the asterisk denotes the complex conjugate, the group delay τ can be determined by maximizing the cross-correlation function R (Sovers *et al.*, 1998):

$$R(\tau) = \frac{1}{T} \int_0^T V_1(t) \cdot V_2^*(t - \tau) \cdot dt. \tag{2.2}$$

Due to Doppler shifts caused by the Earth rotation, VLBI observations at X-band (8.4 GHz) would be oscillating at several kHz if not 'counter-rotated' first (Sovers *et al.*, 1998). In recent years, also software correlators have been developed (e.g. Kondo *et al.* 2004, Tingay *et al.* 2009) because correlation algorithms for geodetic VLBI can be effectively implemented on parallel computers or on distributed systems. Software correlation is already well beyond the development stage. For example, the Bonn correlator has processed all IVS (International VLBI Service for Geodesy and Astrometry) sessions with the DiFX software correlator from November 2010 onwards. During the correlation process, amplitudes and phases are determined every 1 to 2 seconds in parallel for typically 14 frequency channels ω_i. The post-correlation software applies corrections for the phase calibration and fits the phase Φ_0, the group delay τ_{gd}, and the phase rate τ'_{pd} to the phase samples $\Phi(\omega_i, t_j)$ from the various frequency channels ω_i and times t_j. The phase-derived observables are determined (for phase Φ and circular frequency ω) from a bilinear least-squares fit to the measured phases $\Phi(\omega, t)$ with (Sovers *et al.*, 1998)

$$\Phi(\omega, t) = \Phi_0(\omega_0, t_0) + \frac{d\Phi}{d\omega}(\omega - \omega_0) + \frac{d\Phi}{dt}(t - t_0), \tag{2.3}$$

where the phase delay τ_{pd}, group delay τ_{gd}, and phase delay rate τ'_{pd} are defined, respectively, as

$$\tau_{pd} = \frac{\Phi_0}{\omega_0}, \tau_{gd} = \frac{d\Phi}{d\omega}, \tau'_{pd} = \frac{1}{\omega_0}\frac{d\Phi}{dt}. \tag{2.4}$$

The group delay rate τ'_{gd} is not accurate enough to be useful for geodetic or astrometric purposes, however, it is needed to resolve group delay ambiguities in a first solution step. The amplitudes are usually not used in geodetic/astrometric VLBI. The natural ultra-wide band continuum radiation provides the means to use the essentially unambiguous wide band group delay as the prime geodetic VLBI observable. The group delay resolution is proportional to the inverse of the signal-to-noise-ratio (SNR) and the root mean square (rms) of the frequency about the mean (sometime called rms spanned bandwidth) B_{eff} (Rogers, 1970):

$$\sigma_\tau = \frac{1}{2\pi} \cdot \frac{1}{\mathrm{SNR} \cdot B_{eff}}. \tag{2.5}$$

If we increase the rms spanned bandwidth B_{eff} at a given SNR by a factor of ten, the group delay uncertainty will be reduced by the same factor, a relation with tremendous consequences (Campbell, 2000). On the other hand, the SNR is dependent on the recorded bandwidth B with

$$\mathrm{SNR} = \eta \cdot \rho_0 \cdot \sqrt{2 \cdot B \cdot T}, \tag{2.6}$$

where T is the so-called coherent integration time, η is the digital loss factor, and ρ_0 is the correlation amplitude which depends on the system noise temperatures and on the equivalent noise temperature of the source signal (Takahashi *et al.*, 2000). There are virtually no limitations to further improve the statistical precision of the geodetic group delay, except technological

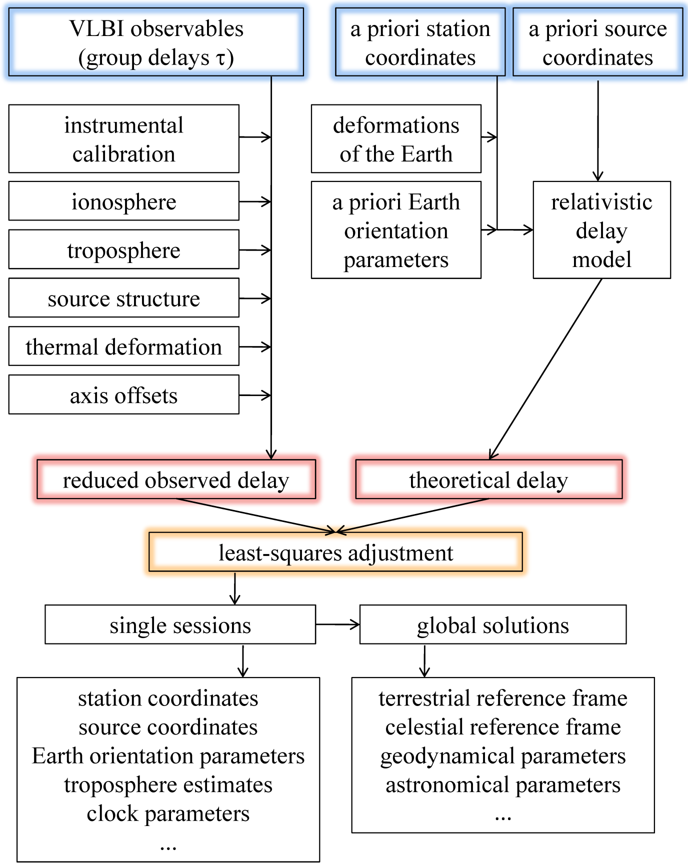

Figure 2.4: Flow diagram of geodetic VLBI data analysis (according to Schuh, 1987)

constraints and costs. For the upcoming VLBI2010 system, a four-band system is recommended that uses a broadband feed to span the entire frequency range from 2 to 14 GHz (see Section 2.6). This will also allow the use of phase delays, which are still an issue of research with the current system where they provide very high accuracy, but only on very short baselines (Herring 1992, Petrov 1999) as on longer baselines the phase ambiguities are still an unsolved problem.

2.1.4 Data Analysis

The VLBI data analysis model is developed using the best presently available knowledge to mathematically recreate, as closely as possible, the situation at the time of observation (see Section 2.2). Then, a least-squares parameter estimation algorithm or other estimation methods can be used to determine the best values of the quantities to be solved for (Section 2.3). Before this process starts, the raw observations have to be cleaned from several systematic effects, which in fact limit the final accuracy of the results (Schuh, 2000). The flow diagram of a geodetic VLBI data analysis (according to Schuh, 1987) is shown in Fig. 2.4. The system can be seen to have two main streams, one containing the actual observations which undergo instrumental and environmental corrections to obtain the reduced delay observables, and the other to produce the theoretical delays, starting with the a priori parameter values, a set of initial values for the parameters of the VLBI model. Both streams converge at the entrance to the parameter estimation algorithm, e.g. the least-squares fit, where the 'observed minus computed' values are formed. The instrumental effects include systematic clock instabilities, electronic delays in cables and circuitry, and the group delay ambiguities. The latter are due to observation by the multichannel frequency setup described in 2.1.2 covering the total spanned bandwidth around each of the two observing frequencies ($f_S = 2.3$ GHz (S-band) and $f_X = 8.4$ GHz (X-band)). As the group delay ambiguity spacing is comparably large and well-known the analyst can select – from a first solution using the observed group delay rates τ'_{gd} only – one level on which all residuals and thus the corresponding group delay observables are shifted. Care has to be taken that the group delay closure within each triangle of a multi-station VLBI network is zero (Schuh, 2000). The ionosphere, which is a dispersive medium in the radio frequency band, can be dealt with to first order by using two different observing frequencies, i.e. the ionosphere group delay corrections for the X-band observations are computed from the differences of group delay measurements at X-band and S-band:

$$\Delta\tau_X^{ion} = (\tau_X - \tau_S) \cdot f_S^2/(f_X^2 - f_S^2). \tag{2.7}$$

In contrast to the Global Positioning System (GPS), where a very close frequency pair has been chosen, the factor in VLBI to convert the difference into a correction for the higher band is very small: 0.081, so that the error contribution from the S-band observations is marginal (Schuh, 2000). Unlike GPS, ionospheric second order effects can be neglected in VLBI analysis as was demonstrated by Hawarey *et al.* (2005).

2.2 Theoretical Delays

In order to calculate observed minus computed values for the least-squares adjustment (see Section 2.3), several models need to be applied. At first, the station coordinates at the observation epoch have to be determined (Section 2.2.1). Then the station coordinates are rotated from the terrestrial to the celestial system (Section 2.2.2) where the computed delays between two stations forming a baseline and a radio source are built (Section 2.2.3), taking into account relativistic corrections and applying troposphere delay (Section 2.2.4), and other corrections. For all the modeling details the reader is referred to the Conventions of the International Earth Rotation and Reference Systems Service (e.g. Petit & Luzum, 2010) and its online updates at `http://tai.bipm.org/iers/convupdt/convupdt.html`, as well as to special IVS Conventions such as those for the treatment of the thermal expansion of radio telescopes (Nothnagel, 2009).

2.2.1 Station Coordinates at the Time of Observation

At first, coordinates (valid at a reference epoch; e.g. J2000.0 = 1 January 2000 at 12 h Terrestrial Time TT) and velocities of a specific realization of the International Terrestrial Reference System (ITRS) are taken to determine the mean coordinates at the time of observation. It should be mentioned already here that typically these realizations are TT frames and that the coordinates are provided in a conventional tide-free system. Examples are the International Terrestrial Reference Frame 2008 (ITRF2008; Altamimi *et al.*, 2011) or specific VLBI realizations like the VTRF2008 (Böckmann *et al.*, 2010), the VLBI contribution to ITRF2008.

Then several corrections are added to get closer to the true station coordinates at the observation epoch. These corrections include periodic and aperiodic deformations of the Earth's crust. The largest periodic corrections are for the solid Earth tides, ocean tide loading, and pole tide loading. Solid Earth tides show mainly diurnal and semidiurnal oscillations which cause vertical deformations in a range of ±20 cm and horizontal displacements of about 30% of the vertical effect (e.g. Mathews *et al.*, 1997). More difficult to model is the loading by the water masses of ocean tides and currents (ocean loading), which amounts to as much as a decimeter on some coastal or island sites (e.g. Scherneck, 1991, Schuh, 2000). Additionally, there is also a periodic deformation at the S1 (24 hours) and S2 (12 hours) periods caused by pressure tides due to thermal heating of the atmosphere. All these effects, which should be corrected at the observation level, are described in detail in the IERS Conventions 2010 (Petit & Luzum, 2010) and its electronic updates. The analysis strategy is not so clear with aperiodic deformations, e.g. with non-tidal atmosphere (but also non-tidal ocean and hydrological) loading, although their significance in VLBI analysis has been shown repeatedly (e.g. Rabbel & Schuh, 1986, vanDam & Herring, 1994). So far, there is no general agreement within the international space geodesy community whether these corrections should be applied at the observation level: Arguments against the application of non-tidal atmosphere loading at the observation level are that there is no consensus model available, that the accuracy of existing models (e.g. Petrov & Boy, 2004) is still not sufficient, and that geophysicists are interested in station coordinate time series which would show the loading signals. On the other hand – and this holds in particular for VLBI with a small number of stations (6 to 8) taking part in typical 24 hour sessions – neglected a priori atmosphere loading is partly absorbed by no-net-rotation (NNR) and no-net-translation (NNT) conditions and does not show up in the estimated station coordinate time series (Böhm *et al.*, 2009b). Furthermore, there is significant variation in non-tidal atmospheric loading corrections within 24 hours which would be neglected if the correction was applied at a later stage of data analysis.

2.2.2 Earth orientation

In the next step, we need to transform the station coordinates from the International Terrestrial Reference System (ITRS) into the Geocentric Celestial Reference System (GCRS) at the epoch of the observation t. The transformation matrix can be written as

$$[GCRS] = Q(t) \cdot R(t) \cdot W(t) \cdot [ITRS]\,, \tag{2.8}$$

where $Q(t)$, $R(t)$, and $W(t)$ are the transformation matrices arising from the motion of the celestial pole in the celestial reference system, from the rotation of the Earth around the axis associated with the pole, and from polar motion respectively (Petit & Luzum, 2010). Matrix W ('wobble') includes as parameters the coordinates x_p and y_p (polar motion) of the Celestial Intermediate Pole (CIP) in the Earth-fixed frame and the correction angle s' which locates the position of the Terrestrial Intermediate Origin (TIO) on the equator of the CIP. Terrestrial (TIO) and Celestial Intermediate Origin (CIO) realize reference meridians in the respective systems. These terms are part of the 'CIO-based' transformation concept following the Non-Rotating Origin (NRO), which replaces the former 'equinox-based' transformation. Matrix $R(t)$ is the Earth rotation matrix with the angle θ between TIO and CIO. The conventional relationship defining UT1 from the Earth rotation angle θ is given by Capitaine (2000) as

$$\theta(T_u) = 2\pi \cdot (0.7790572732640 + 1.00273781191135448 \cdot T_u), \tag{2.9}$$

where T_u = (Julian UT1 date – 2451545.0), and UT1 = UTC + (UT1-UTC). The difference between Universal Time (UT1) and Universal Time Coordinated (UTC, which differs by a known integer number of SI-seconds from TAI, the International Atomic Time, realized as a weighted mean of signals provided by atomic clocks located all over the world) can be uniquely observed by VLBI. All satellite techniques like the Global Navigation Satellite Systems (GNSS) or Satellite Laser Ranging (SLR) – due to the direct dependence between UT1 and the right ascension of the ascending node of the satellite orbit – can only observe length-of-day, which is the negative time derivative of (UT1-UTC), but need external information about UT1-UTC every few days.

The precession/nutation matrix, denoted $Q(t)$, includes the rotations around the angles X and Y (which are the coordinates of the CIP in the celestial frame) and the correction angle s which positions the CIO on the equator of the CIP. The CIP is the reference pole for space geodetic measurements, i.e. it defines the observed axis. This is a pure convention realized by an appropriate theory of precession and nutation as will be described below. The orientation of the CIP does not coincide with that of a physical axis like the rotation axis, the figure axis, or the angular momentum axis, but it can be related to all of them. By definition the CIP is an intermediate pole which divides the motion of the pole of the ITRS w.r.t. the GCRS into a celestial and a terrestrial part. The celestial part (precession and nutation, $[X, Y]$) includes all motions with periods ¿2 days observed in the celestial frame, and this corresponds to all frequencies between 0.5 (retrograde) and +0.5 (prograde) cycles per sidereal day in the GCRS. The terrestrial part (polar motion, $[x_p,\, y_p]$) includes all motions outside of the retrograde daily band in the ITRS, i.e. it includes frequencies below 1.5 and above 0.5 cycles per sidereal day in the ITRS. The largest part of the celestial motion of the CIP can be calculated with a conventional precession/nutation model. Presently the model IAU 2006/2000A is recommended by the IERS Conventions 2010. However, remaining unmodeled parts of the celestial motion can be observed with VLBI and are provided by the IERS as so-called celestial pole offsets $[dX,\, dY]$. These offsets stem from residual errors of the a priori precession/nutation model and the phenomenon of the Free Core Nutation (FCN) which is a resonance mode due to the deviation of the rotation axis of the mantle from the rotation axis of the core (Dehant & Mathews, 2009). This retrograde motion with a period of about 430 days in the GCRS and a varying amplitude of up to 0.3 mas ($\sim$ 10 mm on the Earth surface) (e.g Herring *et al.*, 2002) is not predictable and cannot be neglected if someone wants to achieve highest positioning accuracies. Thus, neither precession/nutation nor polar motion and UT1-UTC can be predicted accurately enough with models but have to be observed by space geodetic techniques. A combination of these estimates is provided by the IERS, e.g. in the IERS 05 C04 series (Bizouard & Gambis, 2009), which can be used by space geodetic techniques as a priori information. If not estimated from the observations, the standard pole coordinates to be used are those published by the IERS $(x, y)_{IERS}$ with additional terms to account for the diurnal and semi-diurnal variations caused by ocean tides $(\Delta x, \Delta y)_{ocean\_tides}$ (Englich *et al.*, 2008, see also Figure 2.8) and for libration $(\Delta x, \Delta y)_{libration}$:

$$(x_p, y_p) = (x, y)_{IERS} + (\Delta x, \Delta y)_{ocean\_tides} + (\Delta x, \Delta y)_{libration}. \tag{2.10}$$

Here $(\Delta x, \Delta y)_{libration}$ are the forced variations in pole coordinates corresponding to motions with periods less than two days in space that are not part of the IAU 2000A nutation model. The IERS Earth Orientation Parameters (EOP) Product Center provides a subroutine to interpolate ('Lagrange' interpolation) in the $(x, y)_{IERS}$ pole coordinates which are typically released at midnight. However, this kind of interpolation (unlike linear interpolation) does not allow the rigorous estimation of estimated polar motion rates to be used for Earth rotation excitation studies. The situation is similar for the Earth rotation angle θ with models for the effects of ocean tides and libration that have to be added to the IERS 05 C04 values of UT1-UTC. In the case of the Earth rotation angle, tidal terms (with periods from 5 to 35 days) are usually removed before the Lagrange interpolation of the IERS values, and are restored afterwards.

2.2.3 General relativistic model for the VLBI time delay

The general relativistic model for the time delay is developed in the frame of the IAU Resolutions, i.e. general relativity using the Barycentric Celestial Reference System (BCRS) and the Geocentric Celestial Reference System (GCRS). The procedure to compute the VLBI time delay according to the so-called consensus model is taken from Eubanks (1991), and it is summarized in the IERS Conventions 2010 (Chapter 11, Petit & Luzum, 2010). The model has been developed for VLBI observations to extragalactic radio sources taken from the Earth surface, but not for observations to objects in our solar system like Earth- or Moon-orbiting satellites. In the model, which is accurate to the picosecond-level, it is assumed that the ionospheric delays have already been removed (see Eq. 2.7 in Section 2.1).

Theoretically, the VLBI time delays are measured in proper times of the station clocks, whereas the VLBI model 2.19 is expressed in terms of coordinate time in a given reference system. We consider the VLBI time delay from the correlator to be equal to the Terrestrial Time (TT, agrees with SI second on the geoid and is equal to TAI, apart from a constant offset: TT = TAI + 32.184 sec) coordinate time interval d_{TT} between the arrival of a radio signal at the reference point of the first station and the arrival of the same signal at the reference point of the second station. From a TT coordinate interval, d_{TT}, the Geocentric Coordinate Time (TCG) coordinate interval, d_{TCG}, can be determined by scaling: $d_{TCG} = d_{TT}/(1 - L_G)$ with $L_G = 6.969290134 \times 10^{-10}$ (Petit & Luzum, 2010).

The Terrestrial Reference System (TRS) space coordinates from the analysis of VLBI observations, x_{VLBI}, are termed 'consistent with TT' if derived from d_{TT} intervals, and the TRS coordinates recommended by the IAU and IUGG resolutions, x_{TCG}, can be derived with $x_{TCG} = x_{VLBI}/(1 - L_G)$ (Petit, 2000). Presently, all VLBI analysis centers provide their coordinate solutions as consistent with TT. Since also SLR analysis centers submit their solutions consistent with TT, it was decided that the coordinates should not be re-scaled to x_{TCG} for the computation of ITRF2008 so that the scale of ITRF2008 (and earlier realizations) in this respect does not fully comply with IAU and IUGG resolutions (Petit & Luzum, 2010).

In the remaining part of this section, we provide the equations for the general relativistic VLBI time delay model and follow the IERS Conventions 2010 (Petit & Luzum, 2010). Although the delay to be calculated is by convention the time of arrival at station 2 minus the time of arrival at station 1, it is the time of arrival at station 1, t_1, that serves as the time reference for the measurement. Thus, all quantities are assumed to be calculated at t_1, including the effects of the troposphere. Assuming that the reference time is the UTC time of arrival of the VLBI signal at receiver 1, and that it is transformed to the appropriate timescale (e.g., UT1 or TT) to be used to compute each element of the geometric model, the following steps are carried out to calculate the VLBI time delay. First, the barycentric station vectors $\boldsymbol{X}_i(t_1)$ for the receivers are determined with

$$\boldsymbol{X}_i(t_1) = \boldsymbol{X}_\oplus(t_1) + \boldsymbol{x}_i(t_1) \tag{2.11}$$

where t_1 is the TCG time of arrival of the radio signal at the first receiver, $\boldsymbol{X}_\oplus(t_1)$ is the barycentric radius vector of the geocenter, and $\boldsymbol{x}_i(t_1)$ the GCRS radius vector of the i-th receiver. Then, we calculate the vectors $\boldsymbol{R}_{iJ}$ from the Sun, the Moon, and each planet (with the barycentric coordinates $\boldsymbol{X}_J$) except the Earth to receivers 1 and 2. The time t_{1J} of the closest approach of the signal to the gravitating body J can be determined with

$$t_{1J} = min\left[t_1, t_1 - \frac{\boldsymbol{K} \cdot (\boldsymbol{X}_J(t_1) - \boldsymbol{X}_1(t_1))}{c}\right] \tag{2.12}$$

so that

$$\boldsymbol{R}_{1J}(t_1) = \boldsymbol{X}_1(t_1) - \boldsymbol{X}_J(t_{1J}) \tag{2.13}$$

and

$$\boldsymbol{R}_{2J}(t_1) = \boldsymbol{X}_2(t_1) - \frac{\boldsymbol{V}_\oplus}{c}(\boldsymbol{K} \cdot b) - \boldsymbol{X}_J(t_{1J}) \tag{2.14}$$

with $\boldsymbol{V}_\oplus$ the barycentric velocity of the geocenter, $\boldsymbol{b} = \boldsymbol{x}_2(t_1) - \boldsymbol{x}_1(t_1)$ the GCRS baseline vector at the TCG time of arrival t_1, $\boldsymbol{K}$ the unit vector from the barycenter to the source in the absence of gravitational or aberrational effects, and c the velocity of light. The differential TCB gravitational delay for each of those bodies J can then be calculated by

$$\Delta T_{grav,J} = (1+\gamma)\frac{GM_J}{c^3} ln \frac{|\boldsymbol{R}_{1J}| + \boldsymbol{K}\cdot\boldsymbol{R}_{1J}}{|\boldsymbol{R}_{2J}| + \boldsymbol{K}\cdot\boldsymbol{R}_{2J}}, \tag{2.15}$$

where M_J is the rest mass of the J^{th} gravitating body and G is the gravitational constant (Petit & Luzum, 2010). According to the General Theory of Relativity (GRT) the so-called light deflection parameter γ is usually set to unity, but γ can also be estimated as a solve-for parameter in a VLBI global solution comprising many or all VLBI sessions that have ever been carried out. See Lambert & Le Poncin-Lafitte (2009), Heinkelmann & Schuh (2010), or Lambert & Le Poncin-Lafitte (2011) for further details.

Analogously, we determine the TCB gravitational delay due to the Earth with

$$\Delta T_{grav\oplus} = (1+\gamma)\frac{GM_\oplus}{c^3} ln \frac{|\boldsymbol{x}_1| + \boldsymbol{K}\cdot\boldsymbol{x}_1}{|\boldsymbol{x}_2| + \boldsymbol{K}\cdot\boldsymbol{x}_2}, \tag{2.16}$$

where $M_\oplus$ is the rest mass of the Earth, and we sum up the effects of all gravitating bodies to find the total differential TCB gravitational delay with

$$\Delta T_{grav} = \sum_J \Delta T_{grav,J}. \tag{2.17}$$

We need to consider the Sun, Earth, Jupiter, the Earth's moon, and the other planets. If observations pass close to them, the major satellites of Jupiter, Saturn, and Neptune should also be added. If the ray path passes very close to some massive bodies, extra terms need to be included for accuracies better than 1 ps (see Klioner, 1991). For observations made very close to the Sun, higher order relativistic time delay effects become increasingly important. The largest correction is due to the change in delay caused by the bending of the ray path by the gravitating body J described in Richter & Matzner (1983) and Hellings (1986). The correction is

$$\delta T_{grav,J} = \frac{4G^2M_J^2}{c^5}\frac{\boldsymbol{b}\cdot(\boldsymbol{N}_{1J}+\boldsymbol{K})}{(|\boldsymbol{R}|_{1J} + \boldsymbol{R}_{1J}\cdot\boldsymbol{K})^2}. \tag{2.18}$$

which should be added to ΔT_{grav} in 2.17. N_{1J} is the unit vector from the J^{th} gravitating body to the first receiver, and M_J is the rest mass of the J^{th} gravitating body. Next, we compute the vacuum delay between t_{vi}, which are the 'vacuum' TCG times of arrival of a radio signal at the i^{th} VLBI receiver including the gravitational delay but neglecting the troposphere propagation delay and the change in the geometric delay caused by the existence of the troposphere propagation delay:

$$t_{v2} - t_{v1} = \frac{\Delta T_{grav} - \frac{\boldsymbol{K}\cdot\boldsymbol{b}}{c}\left[1 - \frac{(1+\gamma)\cdot U}{c^2} - \frac{|\boldsymbol{V}_\oplus|^2}{2c^2} - \frac{\boldsymbol{V}_\oplus \boldsymbol{\omega}_2}{c^2}\right] - \frac{\boldsymbol{V}_\oplus \boldsymbol{b}}{c^2}(1 + \boldsymbol{K}\cdot\boldsymbol{V}_\oplus/2c)}{1 + \frac{\boldsymbol{K}\cdot(\boldsymbol{V}_\oplus + \boldsymbol{\omega})}{c}}. \tag{2.19}$$

In 2.19 ω_i is the geocentric velocity of the i^{th} receiver. The aberrated radio source vectors $\boldsymbol{k}_i$ (the unit vector from the i^{th} station to the radio source after aberration) for use in the determination of the troposphere propagation delays are calculated with

$$\boldsymbol{k}_i = \boldsymbol{K} + \frac{\boldsymbol{V}_\oplus + \boldsymbol{\omega}_i}{c} - \boldsymbol{K}\frac{\boldsymbol{K}\cdot(\boldsymbol{V}_\oplus + \boldsymbol{\omega}_i)}{c}. \tag{2.20}$$

Thus, we can add the geometric part of the troposphere propagation delay to the vacuum delay with

$$t_{g2} - t_{g1} = t_{v2} - t_{v1} + \Delta L_1 \cdot \frac{\boldsymbol{K}\cdot(\boldsymbol{\omega}_2 - \boldsymbol{\omega}_1)}{c}. \tag{2.21}$$

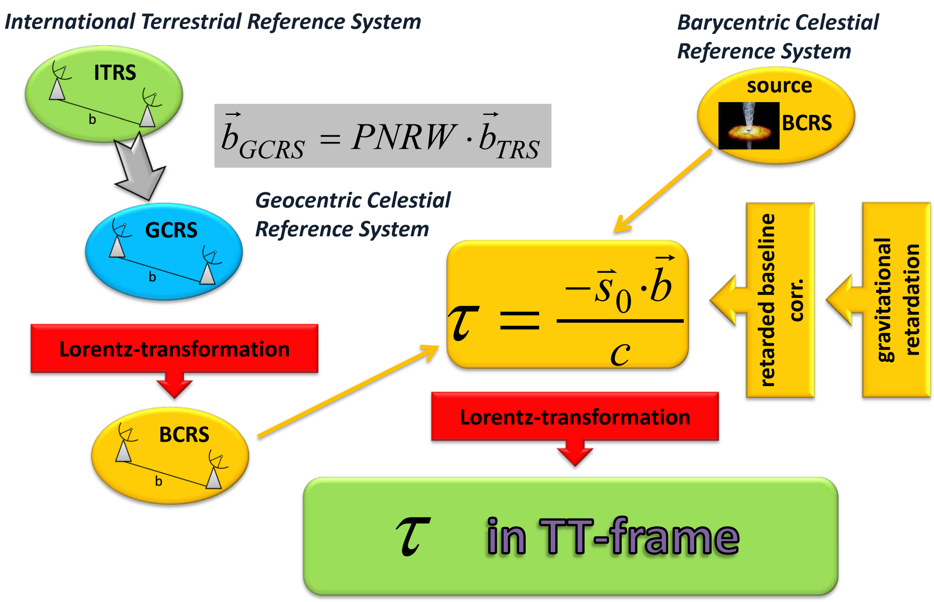

Figure 2.5: Symbolic representation of the derivation of the time delay τ in the TT frame starting with station coordinates in the ITRS and source coordinates in the ICRS (by courtesy of Lucia Plank)

where ΔL_i is the troposphere propagation TCG delay for the i^{th} receiver ($= t_i - t_{gi}$). The total delay can be found by adding the best estimate of the troposphere propagation delay:

$$t_2 - t_1 = t_{g2} - t_{g1} + (\Delta L_2 - \Delta L_1). \tag{2.22}$$

The troposphere propagation delays in 2.21 and 2.22 need not be from the same model. The estimate in 2.22 should be as accurate as possible (see 2.2.4), while the ΔL_1 model in 2.21 need only be accurate to about 10 ns (Petit & Luzum, 2010). Sections 2.2.2 (Earth orientation) and 2.2.3 (Relativistic delay model) are symbolically summarized in Fig. 2.5.

2.2.4 Troposphere delay modeling

The troposphere path delay $\Delta L(e)$ at the elevation angle e is usually represented as the product of the zenith delay ΔL^z and an elevation-dependent mapping function $mf(e)$:

$$\Delta L(e) = \Delta L^z \cdot mf(e). \tag{2.23}$$

This concept is not only used to determine a priori slant delays for the observations, but the mapping function is also the partial derivative to estimate residual zenith delays, typically every 20 to 60 minutes. In the analysis of space geodetic observations, not only zenith delays are estimated, but also other parameters like stations heights and clocks. Whereas the partials for the clocks ($= 1$) and the station heights ($= \sin(e)$) are exactly known, the partial derivative for the zenith delays (i.e., the mapping function) is only known with a limited accuracy. Via the correlations between zenith delays, station heights, and clocks, any imperfection of the mapping function is also manifested as station height error (and clock error) (Nothnagel *et al.*, 2002). To reduce these correlations, observations at low elevations need to be included in the analysis; however, care has to be taken because mapping function errors increase rapidly at very low elevations, i.e. at 5° or below. Presently, the best trade-off between reduced correlations and increasing mapping function errors is found for cutoff elevation angles of about 7° (MacMillan & Ma 1994, Teke *et al.* 2008) or by appropriate down-weighting (Gipson & MacMillan, 2009). Simulations of VLBI2010 observing scenarios indicate that in the future with faster antennas and significantly more observations the cutoff elevation angle can be increased so that the mapping function is less critical for the accuracy of VLBI analysis (Petrachenko, 2009).

Considering 2.23 we find the following relationship: If the erroneous mapping function was too large, the estimated zenith delay ΔL^z becomes too small, because the observed troposphere delay $\Delta L(e)$ stays the same. Consequently, the estimated station height moves up to account for the reduced zenith delay. MacMillan & Ma (1994) set up a rule of thumb specifying that the error in the station height is approximately 0.22 of the delay error at the lowest elevation angle included in the analysis. Böhm (2004) confirmed this rule of thumb for VLBI analysis (and a cutoff elevation angle of 5°) specifying that the station height error is about one fifth of the delay error at 5° elevation angle. The corresponding decrease of the zenith delay becomes about one half of the station height increase. Assuming azimuthal symmetry of the neutral atmosphere around the station (i.e., at a constant elevation angle the delay is not dependent on the azimuth of the observation), the approach as described in Eq. 2.24 (e.g. Davis *et al.*, 1985) is generally applied:

$$\Delta L(e) = \Delta L_h^z \cdot mf_h(e) + \Delta L_w^z \cdot mf_w(e), \tag{2.24}$$

where $\Delta L(e)$ is the total path delay of the microwaves in the neutral atmosphere and e is the elevation angle of the observation to the quasar (vacuum or geometric elevation angle). ΔL_h^z and ΔL_w^z are the a priori zenith hydrostatic and the estimated zenith wet delays, and $mf_h(e)$ and $mf_w(e)$ are the mapping functions which provide the ratio of the slant delay to the delay in zenith direction. The input to both mapping functions is the vacuum elevation angle e, because the bending effect is accounted for by the hydrostatic mapping function. The underlying continued fraction form to all mapping functions is that proposed by Herring (1992):

$$mf(e) = \frac{1 + \frac{a}{1+\frac{b}{1+c}}}{\sin(e) + \frac{a}{\sin(e)+\frac{b}{\sin(e)+c}}}. \tag{2.25}$$

Presently, the most accurate mapping functions globally available are the Vienna Mapping Functions 1 (VMF1, Böhm *et al.*, 2006). Whereas the b and c coefficients of 2.25 are provided as analytical functions depending on day of the year and station latitude, the a coefficients (hydrostatic and wet) are provided as time series with a 6 hour time resolution on global (2.0° in latitude times 2.5° in longitude) grids as well as for all VLBI sites for the complete history of VLBI observations. The coefficients are available from the website `http://ggosatm.hg.tuwien.ac.at/` of the Vienna University of Technology as derived from operational analysis data as well as from forecast data of the European Centre for Medium-Range Weather Forecasts (ECMWF). Vienna Mapping Functions 1 coefficients from forecast data can be used for VLBI real-time applications without significant loss of accuracy as shown by Böhm *et al.* (2009a). Böhm *et al.* (2006) tested the concept of a 'total' Vienna Mapping Function 1, i.e. using the same function for mapping the a priori zenith delay to the elevation of the observation and for the estimation of the residual zenith delays. This concept was not as successful (in terms of baseline length repeatability, which is the standard deviation after removing a linear trend from a time series of baseline lengths) as the separation into a hydrostatic and a wet part, because the variation of the zenith wet delay is faster than can be described by coefficients with a 6 hour time resolution. A total mapping function (which is close to the hydrostatic mapping function) cannot account for this variation whereas the wet mapping function is able to account for it by estimating zenith wet delays every hour or even faster.

The a priori zenith hydrostatic delays in 2.24 can be determined very accurately from the atmosphere pressure at the site (see Saastamoinen, 1972, Davis *et al.*, 1985). If locally recorded pressure values are not available, it is recommended to take values retrieved from numerical weather models as e.g. provided by the Vienna University of Technology [2] together with the coefficients of the VMF1. If those are also not accessible, it is recommended to use an analytical expression like the Global Pressure and Temperature model (GPT; Böhm *et al.*, 2007). Zenith wet delays are usually fully estimated in the VLBI analysis, although Gipson & MacMillan (2009) found a slight improvement if zenith wet delays were already added to the a priori delays and only residual zenith delays were estimated. Approximate values of zenith wet delays are provided with the VMF1 files. Errors in the zenith hydrostatic delays or the mapping functions have an influence on station heights as can be described with the rule of thumb by Böhm (2004) mentioned above: Exemplarily, the zenith hydrostatic and wet delays shall be 2000 mm and 200 mm, respectively, the minimum elevation angle is 5°, and the corresponding values for the hydrostatic and wet mapping functions are 10.15 ($mf_h(5°)$) and 10.75 ($mf_w(5°)$).

1. We consider an error in the wet mapping function of 0.1 ($mf_w(5°) = 10.85$ instead of 10.75) or in the hydrostatic mapping function of 0.01 ($mf_h(5°) = 10.16$ instead of 10.15). The error at 5° elevation in both cases is +20 mm, i.e. the error in the station height is approximately +4 mm.

2. We assume an error in the total pressure measured at the station of -10 hPa. Let us assume that we take the 'mean' pressure from GPT (Böhm *et al.*, 2007) although the real pressure at the site is larger by 10 hPa. -10 hPa correspond to about -20 mm zenith hydrostatic delay (Saastamoinen, 1972), which is then mapped with the wrong mapping function (factor $0.6 = 10.75 - 10.15$). At 5° elevation the mapping function error causes +12 mm delay error, and one fifth of it, i.e. +2.4 mm, is the resulting station height error (Böhm *et al.*, 2006).

On the other hand – due to atmosphere loading – the station height is decreased by about 4 mm (assuming a regression coefficient of 0.4 mm/hPa) if the actual pressure is larger than the mean pressure (from GPT) by 10 hPa. This implies that the application of GPT (or any other mean pressure model) for the determination of the a priori zenith hydrostatic delays of VLBI observables (or any other technique using microwave signals) partly corrects for atmosphere loading (see also Steigenberger *et al.*, 2009). In our example 2.4 mm out of 4.0 mm are compensated, because the application of GPT causes an error that goes into the same direction as the atmosphere loading corrections. In addition to the azimuthal symmetry of the troposphere delays according to Eq. 2.24, we need to take azimuthal asymmetry into account, which in North-South direction is caused by the larger extension of the troposphere above the equator compared to the poles and which can also be due to local weather phenomena, e.g. if a VLBI site is located close to the coast. Typically, North and East gradients are estimated in VLBI analysis with a resolution of 2 to 24 hours. MacMillan (1995) proposed to use the equation

$$\Delta L(a,e) = \Delta L_0(e) + mf_h(e) \cdot \cot(e) \cdot [G_n \cos(a) + G_e \sin(a)] \tag{2.26}$$

which goes back to Davis *et al.* (1993) with a denoting the azimuth and ΔL_0 the symmetric delay (see Eq. 2.24). Chen & Herring (1997) published the formula

$$\Delta L(a,e) = \Delta L_0(e) + \frac{1}{\sin(e)\tan(e) + C} \cdot [G_n \cos(a) + G_e \sin(a)] \tag{2.27}$$

[2] at `http://ggosatm.hg.tuwien.ac.at/`

and recommended to use $C = 0.0032$ if the total (hydrostatic plus wet) gradients are estimated. Böhm & Schuh (2007) tested the application of a priori gradients derived from data of the ECMWF and found that estimating gradients from VLBI observations provides better baseline length repeatabilities than keeping those values fixed to non-zero a priori values derived from numerical weather models.

At present, many investigations are carried out on 'direct ray-tracing', i.e. deriving the slant delay for every single observation from numerical weather models (Hobiger *et al.*, 2008). Gipson & MacMillan (2009) found better baseline length repeatabilities for CONT08 (a 14-days VLBI campaign in August 2008) with slant delays derived from data of the Goddard Modelling and Assimilation Office (GMAO) compared to using VMF1. Böhm *et al.* (2010) obtained improvement for UT1 estimates from Intensive sessions on the baseline Wettzell-Tsukuba if using ray-traced delays at station Tsukuba.

2.2.5 Antenna deformation

It has already been mentioned that in addition to the troposphere delays, there are other effects which depend on azimuth and elevation of the observations and need to be taken into account. For instance, deformations of the radio telescope structure which occur during the 24 hours of an observing session or between the observing sessions have to be considered if we want to achieve highest accuracies. They can be caused by snow and ice loading of the antenna (Haas, 1999) or thermal expansion of the radio telescopes (Nothnagel, 2009). Wresnik *et al.* (2007) compared thermal deformation measurements with invar rods at Wettzell (Germany) and Onsala (Sweden) to thermal deformation models applying local air temperatures as well as structure temperatures measured at those sites. They found an improvement if the air temperatures are first converted to structure temperatures before using them for modeling the thermal deformation of the radio telescopes (see Fig. 2.6). Recent investigations also deal with gravitational deformations (Abbondanza & Sarti, 2010) which can significantly influence the estimated station heights if neglected in VLBI analysis (Sarti *et al.*, 2011).

2.2.6 Axis offsets

At the radio telescope the distance between the feed horn and the axis intersection, which constitutes the baseline reference point, is assumed to be constant at the millimeter-level. In this case the corresponding time offset becomes part of the clock offset parameter. However, an axis offset model is applied to each antenna where the pointing axes do not intersect (Sovers *et al.*, 1998). The axis offsets are provided by the IVS Analysis Coordinator together with the coefficients of the thermal expansion models (Nothnagel, 2009). Large radio telescopes such as the Effelsberg 100 m antenna exhibit elevation-dependent changes in the focal distance which can however be modeled to a level of a few millimeters (Rius *et al.*, 1987). In the case of radio telescopes of the type alt-azimuth, the correction $\Delta\tau$ due to an axis offset AO can be calculated with

$$\Delta\tau = -AO \cdot \sin(zd') \tag{2.28}$$

if zd' is the zenith distance corrected for refraction.

2.2.7 Source structure

A major problem is constituted by the fact that most of the observed radio sources tend to show structure at the level of a few milliarcseconds which often varies with time. These effects, in particular the changes in the source structure, pose a limit on the accuracy of the radio reference frame. For highest accuracies, a regular monitoring of the structure, which is also accomplished

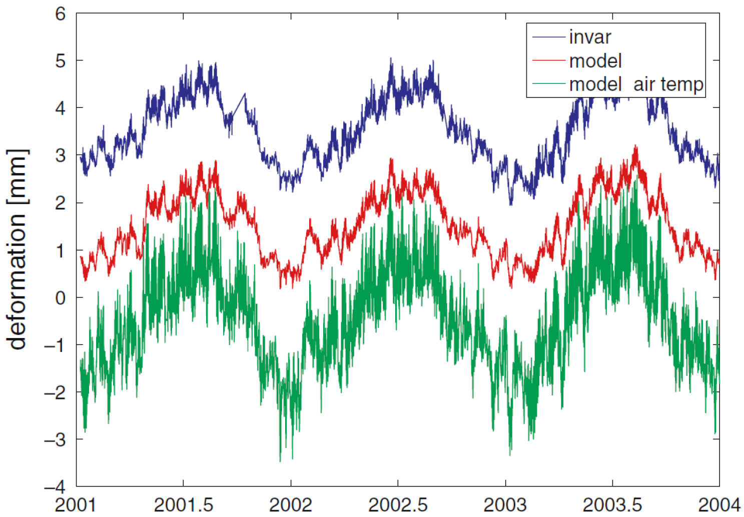

Figure 2.6: Measured vertical deformation (invar rod, upper curve), calculated antenna deformation using the air temperature to model the structure temperature (central curve), and the thermal deformation using the measured air temperature directly at Wettzell. The curves are offset by 2 mm for clarity (Wresnik *et al.*, 2007).

by analyzing VLBI data, can be done in parallel to the geodetic analysis, thus providing a means to correct for the source structure effects (see Collioud & Charlot, 2009, Schuh, 2000, and other references therein).

2.2.8 A few examples of constituents to the delay

The various effects that have been described in the previous sections on the calculated time delay τ for simulated observations with stations Westford (U.S.A) and Wettzell (Germany) to source 0642+449 are evident in Fig. 2.7. These effects are ordered by magnitude from top to bottom. The upper plot displays the total delay which is mainly caused by the Earth rotation (Section 2.2.2) and can be as large as one Earth radius. The next plot depicts the contribution of the hydrostatic delays at both sites to the total delay, i.e., the delay at Wettzell minus the delay at Westford. At each site, the hydrostatic delay at low elevation angles can be larger than 20 m, and it increases rapidly as the elevation angle decreases (Section 2.2.4). The third sub-plot illustrates the influence of the axis offsets at Wettzell and Westford (Section 2.2.6), of the gravitational effect of the Sun (Section 2.2.3), and of the solid Earth tides (Section 2.2.1). The bottom plot contains the influence of the high-frequency Earth rotation model accounting for the ocean tides (Section 2.2.2), as well as the effect of ocean loading (Section 2.2.1) at the sites on the calculated delay τ.

2.3 Least-squares adjustment in VLBI

As can be seen in the flowchart of Fig. 2.4 the theoretical delays are then compared with the reduced observed delays by a parameter estimation process, e.g. a classical Gauß-Markov model as will be described below, or Kalman filtering (Herring *et al.*, 1990), or collocation (Titov & Schuh, 2000) – all three following the least-squares concept – or a square-root information filter (Bier-

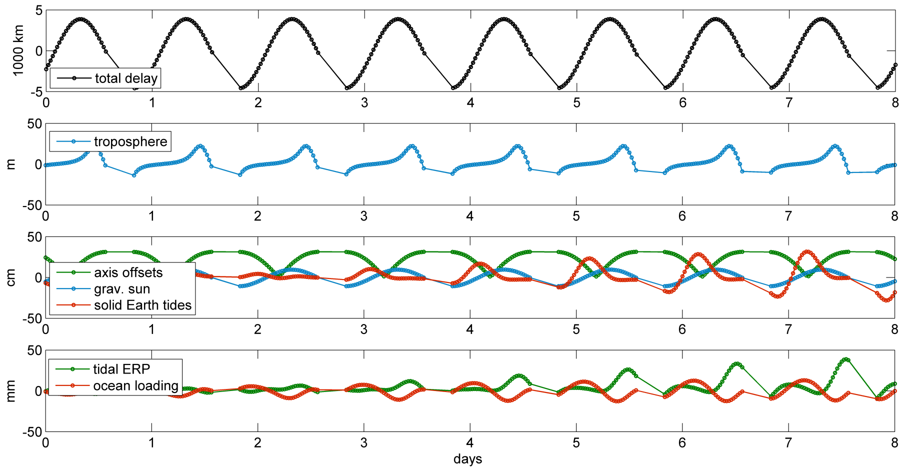

Figure 2.7: Influence on the calculated time delay τ for simulated observations with stations Westford (U.S.A) and Wettzell (Germany) to radio source 0642+449. From top to bottom: Total delay (mainly caused by Earth rotation), troposphere, axis offsets, gravitational effect of the Sun, solid Earth tides, high-frequency model for the Earth rotation caused by ocean tides, and ocean loading (by courtesy of Lucia Plank)

man, 1977). The least-squares adjustment theory allows estimating unknown parameters in an over-determined system of equations. Since there are more equations than unknown parameters, the solution will not be exactly correct for each equation, but the adjustment provides a unique solution dx and minimizes the squared sum of the weighted residuals v. Functional and stochastic models are based on linearized observation equations:

$$A \cdot dx = l + v \quad \text{or} \quad \left[\begin{array}{c} A_{ro} \\ A_{po} \end{array} \right] \cdot dx = \left[\begin{array}{c} l_{ro} \\ l_{po} \end{array} \right] + \left[\begin{array}{c} v_{ro} \\ v_{po} \end{array} \right], \tag{2.29}$$

$$P = \left[\begin{array}{cc} P_{ro} & 0 \\ 0 & P_{po} \end{array} \right]. \tag{2.30}$$

The design matrix A_{ro} contains the first derivatives of the function of the real observations w.r.t. the estimated parameters. Short estimation intervals (e.g. 20 minutes for zenith wet delays) could lead to singularity problems if there was no observation within a time segment. Therefore, the A_{ro} matrix is extended by a pseudo-observation matrix A_{po}, which constrains the value of variability of the parameters, either by constraining the absolute values to zero (typically used for troposphere gradients in early VLBI sessions) or by constraining the relative variation of the continuous piecewise linear functions. The reduced observations, i.e. the observed minus calculated time delays, are listed in the l_{ro} vector (real observations) whereas the l_{po} vector (pseudo-observations) is typically filled with zeros. The weighting of the observations is done by the weight matrix P.

There are different groups of parameters. Auxiliary parameters, e.g. clock parameters and sometimes also the troposphere parameters like zenith wet delays or gradients, have to be computed but are usually not of interest for the geodesists. As clock parameters, linear or quadratic polynomials (over the 24 hour session accounting for clock offset, clock frequency offset, and clock frequency drift) are estimated. Additionally, continuous piecewise linear functions with, e.g. hourly segments, are estimated with respect to a reference clock that is set to zero in order to account for rapid clock instabilities. A typical constraint for the relative variation of the piecewise linear clock function is 0.5 ps^2/s; and for time segments e.g. of 60 min this would correspond to a variance of 1800 ps^2 over that time span of one hour, meaning that the difference between two adjacent clock offsets is 0 ± 13 mm. Special care has to be paid to the detection of clock breaks that sometime occur at some station clocks (hydrogen masers, described in Section 2.1.1) during a VLBI session. The epochs of those clock breaks have to be introduced in the analysis of VLBI sessions, because separate, quadratic polynomials are used to describe the behavior of the clock before and after the break.

2.3.1 The concept of piecewise linear offsets

In the Vienna VLBI Software (VieVS; Böhm *et al.*, 2011) zenith wet delays are typically estimated every 20 to 60 minutes, and rather loose constraints are put on the variation of the zenith wet delays (0.7 ps^2/s). So-called 'piecewise linear offsets' are used in VieVS, i.e. the functional model is based on offsets only (no rates) (see Eq. 2.31). These piecewise linear offsets are estimated at integer hours (e.g., at 18 UTC, 19 UTC, ...), at integer fractions of integer hours (e.g., 18:20 UTC, 18:40 UTC, ...) or at integer multiples of integer hours (e.g. 18:00 UTC, 0:00 UTC, 6:00 UTC, ...). In VieVS, this representation is not only possible for troposphere zenith delays and gradients, station clocks, and Earth orientation parameters, but also for coordinates of selected stations and radio sources. Equation 2.31 denotes the functional model of the wet delay ΔL_w at one station represented by piecewise linear offsets x_1 and x_2 of the zenith wet delays at the integer hours t_1 and t_2. The wet mapping function at epoch t of an observation which is in between the integer hours is expressed by $mf_w(t)$. The partial derivatives which have to be entered in the design matrix are given in Eqs. 2.32 and 2.33. This concept is similar for all parameters, and with this kind of parameterization all combinations (at the normal equation level) with other space geodetic techniques will be easy and straight-forward.

$$\Delta L_w(t) = mf_w(t) \cdot x_1 + mf_w(t) \cdot \frac{t - t_1}{t_2 - t_1} \cdot (x_2 - x_1) \tag{2.31}$$

$$\frac{d\Delta L_w}{dx_1} = mf_w(t) - mf_w(t) \cdot \frac{t - t_1}{t_2 - t_1} \tag{2.32}$$

$$\frac{d\Delta L_w}{dx_2} = mf_w(t) \cdot \frac{t - t_1}{t_2 - t_1} \tag{2.33}$$

In addition to the clock and troposphere parameters (zenith wet delays and gradients) mentioned above, there are many other geodetic/astrometric parameters which can by estimated from VLBI sessions (see Section 4). Earth orientation parameters – although typically estimated once per session – can also be retrieved with a higher temporal resolution applying the concept of the piecewise linear offsets. Figure 2.8 shows hourly estimates of (UT1-UTC) during CONT08.

2.3.2 Global VLBI solutions

Other 'global' parameters such as station or source coordinates can in principle also be estimated from single VLBI sessions, but they are preferably determined in a global solution, i.e., from a large number of VLBI sessions connected to a common least-squares parameter estimation. Due to limited computer memory capacity it is essential to keep the equation system small. In VLBI analysis there are auxiliary parameters in the observation equations which cannot be fixed to a priori values, even if we are not interested in them, e.g., clock parameters. Therefore, a reduction algorithm is used which is based on a separation of the normal equation system into

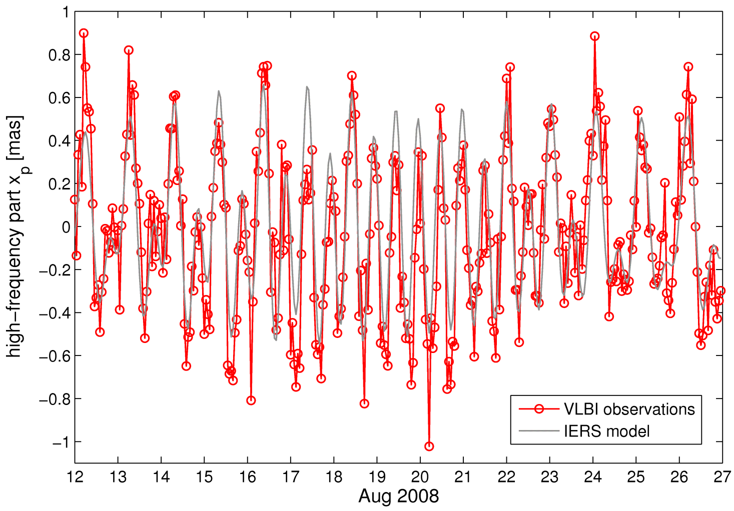

Figure 2.8: Hourly x-pole values in mas estimated with VieVS for CONT08 in red. For comparison high-frequency (UT1-UTC) values as derived from the IERS Conventions model (ocean tides and libration; Petit & Luzum, 2010) are shown in grey (by courtesy of Sigrid Böhm).

two parts. The first part contains parameters which we want to estimate and the second part those parameters which will be reduced. Even if we 'reduce' parameters, they still belong to the functional model of unknown parameters and will be estimated implicitly.

$$\begin{bmatrix} N_{11} & N_{12} \\ N_{21} & N_{22} \end{bmatrix} \cdot \begin{bmatrix} dx_1 \\ dx_2 \end{bmatrix} = \begin{bmatrix} b_1 \\ b_2 \end{bmatrix}. \tag{2.34}$$

In 2.34 $N = A^T PA$ and $b = A^T Pl$, and the reduction of dx_2 is done by executing the matrix operation

$$(N_{11} - N_{12}N_{22}^{-1}N_{21}) \cdot dx_1 = b_1 - N_{12}N_{22}^{-1}b_2 \text{ or } N_{reduc} \cdot dx_1 = b_{reduc}. \tag{2.35}$$

Stacking is used for combining normal equation systems if a parameter is contained in at least two normal equation systems and only one common value in the resulting combined system should be estimated. For a combined solution of the identical parameters (dx_1), the normal matrices (N_{reduc}) and the right hand side vectors (b_{reduc}) from n single sessions have to be summed up:

$$N_{REDUC} = N_{reduc\_1} + N_{reduc\_2} + \ldots + N_{reduc\_n}, \tag{2.36}$$

$$b_{REDUC} = b_{reduc\_1} + b_{reduc\_2} + \ldots + b_{reduc\_n}. \tag{2.37}$$

Conditions on the N_{REDUC} matrix are applied in order to prevent the matrix from being singular. From the analysis of VLBI sessions we get free station networks, which are the result of adjusting observations in a model where coordinates are unknowns without fixing the coordinate system (Sillard & Boucher, 2001). With three-dimensional VLBI station networks the rank deficiency is six (the scale is determined from the observations), which means that at least six conditions have to be applied to remove the rank deficiency. In case of station coordinates three no-net-translation (NNT) and three no-net-rotation (NNR) conditions are applied on selected datum stations, and in the case of source coordinates an NNR condition is usually applied on a selected set of datum sources. In case of longer time spans NNR-rate/NNT-rate conditions are also applied on station coordinate velocities. It is very important to use stable stations and sources for the datum, because otherwise the quality of the terrestrial and celestial reference would be deteriorated. Moreover, it is absolutely necessary to take into account any episodic changes in the station coordinates, e.g. due to instrumental changes or earthquakes. Unlike positions and velocities, no scale or scale rate parameters are estimated in VLBI, as the scale directly depends on the speed of light, c, one of the defining natural constants. The final solution is obtained by an inversion of the normal matrix:

$$dx_1 = N_{REDUC}^{-1} \cdot b_{REDUC}. \tag{2.38}$$

Since the least-squares adjustment minimizes the squared sum of weighted residuals, this value is used to scale the standard deviations of the estimates. It is determined with

$$v^T Pv = (l^T Pl)_{REDUC} - x_1^T b_{REDUC}, \tag{2.39}$$

where the first part $(l^T Pl)_{REDUC}$ depends only on observations; it has to be corrected for the influence of the reduced parameters which is known from the single normal equation systems:

$$(l^T Pl)_{REDUC} = \sum_{i=1}^{n} (l^T Pl - b_2^T N_{22}^{-1} b_2). \tag{2.40}$$

The second part in 2.39, $x_1^T b_{REDUC}$, depends on the combined solution. The a posteriori variance of unit weight σ_0^2 is a scaling factor for the inverse normal equation matrix, i.e., for the covariance matrix Q of the estimated parameters:

$$Q = \sigma_0^2 \cdot N^{-1}. \tag{2.41}$$

It is determined with

$$\sigma_0^2 = \frac{v^T Pv}{k - u + d}, \tag{2.42}$$

where k is the number of observations, u the number of estimated and reduced parameters, and d the number of additional condition equations.

2.4 Results from geodetic VLBI and the International VLBI Service for Geodesy and Astrometry (IVS)

The Very Long Baseline Interferometry (VLBI) technique has been employed for more than 30 years in geodesy, geophysics, and astronomy, and results of geodetic VLBI have been presented and interpreted in a multitude of publications by hundreds of authors. During the first two decades, most of the scientific and operational activities were organized through national or bilateral agreements, only, which was not a basis sufficiently strong for carrying out VLBI sessions in global networks. In 1999 the International VLBI Service for Geodesy and Astrometry (IVS) was established to coordinate the global VLBI components and resources on an international basis. All international collaboration, in accordance with the IVS terms of reference, is based on a standing call for participation that was first issued in 1998. Any institution that is prepared to participate in IVS activities may join at any time after getting accepted by the IVS Directing Board (Schlüter & Behrend, 2007). The inauguration of the IVS took place in March 1999, and the first meeting of the Directing Board was held at the Fundamental Station Wettzell, Germany. The IVS was approved as a service of the International Astronomical Union (IAU), of the International Association of Geodesy (IAG), and of the Federation of Astronomical and Geophysical Data Analysis Services (FAGS); the latter was dissolved in 2010 and replaced in 2011

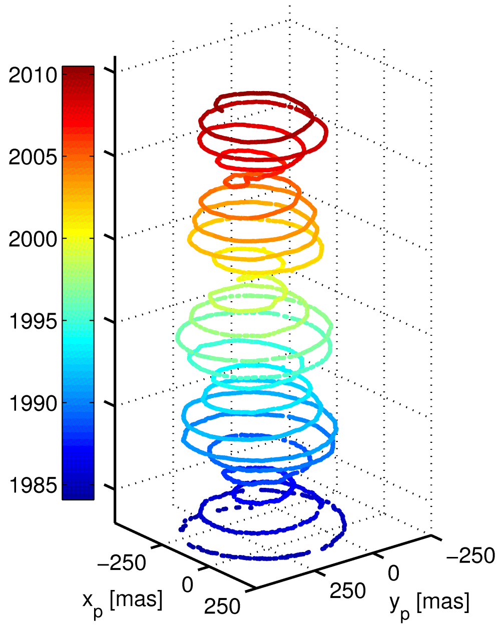

Figure 2.9: Polar motion estimates in milliarcseconds as determined from VLBI observations since 1984. Clearly visible is the modulation between the Chandler wobble period of about 1.18 years and the annual variation (by courtesy of Sigrid Böhm)

by the World Data System (WDS). According to its terms of reference, the IVS is an international collaboration of organizations that operate or support VLBI components for geodetic and astrometric applications. Specific goals are to provide a service to support geodetic, geophysical, and astrometric research and operational activities, to promote research and development activities in all aspects of the geodetic and astrometric VLBI technique, and to interact with the community of users of VLBI products and to integrate VLBI into a global Earth observing system. Since 2003 the Global Geodetic Observing System (GGOS; Plag & Pearlman, 2009) has been developed as a main component of the IAG, and the IVS provides an essential contribution to it (Schlüter & Behrend, 2007).

'Official IVS products' are the realization of the Celestial Reference Frame (CRF) through the positions of extragalactic radio sources, the maintenance of the terrestrial reference frame (TRF), such as station positions and their changes with time, and the generation of series describing the Earth orientation (see table 2.1). Geodetic Very Long Baseline Interferometry (VLBI) is the only space geodetic technique that allows the observation of the full set of Earth orientation parameters (EOP), and it is unique in providing Universal Time (UT1) (see Fig. 2.8) as well as celestial pole offsets over longer time spans. Figure 2.9 depicts polar motion estimates as determined from VLBI observations since 1984 with the Vienna VLBI software VieVS (Böhm *et al.*, 2011). As mentioned above, the IVS plays a key role within GGOS and thus all IVS products are also considered GGOS products, today. Moreover, VLBI is the only technique for the determination of the International Celestial Reference Frame (ICRF). The International Celestial Reference Frame (ICRF1; Ma *et al.*, 1998), defined by positions of 212 compact radio sources (out of in total 608 radio sources), was the first realization at radio frequencies. Since its approval in 1997 by the IAU, the IVS has been in charge of the VLBI realization. At the XXVII General Assembly in 2009 the IAU adopted the ICRF2 including the positions of 3414 compact radio astronomical sources. This is more than five times the

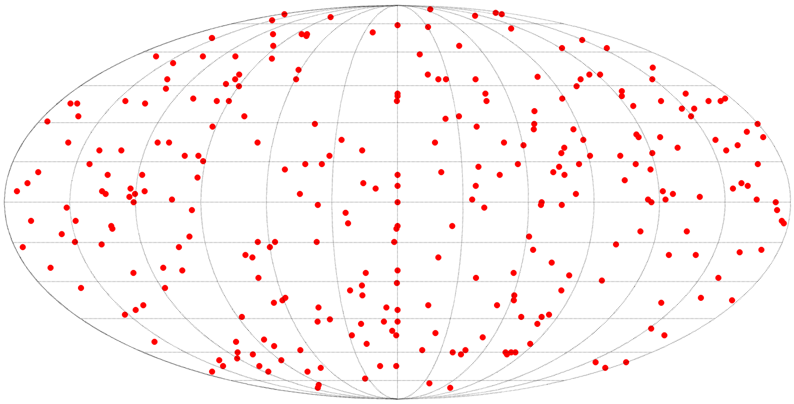

Figure 2.10: Defining ICRF2 sources

number of sources in the ICRF1 (or its later extension, the ICRF1-Ext.2). The noise floor of the ICRF2 is at the level of 40 μas and the axis stability at the level of 10 μas (Fey *et al.*, 2009). The ICRF2 has 295 defining sources with an equal distribution, in particular in the Southern celestial hemisphere, and smaller source structure effects, both weaknesses in the ICRF1 (Fey *et al.*, 2009). Geodetic VLBI also contributes to the realization of the International Terrestrial Reference Frame (ITRF) by measuring long intercontinental baselines within global networks. Compared to those space geodetic techniques using satellites, VLBI has the principal advantage that its realization of the ITRF scale only depends on the speed of light c, which is used to transform the delay observables into metric units. There exists no evidence at all that during the last three decades a bias or rate of this conversion has occurred due to technical reasons. Figure 2.11 illustrates the horizontal velocities of the VLBI stations included in the VTRF2008 (Böckmann *et al.*, 2010), the VLBI contribution to the ITRF2008 (Altamimi *et al.*, 2011).

Table 2.1 provides a summary of current IVS main products (Schlüter & Behrend, 2007). Observations of geodetic VLBI have been carried out for more than three decades providing a basis for the precise determination of geodynamic and astronomical parameters including their long-term variations. For example, VLBI can determine Love numbers h and l of the solid Earth tides model (Spicakova *et al.*, 2010), ionosphere models (Hobiger, 2006), or troposphere parameters. The long-term VLBI zenith wet delays are of interest for climatologists because they contain information about the precipitable water above the stations for their complete history (Heinkelmann, 2008); they can also be used to validate troposphere parameters from other space geodetic techniques (Snajdrova *et al.*, 2005, Teke *et al.*, 2011). Another interesting phenomenon, which can be observed by VLBI, is the gravitational deflection of radio waves by the solar gravity field according to general relativity. As described in Section 2.2.3, radio waves are subject to space-time curvature caused by any massive body (in our solar system mainly those by the Sun has to be considered but also that one by Jupiter for close approaches). At the elongation angle of 2.5° to the Sun, which was the minimal angle of VLBI observations till 2002, the differential deflection reaches 150 mas (Robertson *et al.*, 1991) causing a significant effect on the observed group delays. With respect to the noise floor of source coordinates, which is about 40 μas for the ICRF2 (Fey *et al.*, 2009), analysis of source observations in the vicinity of the Sun allows the determination of the post-Newtonian parameter γ ('light deflection parameter') characterizing the space curvature due to gravity (see Eq. 2.15). Although since 2002 the VLBI observations are scheduled for a minimal angle of 15° to the Sun, the gravitational deflection still influences the measurements significantly and the most recent VLBI global solutions provided γ with a precision

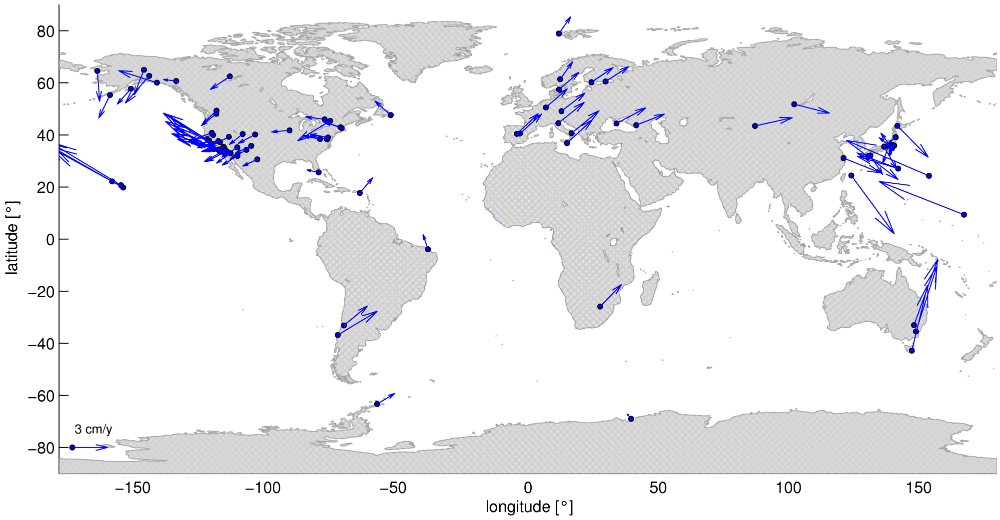

Figure 2.11: VTRF2008 station distribution with horizontal velocities

Products	Specification	Status 2010
Polar motion x_p, y_p	Accuracy	50-80 μas
	Product delivery	8-10 days
	Resolution	1 day
	Frequency of solution	$\sim$ 3 days/week
UT1-UTC	Accuracy	3-5 μs
	Product delivery	8-10 day
	Resolution	1 day
	Frequency of solution	$\sim$ 3 days/week
UT1-UTC (Intensives)	Accuracy	15-20 μas
	Product delivery	1 day
	Resolution	1 day
	Frequency of solution	7 days/week
Celestial pole dX, dY	Accuracy	50 μas
	Product delivery	8-10 days
	Resolution	1 day
	Frequency of solution	$\sim$ 3 days/week
TRF (x, y, z)	Accuracy	5 mm
CRF (α, δ)	Accuracy	40-250 μas
	Frequency of solution	1 year
	Product delivery	3 months

Table 2.1: Summary of IVS main products (modified from Schlüter & Behrend, 2007)

of 1×10^{-4} (Lambert & Le Poncin-Lafitte, 2009, 2011). The series of VLBI data is also sensitive to a possible acceleration of the solar system barycenter which might cause a secular drift of aberration with a magnitude of 4 μas/year (Sovers *et al.*, 1998, Titov, 2010). Furthermore, the solar system motion relative to the cosmic microwave background might produce a dipole pattern that decreases with red shift (Titov, 2010).

2.5 The next generation VLBI system, VLBI2010

In September 2005 the IVS Directing Board accepted the final report of its Working Group 3 (WG3) entitled "VLBI2010: Current and Future Requirements for Geodetic VLBI Systems" (Niell *et al.*, 2006) which recommended a review of all current VLBI systems and processes from antennas to analysis and outlined a path to a next-generation system with unprecedented new capabilities: 1 mm position and 0.1 mm/yr velocity accuracy on global scales, continuous measurements for time series of station positions and Earth orientation parameters, and a turnaround time to initial geodetic results of less than 24 hours.

As a consequence, the IVS established the VLBI2010 Committee (V2C) to carry out a series of studies and to encourage the realization of the new vision for geodetic VLBI. Making rational design decisions for VLBI2010 requires an understanding of the impact of new strategies on the quality of VLBI products. To serve this purpose, Monte Carlo simulators were developed which have been used to study the effects of the dominant VLBI random error processes (related to the atmosphere, the reference clocks, and the delay measurement noise; Pany *et al.*, 2010) and new approaches to reduce them, such as decreasing the source-switching interval and improving analysis and scheduling strategies. Shortening the source-switching interval results in a higher number of observables leading to a significant improvement in station position accuracy (Petrachenko, 2009). In any case, the simulators confirm that the dominant error source is the troposphere. It is recommended that research on analysis strategies for the atmosphere continues to be a priority for the IVS. Based on the findings from the Monte Carlo studies, the source-switching interval should be reduced. This includes decreasing both the on-source time needed to make a precise delay measurement and the time required to slew between sources. From these two somewhat competing goals, recommendations for the VLBI2010 antennas are emerging, e.g., either a single $\sim$ 12 m diameter antenna or larger with very high slew rates, e.g., 12°/s in azimuth, or a pair of $\sim$ 12 m diameter antennas (or larger), each with more moderate slew rates, e.g., 5°/s in azimuth (Petrachenko, 2009).

In order to reduce the on-source observing time, it is important to find a means for measuring the delay with the requisite precision even at a modest signal-to-noise ratio. To do this a new approach is being developed in which several widely spaced frequency bands are used to unambiguously resolve the interferometric phase. The new observable is being referred to as the broadband delay. A four-band system is recommended that uses a broadband feed to span the entire frequency range from 2 to 14 GHz (Petrachenko, 2009). A total instantaneous data rate as high as 32 Gbps and a sustained data storage or transmission rate as high as 8 Gbps are necessary to detect an adequate number of high-quality radio sources (Petrachenko, 2009). NASA is funding a proof-of-concept effort till 2012 to test the broadband delay technique, and first fringes have been already detected in all bands. In addition to random errors, systematic errors need to be reduced, too. For example, updated calibration systems are being developed to account for electronic biases. Conventional surveying techniques have to be refined to observe antenna deformations, and the application of small reference antennas is considered for generating deformation models and establishing site ties. Furthermore, corrections based on images derived directly from the VLBI2010 observations are under study to mitigate errors due to source structure (Petrachenko, 2009).

The progress report of the IVS VLBI2010 Committee (Petrachenko, 2009) recommends that a globally distributed network of at least 16 VLBI2010 antennas observes every day to determine Earth orientation parameters, and that other antennas be added as needed for the maintenance of the celestial and terrestrial reference frames. Antennas with access to high-speed fiber networks are also required to enable daily delivery of initial IVS products in less than 24 hours. A high priority is placed on increasing the number of stations in the Southern hemisphere. Since IVS products must be delivered without interruption, a transition period to VLBI2010 operations is required in which there will be a mix of antennas with current and next-generation receiving systems. For this period a compatibility mode of operation has been identified and tested to a limited extent with the NASA proof-of-concept system. In order to increase reliability and to reduce the cost of operations, enhanced automation will be introduced both at the stations and in the analysis process. Stations will be monitored centrally to ensure compatible operating modes, to update schedules as required, and to notify station staff when problems occur. Automation of the analysis process will benefit from the work of the current IVS Working Group 4, which is updating data structures and modernizing data delivery (Petrachenko, 2009).

For more details the authors refer to various reports, memos, and other documents describing the concept and realizations of VLBI2010. Many of those are accessible via the webpage of the IVS at `http://ivscc.gsfc.nasa.gov/`.

2.6 Concluding remarks

Very Long Baseline Interferometry plays a unique and fundamental role in the maintenance of the global (terrestrial and celestial) reference frames and in monitoring the Earth orientation parameters, which are required for precise positioning and navigation on Earth and in space. Furthermore, very valuable information on various time scales can be obtained about several other parameters needed for the investigation of phenomena such as meteorological and climatologic changes, and geodynamical or astronomical effects. Thus, geodetic VLBI is essential for the Global Geodetic Observing System (GGOS), the flagship component of the International Association of Geodesy (IAG). The IVS has served this task very successfully in the past, and with the upcoming VLBI2010 concept, it is advancing to a bright and challenging future.

Acknowledgements

We are grateful to the International VLBI Service for Geodesy and Astrometry (IVS) with all its components and contributing agencies for acquiring and providing the data used in the examples given in this chapter and for the very fruitful cooperation in the past decades. The authors would like to acknowledge all individuals mentioned in this chapter and many other VLBI experts who developed the VLBI technology, correlator, and data analysis since the mid-sixties of the last century. Their continuous efforts made it such an exciting space geodetic technique providing scientific results of highest quality but also producing regular measurements with highest impact on society and our Earth in general. Also, we would like to thank all members of the VLBI group at the Vienna University of Technology who contributed with their efforts to this summary; their continuous enthusiasm is advancing VLBI. We are also grateful to Brian Corey (MIT Haystack Observatory), Axel Nothnagel (University Bonn), and Ludwig Combrinck (Hartebeesthoek Radio Astronomy Observatory) for their comments on the manuscript.

Chapter 3

User Guide

3.1 General concept of VieVS

The VieVS software was written by the Institute of Geodesy and Geophysics (IGG), Vienna University of Technology. It includes state of the art models that coincide with the latest International Earth Rotation Service (IERS) conventions. It is written in Matlab (version 7.6 (R2008a) or later is required) which has the advantages of being easy to use and source code changes can be applied without much effort. Unfortunately Matlab is expensive and is not as fast as C++ or FORTRAN. Matlab is, however, widely used, hence many research facilities are already in possession of a licence. The slower speed is not a big disadvantage since today's computer hardware is fast enough for normal usage of the software.

The VieVS software is structured in different parts (a flow chart is illustrated in Figure 3.1):

- The first part, VIE_INIT (INIT stands for initialising), is responsible for reading the data; currently VieVS needs session files (files with the actual measurements) in NGS format. Data created here is saved in the LEVEL 0 folder.

- The second part, VIE_MOD (MOD stands for modelling), calculates the theoretical delays, and its partial derivatives, models according to the IERS conventions are implemented. Data created here is saved in the LEVEL 1 folder.

- The third part, VIE_LSM (LSM stands for least squares matching), is responsible for the least squares estimation. Parameters such as EOPs, station coordinates and clock offsets etc. are estimated and saved in the LEVEL 3 folder for further investigation.

Apart from the main structure in VieVS there are three other modules, namely VIE_SCHED, VIE_SIM and VIE_GLOB.

- VIE_SCHED (SCHED stands for scheduling) is the scheduling package of VieVS. With this module an observation plan for a specific time and network can be created.

- VIE_SIM (SIM stands for simulating) creates simulated observations for an observation plan (could either be from a real session or scheduled). It combines the theoretical delay with simulated values for zenith wet delay, clocks and observation noise at each epoch, in order to create realistic observations. The output is saved as NGS format and can then be analysed with the main VieVS methods.

- VIE_GLOB (GLOB stands for global) combines the normal equations of several sessions into a global solution in order to calculate reference frames and global parameters.

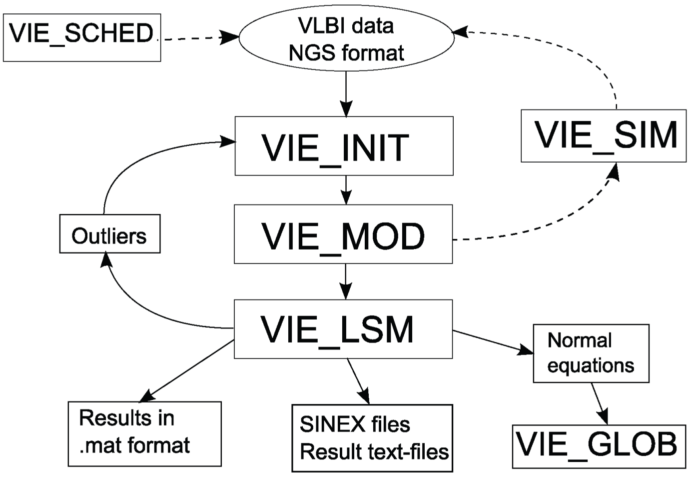

Figure 3.1: Different modules of VieVS and their relation

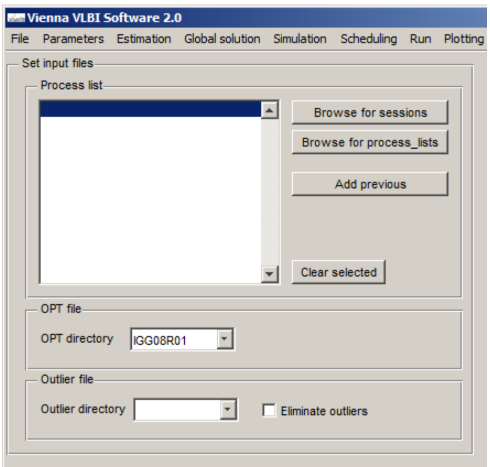

Figure 3.2: VieVS graphical user interface

Parameters and models can be easily selected using the graphical user interface (GUI) of VieVS. The output is written to the command window of Matlab, the results are saved as Matlab files.

3.2 GUI and batch

A graphical user interface (GUI) for VieVS (Figure 3.2), 'VIE_SETUP' is provided. All the different modules are integrated in the GUI and can be selected with the drop down menu. Additionally a plotting tool is implemented. The GUI can be started by typing `vievs` in the Matlab command window (be sure that the *VieVS/WORK* directory is set as current directory in Matlab).

3.2.1 Processing preparation done by the GUI

The final purpose of the interface before processing is to save the required files at their required destination ('prepare processing'). The only difference between the buttons *Save runp* and *Save + Run* is that the latter also starts the processing (*vie_batch*). Following files are created when clicking either *Save runp* or *Save + Run*.

- input_protocol.txt - not required for processing (see Chapter 3.11.4)
- runp.mat - required in folder */WORK/* (see Chapter 3.3.2)
- process_list.mat - required in folder */WORK/* (see Chapter 3.3.3)
- parameter.mat - required in folder*/DATA/LEVEL0/subdir/* (see Chapter 3.3.1)
- Scheduling parameters - required for VIE_SCHED (see Chapter 3.7)
- Simulation parameters - required for VIE_SIM (see Chapter 3.8)
- Global parameters - required for VIE_GLOB (see Chapter 3.6)

3.2.2 Batch processing

To start the processing, the user has to click either on *Save + Run* in the GUI or type `vievs('batch')` in the command window (a *runp.mat* file has to be created beforehand). The chart in Figure 3.4 shows the work flow of *vie_batch*. You can see the required input files on the left and the directory where intermediate and final results are saved on the right. In the middle you can see the modules which are used according to the input.

3.2.3 Parallel computing

To speed up the processing of several sessions with the same parametrization, parallel computing, allows Matlab to use more than one core. Parallel computing can be enabled in *Run - run options* (see Figure 3.3). The Parallel Computing Toolbox in Matlab is required to run parallel jobs.

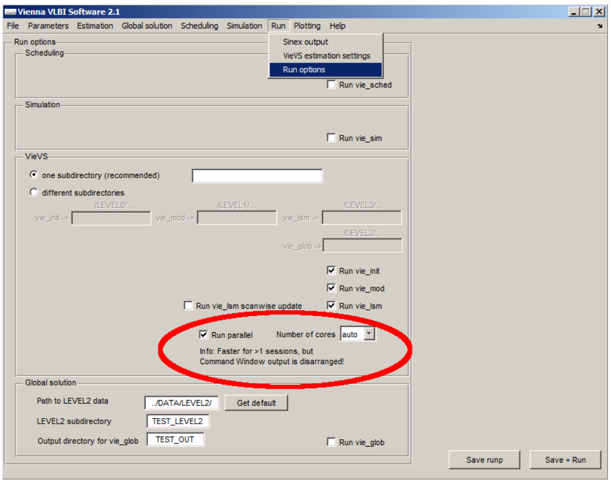

Figure 3.3: Enable parallel computing for faster multi-session processing

When parallel computing is enabled, the sessions run in a parfor instead of a for loop. This decreases the computation time roughly by a factor of the number of cores (usually 2 or 4). If the number of cores in the GUI is set to *auto*, Matlab uses the number of pools specified by the default parallel configuration.

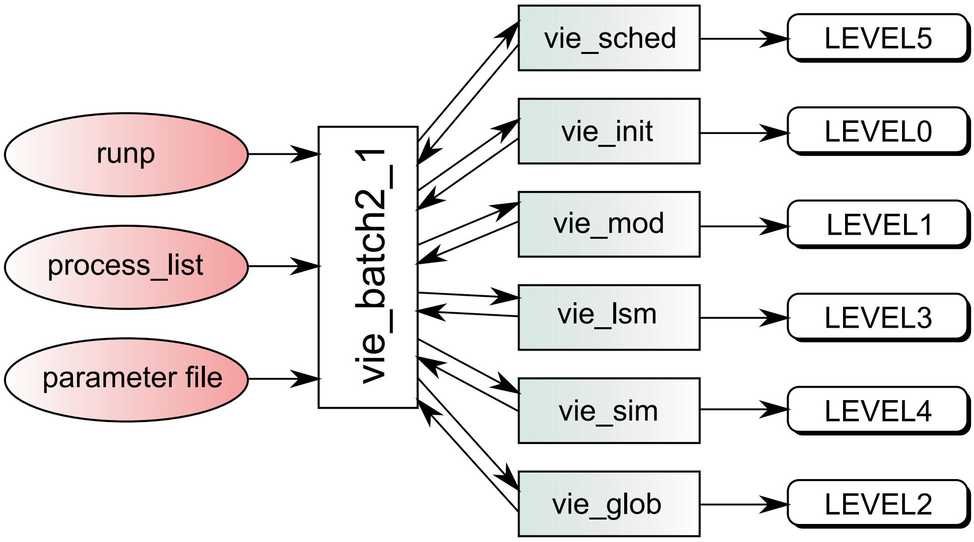

Figure 3.4: Workflow of vie_batch

3.3 Important files

3.3.1 Parameter files

The parameter files are of type *.mat* (Matlab internal binary format) and contain the VieVS processing options (e.g. minimum elevation angle, quality limit, EOP models, estimation intervals and constraints). This file can be used both in the processing (vie_batch) as well as in the interface (vie_setup) for loading the parameters into the GUI.

The parametrization for the 'main' VieVS (except parameters for Simulation, Scheduling and Global solution) is saved in a parameter file (see Chapter 3.3.1). After every modification (e.g. button click, checkbox value change), the current parametrization is saved automatically as *auto_save_fromGUI_yyyymmdd.mat* in */WORK/PARAMETERS/*. This 'last' parametrization can be loaded by selecting *File - Parameter files - Load current*. This might be useful when you want to use the same parametrization in several runs (but keep in mind that this file is changed every time the GUI is changed!).

It is also possible to save a desired parametrization in an own parameter file. Simply go to *File - Parameter files - Save parameters as...*, select a filename and save it. Later you can load this parametrization (*File - Paramter files - Load parameters*).

3.3.2 runp

The file *runp.mat* is one of the main files in a VieVS processing run. This Matlab struct is created in the interface (vie_setup) and contains the subdirectories for all three modules (init_path for VIE_INIT - LEVEL0, mod_path for VIE_MOD - LEVEL1, lsm_path for VIE_LSM - LEVEL3), as well as a logical variable for all six modules (sched, sim, init, mod, lsm, glob), defining whether or not this module should be run. The file must be in */WORK/* and is overwritten for every single processing run.

3.3.3 Process lists

The process list is a *.mat* file, which contains a list of sessions to be processed (multiple sessions can be selected). The file *process_list* in */WORK/* is loaded by *vie_batch* and the sessions written in that file are processed. User defined process lists (e.g. CONT campains, Intensives in 2010, ...) can be loaded and saved in the interface of VieVS.

File - Parameter files - Save process list as saves the selected sessions from the listbox in *File - Set input files* to a process list.

This process list can be loaded in *File - Set input files* by selecting *Browse for process_lists.* All the containing sessions should appear in the listbox of *File - Set input files.*

A function for automatically generating process lists is mk_list, see Chapter 3.3.6 for more information.

3.3.4 Outlier files

Outlier files are simple ASCII files containing line-per-line observations which have been (automatically or manually) set as outliers. This is usually done for observations with large residuals. One line contains the two participating stations and the mjd of the observation. Three example lines of such a file are:

```
NYALES20 SVETLOE  56009.261099537034
SVETLOE  WETTZELL 56009.261099537034
KOKEE    NYALES20 56009.256249999999
```

If an outlier file does already exist, all new outliers will be appended (the old ones will not be removed!).

Different folders may exist in the */DATA/OUTLIER/* directory. One can select the folder where outlier files are written to, in the *File - Set input files* part of the GUI.

The outlier file of a session can be opened by right-clicking on the session in the listbox and selecting the Outlier file.

Define outliers

They can either be defined (A) automatically or (B) manually:

(A) In *Run - VieVS estimation settings* the user can select one of two outlier tests. The 'simple' outlier test (1) sets observations as outliers which have larger residuals than $c \cdot m_0$ where c is a user-definable number (e.g. 5) and m_0 is the a posteriori standard deviation of unit weight. The 'normal' outlier test (2) has a outlier-threshold of $c \cdot m_0 \cdot \sqrt{Q_{vv}}$ where Q_{vv} is the variance-covariance matrix a posteriori of the observations. If no automatic outlier selection should be used, the two checkboxes should be unclicked!

(B) Outliers can be selected manually in the plotting of residuals. The button *Select outliers* lets the user drag open a box (left mouse-button) and select observations. A click on *Remove outliers* writes the selected observations to the outlier file.

Treatment of outliers

VieVS removes outliers always at the beginning. If no outlier file is specified before the processing starts no outliers will be removed in this run. This means that if you want to have a solution without outliers, you have to process the session twice: One for the detection (automatic or manual) of them, the second with those outliers removed!

The checkbox *Eliminate outliers* in *File - Set input files* tells the program to remove observations which are written in the outlier file specified by the directory.

3.3.5 OPT files

The OPT-file contains several informations related to one session, usually sessions which have large residuals or generate some other 'problem'. In the following lines an example of the content of an OPT file is given (Attention: The OPT file is very sensitive in terms of blanks and characters. Please stick to the format. Remember: a station name MUST have 8 characters!):

```
CLOCK REFERENCE:
WETTZELL

CLOCK BREAKS: 2
BADARY 55454.4
WETTZELL 55372.369

stations down time (optional)
STATIONS TO BE EXCLUDED: 1
MATERA YYMMDDhhmm-YYMMDDhhmm

if no down time:
STATIONS TO BE EXCLUDED: 1
MATERA

BASELINES TO BE EXCLUDED: 3
WETTZELL ZELENCHK
SVETLOE ZELENCHK
BADARY ZELENCHK

SOURCES TO BE EXCLUDED: 1
1936+095
```

Clock reference

Clock parameters in VieVS are estimated relative to a reference clock, which is one of the station clocks (the clock of the first station in the *_antenna* file is chosen by default). This reference clock can be changed in the OPT file as shown in the example lines (the clock of station WETTZELL is set as reference clock in this example). This is usually important when there is a problem (e.g. a clock break) at exactly this station. Hence the reference clock should be a clock without problems.

Clock break

Station clocks may have discontinuities ('jumps') which - if they are improperly modeled - degrade the estimates. The clock might be modeled as one (e.g. linear) function with respect to the reference clock. If a clock break is specified in the OPT file a separate linear function is estimated before and after the event. Those two functions will model the actual behavior of the clock much more accurately. It is possible to specify more than one clock break per station.

The first-solution residuals are well-suited to identify clock breaks (station and epoch) since there is only one zenith wet delay per station (atmospheric influence is large) and one linear clock function estimated per station: The residuals due to a clock break do not go into the estimated parameters in this solution.

The residuals can be visualized and clock breaks added interactively in the plotting tool (see Chapter 3.10.1).

Exclude stations, baselines and sources

If stations, baselines or sources should not take part in the processing of a session, they have to be excluded in the OPT file. Then they are removed right in the beginning of a VieVS run. It is also possible to deselect the observations of a specific station for a certain time interval.

3.3.6 mk_list

The *mk_list* function can be found in the *WORK* directory. It is a very useful tool that helps the user to select certain sessions with specified attributes (e.g. all IVS-R1 sessions from 2012 where Wettzell contributed). The function can be accessed by typing $[process\_list, sess] = mk\_list(s1, s2, ...)$ in the command window (make sure that the *Current Folder* in Matlab is set to the *WORK* directory). S1, s2, etc. are strings containing the parameters to be set, *process_list* is the list of sessions (can be loaded into the VieVS GUI) and *sess* contains the session names. To make the process list available in the VieVS GUI, save it in the *WORK/PROCESSLIST* directory.

Parameters that can be set: (You also find this information in the header of the function. This can be shown on the command window by typing 'help mk_list')

- include only a specific type of session (e.g. all, R1, EURO etc.)

  process_list=mk_list('all',...)

- include only sessions from specific years

  process_list=mk_list(...,'YEARS',yrs) where yrs is an array with the years you want to include.

- include only a specific station

  process_list=mk_list(...,'REQSTAT',sta) where sta is the two-letter ns-code of the station.

- list of sessions to be excluded

  process_list=mk_list(...,'EXCLUDE',excllist) where excllist is the file name of the list containing the sessions to be excluded.

- include all NGS files (not only the latest)

Here we give some examples on how to use the script:

- Create a list of all R1/R4 between 2003 and 2007:

  process_list=mk_list('R1','R4','YEARS',2003:2007)

- All sessions which Metsähovi has participated in:

  process_list=mk_list('all','REQSTAT','Mh')

- All R1/R4 in 2009, except those listed in exclude.txt:

  process_list=mk_list('R1','R4','YEARS',2009,'EXCLUDE','exclude.txt')

- All CONT02 sessions, including all versions of the NGS files (in case there are more than one):

  process_list=mk_list('C02','ALLVERSIONS')

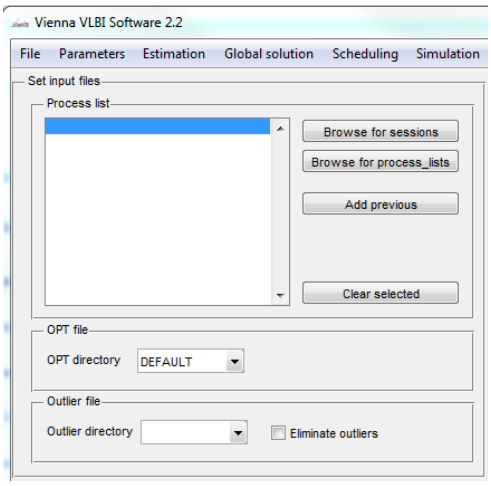

Figure 3.5: GUI screenshot of session selection.

3.4 Input parameters

3.4.1 Select Sessions to be processed

In the tab *File* the sessions to be processed can be selected, a screen shot of the GUI is provided in Figure 3.5. By clicking the button *Browse for sessions* one can select sessions from the *DATA/NGS* directory. VieVS also provides the possibility to use predefined process lists. The selected sessions (more than one can be processed using the specified parametrization) are displayed in the list box. The use of OPT (see Chapter 3.3.5) and outlier files (see Chapter 3.3.4) can also be specified here.

Parameter files and process lists can be saved/loaded with *File - Parameter files - save/load.*

In the tab *Parameters*, variable options concerning the calculation of the theoretical delay and it's partial derivatives can be chosen. When no changes are done here, the processing runs with the default options. The corresponding source code is found in VIE_MOD, with a short introduction of the processing chain given in the next section.

3.4.2 Overview of VIE_MOD

VIE_MOD takes care of the calculation of the theoretical delay and the partial derivatives of the delay with respect to certain parameters. Details on the theory behind is given in chapter 2.2. In Figure 3.6 the flowchart of VIE_MOD is shown.

0. INPUT FILES: As input, VIE_MOD uses the previously prepared files of LEVEL0, namely the structures *sesname_scan, _parameter, _antenna and _sources.*

1. EARTH ORIENTATION: For each observation epoch, the actual Earth orientation is calculated and the transformation matrix between the terrestrial and the celestial system is prepared (eq. 2.8). The source coordinates, originally given as angles in right ascension and declination in the celestial frame, are converted to barycentric direction vectors.

2. STATION COORDINATES: At this point, a loop over all scans, respectively observing epochs, is started. In a second loop over all participating antennas, the coordinates for each station are calculated for the time of observation, as described in chapter 2.2.1.

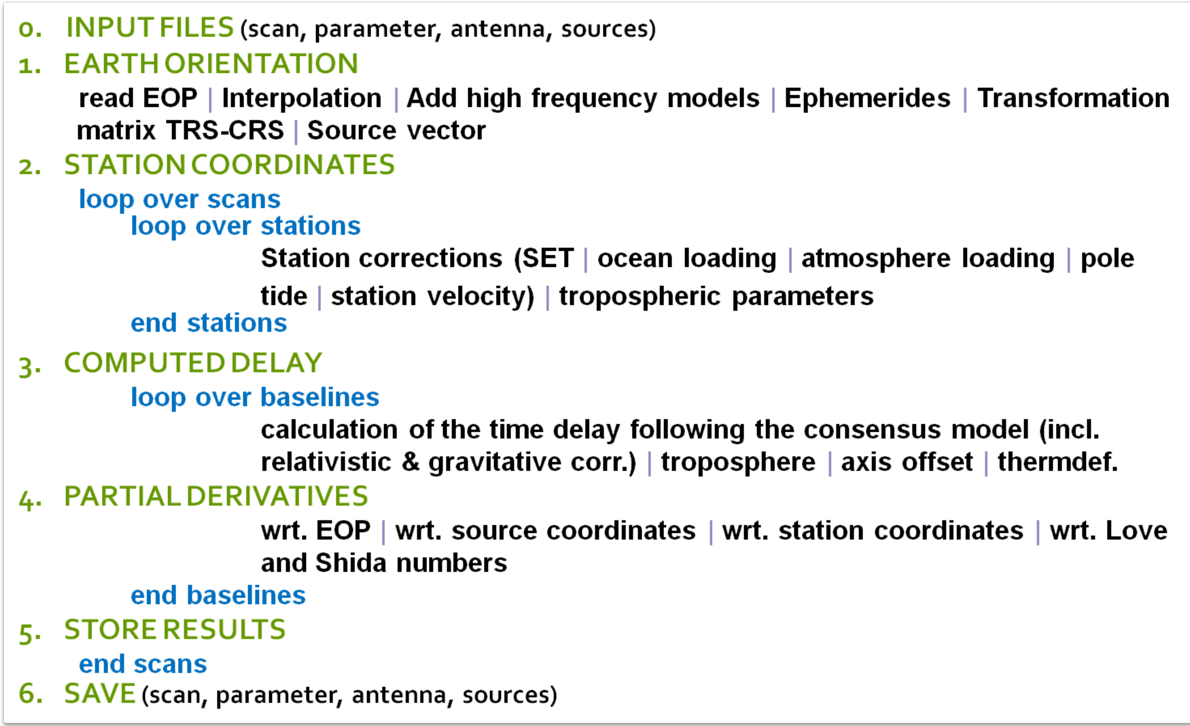

Figure 3.6: Flowchart of VIE_MOD.

3. **COMPUTED DELAY:** The theoretical delay is calculated for each observation, following the Consensus model (IERS Conventions 2010; Petit & Luzum, 2010) as described in chapter 2.2.3.

4. **PARTIAL DERIVATIVES:** The derivatives of the observable (time delay τ) after the target parameters is calculated in VIE_MOD. This is the main input to VIE_LSM. For a detailed formalism please have a look at the source code directly.

5. **STORE RESULTS:** The computed values are stored in the respective structure arrays.

6. **SAVE:** Result of VIE_MOD are the modified structures *sesname_scan, _parameter, _antenna and _sources*, which are stored in the LEVEL1 directory.

3.4.3 Reference frames

Both terrestrial and celestial reference frames can be selected in *Parameters - Reference frames*. By default a 'superstations file' is loaded which contains different reference frames, such as ITRF2005, ITRF2008, VTRF2008 and a special VieVS-TRF. Those can be chosen in the pop-upmenu. A manual TRF file can be loaded by clicking on *other*. The textfile must be put in */VieVS/TRF/*. However, it is recommended to use the superstation file (see Chapter 4.9) to include a user-own TRF. The used coordinates are stored in the *antenna* structure in LEVEL0 and LEVEL1. However, the antenna coordinates in the *antenna* structure are the catalog co-ordinates, in order to get the precise station coordinate for the time of observation, see sec. 3.4.7.

For the CRF, a co-called "supersource file" is used. From this, the chosen catalog is taken and the source coordinates in terms of right ascension and declination are stored in the *sources*

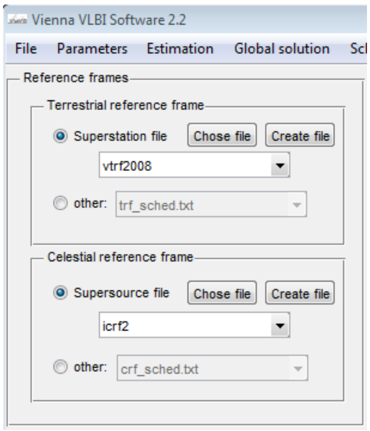

Figure 3.7: Reference frames in VieVS

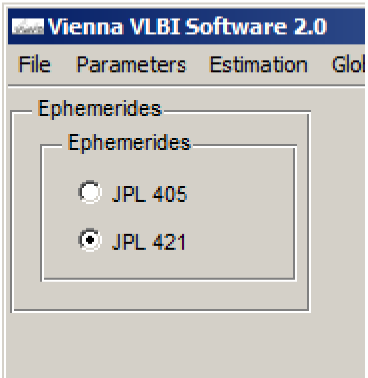

Figure 3.8: Ephemerides options in VieVS

structure. In VIE_MOD, the celestial angles are converted to a barycentric direction vector $\vec{K}$.

$$\vec{K} = \begin{pmatrix} \cos\delta \cos\alpha \\ \cos\delta \sin\alpha \\ \sin\delta \end{pmatrix} \tag{3.1}$$

This source vector is stored in the *scan* structure.
`scan(isc).space.source`

3.4.4 Ephemerides

The ephemerides contain the positions of the Earth, the Sun, the Earth's Moon the the solar system's planets. In VieVS, the planetary and lunar ephemerides DE 405 and DE 421 (Folkner *et al.*, 2008) can be used. Therefore, the files *jpl_405.mat* and *jpl_421.mat* must be available in the *VieVS/EPHEM/* directory. These files contain the Chebychev series coefficients that are distributed by the Jet Propulsion Laboratory (JPL) via plain-text (ASCII) files[1]. The GUI can be found in *Parameter - Ephemerides* with the default use of JPL 421 (3.8). However, the effect of using the different ephemerides is marginal in normal geodetic VLBI. In the processing, the function *load_eph.m* calculates the JPL ephemerides for VieVS, following the JPL guidelines and the idea of OCCAM 6.2 by O. Titov. The respective note on the Command Window is "reading_jpl_421 ephemerides". Output is the structure array *VieVS/EPHEM/jpl_421_sesname.mat*,

[1] `ftp://ssd.jpl.nasa.gov/pub/eph/planets/ascii/de421`

containing the barycentric coordinates and velocities for each observation epoch. Units are m and m/s. In addition, the GM for the planets is given in m^3/s^2. As the calculation for each observing epoch can be time consuming, the software searches for an available ephem-file by looking up the name of the session. If a file is found and the time epochs agree[2], the old file is loaded and a repeated calculation of the planetary positions is omitted. This is documented with "load existing ephemerides ..." in the Command Window.

3.4.5 Troposphere

In *Parameters - Troposphere* the user can select the models used for calculating the a priori tropospheric delay for the VLBI observations. Implemented in VieVS is a mapping function approach, where the user can calculate the hydrostatic zenith delay from (1) pressure measurement at the site *(Pressure from NGS (GPT backup))* or (2) pressure values derived from Global Pressure and Temperature *(GPT)*. The mapping functions *Vienna Mapping Function1 (VMF1)* and *Global Mapping Function (GMF)* can be selected.

In addition you can use a priori tropospheric delays. Two models are implemented: (1) APG (Böhm) and (2) DAO (MacMillan). The user can also use his/her own a priori delays by clicking *External file* and selecting the folder of the wanted files (the folders are folders in */VieVS/TRP/*). The button -> *Create* lets the user create external tropospheric files. The a

Figure 3.9: A priori troposphere parameters

[2]if, in a second run, some observations are left out, e.g. because they were marked as outliers, the time epochs changed and the ephem-file is newly created

priori hydrostatic zenith delay, $zdry$ is calculated following the Marini(?) tropospheric model.

$$zdry[m] = \frac{a1}{f1} = \frac{0.0022768 \cdot press_{stat}}{1 - 0.00266 \cdot \cos(2\phi_{stat}) - 0.28 \cdot 10^{-6} \cdot h_{ell}} \tag{3.2}$$

As described above, the hydrostatic and wet mapping functions mf_h and mf_w as well as the a priori gradient delay apr_{grd} are calculated according to the chosen model. The a priori tropospheric delay for each station, $trop$, is calculated as

$$trop[sec] = (zdry \cdot mf_h + apr_{grd})/\mathrm{c} \tag{3.3}$$

The corresponding values for each station are stored in the LEVEL1 scan structure.

```
scan(isc).stat(stnum).mfh
scan(isc).stat(stnum).mfw
scan(isc).stat(stnum).zdry [m]
scan(isc).stat(stnum).aprgrd [m]
scan(isc).stat(stnum).trop [sec]
```

Following the Consensus model (Petit & Luzum, 2010) and equations 2.21 and 2.22, the theoretical delay is corrected for the influence of the troposphere by adding the geometric part of the troposphere ($t_{g2} - t_{g1}$) and by adding the troposphere propagation delay for each station.

$$\tau = \tau + (t_{g2} - t_{g1}) + (trop_2 - trop_1) = \tau + trop_1 \cdot \frac{\vec{K} \cdot (v_2 - v_1)}{\mathrm{c}} + (trop_2 - trop_1) \tag{3.4}$$

3.4.6 Ionosphere

In VieVS the information about the ionospheric delay contained in the NGS file is used by default, but there is also the possibility of using external corrections, in this case, derived from GNSS Total Electron Content (TEC) maps.

To use the external corrections you should go to PARAMETERS/IONOSPHERE and select external file. You should also select, in the adjacent box, the folder where your external ionospheric corrections file is (Figure 3.10). Please notice that this file has to be created previously (see section 4.7).

In order to get more information about the external ionospheric file (how it looks like, how it is created...) please see section 4.7.

Please note that it is only recommended to use the GNSS corrections in case of not having observations in both S- and X-band, since the X/S ionosphere values are instantaneous direct measurements while the GNSS values suffer from low spatial and temporal resolution (Gordon, 2010)

By default, in VieVS the ionospheric correction *delion* as given in the NGS file is applied on the observed delay already in LEVEL0, when the data is read in. Alternatively, when an external file is used, *delion* = 0 and the observed delay is corrected in LEVEL1. Then, the ionospheric correction is also saved for each station.

$$\tau_{observed} = \tau_{observed} - iono \tag{3.5}$$

The data can be found in the scan structure.

```
scan(isc).obs(iobs).delion - ionosphere from the NGS file, LEVEL0
scan(isc).obs(iobs).ionDelext (optional) - LEVEL1
scan(isc).stat(stnum).iono (optional) - LEVEL1
```

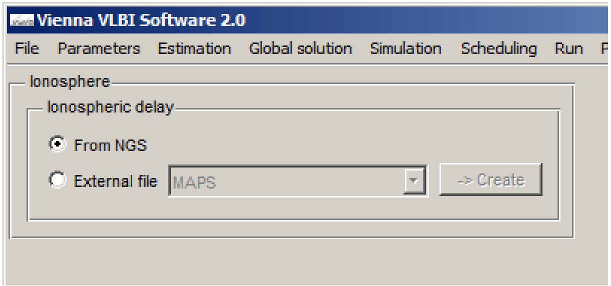

Figure 3.10: A priori ionosphere settings

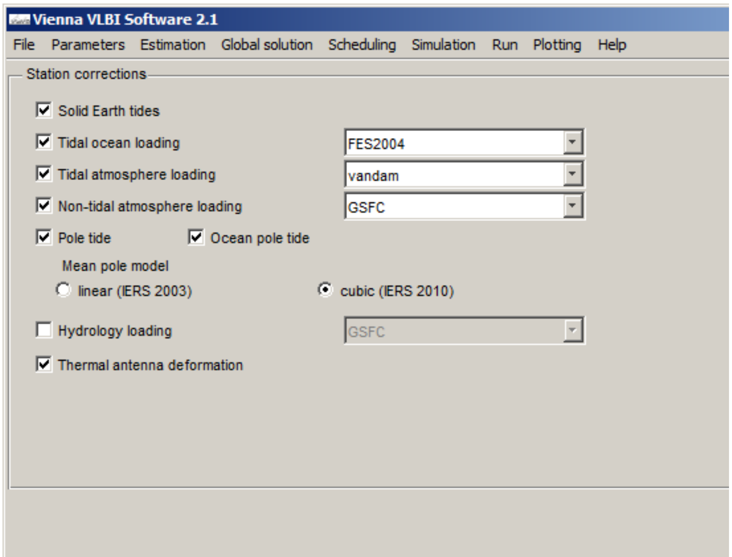

Figure 3.11: A priori station models

3.4.7 Station models

The provision of ITRF happens via tables of station coordinates, modeled linearly, which means there are coordinates $\vec{X}_0$ calculated for a certain reference epoch t_0 and the corresponding velocity $\dot{\vec{X}}$ for each station. These coordinates are calculated for regularized positions, in order to remove high frequency variations. The variations $\Delta\vec{X}_i$, predominantly of geophysical origin, are accounted for with conventional models, as described in chapter 7 of the IERS Conventions (Petit & Luzum, 2010). The instantaneous station position $\vec{X}$ at epoch t composes to:

$$\vec{X}(t) = \vec{X}_0 + \dot{\vec{X}} \cdot (t - t_0) + \sum_i \Delta\vec{X}_i. \tag{3.6}$$

All models that can be selected in the GUI according to Figure 3.11, except the correction for antenna thermal deformation (see sec. 3.4.10), are calculated for each observation epoch and are applied directly to the antenna coordinates prior to the delay calculation. Additionally, antenna eccentricities are applied. The corrected station position in the TRF as well as in the GCRF is stored in the scan structure.

```
scan(isc).stat(ist).x - corrected station position in TRS [x,y,z], [m]
scan(isc).stat(ist).xcrs - corrected station position in GCRS [x,y,z], [m]
```

3.4.8 EOP

The Earth orientation must be calculated in order to relate the terrestrial co-rotating system where the stations are given in with the space-fixed celestial system of the radio sources. In VieVS, the procedure described in chapter 5 of the IERS Conventions (Petit & Luzum, 2010) is implemented to calculate the transformation matrix for each observation epoch. Hereby, the "CIO-based" transformation concept following the Non-Rotating Origin (NRO) is chosen. Consequently, the Precession/Nutation is accounted for with the coordinates of the CIP in the GCRS, represented by the parameters X and Y. For the processing, an up-to-date time series of

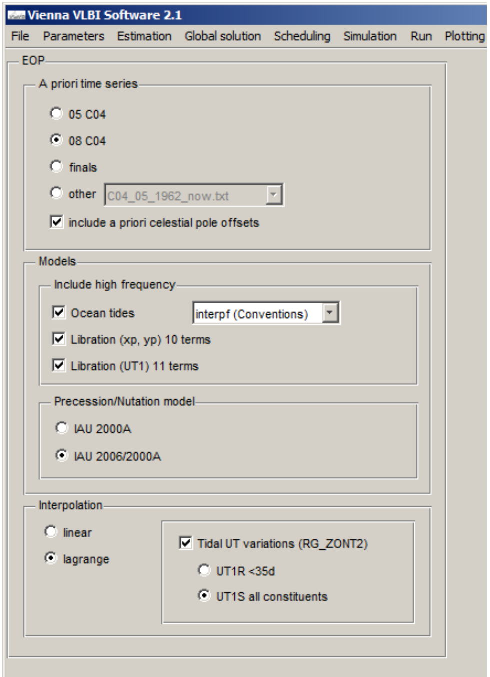

Figure 3.12: A priori EOP settings

the Earth orientation parameters (EOP) is necessary in the directory VIEVS/EOP/. As default, the C04 08 series provided by the IERS is used. However, as this series is updated with some latency, for recent sessions one might need to use the slightly less accurate *finals* EOP series. In this case, the program will crash with the error:

```
time of observation is out of your EOP time limits
please update ../EOP/C04_08_1962_now.txt !!!
```

appearing in the command window (see section A.3). When calculating the Earth orientation, leap seconds must be taken into account. The agreed time epochs when a new leap second was inserted are saved in the routine *tai_utc.m*. In order to be sure that you do not forget to update this file when a new leap second is inserted, there is an automatic warning when you process a session after the given date. What to do if the warning

```
+++ please check for new leap second TAI-UTC tai_utc.m +++
```

appears, is written in A.4.

3.4.9 Observation restrictions

By default all observation above horizon (0° elevation) and a quality code of 0 (best) are used in the analysis. However, the user can modify these two settings in *Parameters - Observation restrictions*. If all observations (not only those of best quality) should be used, type a num-

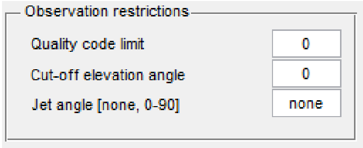

Figure 3.13: Quality code, minimum elevation angle settings and source structure exclusion criterion

Figure 3.14: Settings for source structure correction

ber ≥ 9 into the textfield *Quality code limit*. The input cut-off elevation angle is in unit of degree. Additionally the user can decide to exclude observations with certain jet angles. If no observations should be exculded, type *none* into the corresponding checkbox.

3.4.10 Antenna deformation

The computed delay is corrected for errors due to antenna thermal deformation. The corresponding code can be found in the subroutine */VIE_MOD/thermdef.m*, follwoing (Skurikhina (2001); Haas (1999), Nothnagel (2009)). The parameters for each station are stored in the superstation file, as read in from the *antenna-info.txt* file.

3.4.11 Axis offsets

The additional delay due to the axis offset is calculated in the subroutine */VIE_MOD/axis-stat.m*. The axis offset parameter for each antenna needs to be stored in the superstation file.

3.4.12 Source Structure

First select the source structure catalog you would like to use. Catalogs are saved in *VieVS/-CRF/SOURCE_STRUCTURE_CAT/*. Then you can decide if you want to apply the correction and/or calculate and write the jet angles to *VieVS/DATA/JETANG/*.

3.5 Estimation

In the tab *Estimation*, parameters for the estimation process can be selected. The current version supports parameter estimations with the least squares adjustment (LSM). One of our aims is to develop a Kalman Filter as second parameter estimation algorithm. It has not been implemented yet. For the estimation of a global solution the N matrix has to be prepared with the LSM module (menu item *Global parameters*), see Chapter 3.6 for more information on global solutions. The corresponding source code can be found in VIE_LSM.

3.5.1 Overview of VIE_LSM

The VIE_LSM module was designed by Kamil Teke in the course of his Ph.D. thesis. This section provides a brief discussion of the module and its implementation into VieVS. For further detail see (Teke, 2011). The VIE_LSM module takes care of the parameter estimation process with the least squares method. All the parameters can be estimated as continuous piece-wise linear offsets (CPWLO) in sub-daily and daily temporal resolution. Pseudo observations (constraints) can be introduced to the estimation process. We distinguish between two types of constraints, namely relative and absolute. Relative constraints are used to fill gaps where two parameters have no observation in an estimation interval. Additionally they provide supplementary observations which keep the normal equation matrix N regular. Absolute constraints are used if the preferred value of the parameter is known (e.g. fixing it to the a priori value). A detailed description of the theory can be found in Chapter 2.3.

The design matrix A_{ro} given in Equation 2.29 is formed by 15 sub-matrices,

$$A_{ro} = [A_1\ A_2 \dots A_{15}]. \tag{3.7}$$

The used models are:

- CPWLO of clocks (A_1),
- rate and quadratic terms of polynomials of clocks (A_2),
- CPWLO of zenith wet delay (A_3),
- CPWLO of troposphere north gradients (A_4),
- CPWLO of troposphere east gradients (A_5),
- CPWLO of polar motion coordinates in TRF along the Greenwich meridian (*xpol*) (A_6),
- CPWLO of polar motion coordinates in TRF along 270° east meridian (*ypol*) (A_7),
- CPWLO of Earth's rotation phase (dUT1) (A_8),
- CPWLO of celestial intermediate pole (CIP) coordinate in CRF (X) (A_9),
- CPWLO of celestial intermediate pole (CIP) coordinate in CRF (Y) (A_{10}),
- CPWLO of right ascensions of source in CRF (A_{11}),
- CPWLO of declinations of sources in CRF (A_{12}),
- CPWLO or one offset (optional) of VLBI antenna X coordinate in TRF (A_{13}),
- CPWLO or one offset (optional) of VLBI antenna Y coordinate in TRF (A_{14}),
- CPWLO or one offset (optional) of VLBI antenna Z coordinate in TRF (A_{15}).

3.5.2 Troposphere

The estimation settings for the troposphere can be found in *Estimation - Least squares - Troposphere*, a screen shot of the GUI is depicted in Figure 3.15. We usually estimate the zenith wet delay and north and east gradients. Both are estimated as CPWLO, intervals and constraints can be selected in the GUI. If nothing is changed the predefined default values are used.

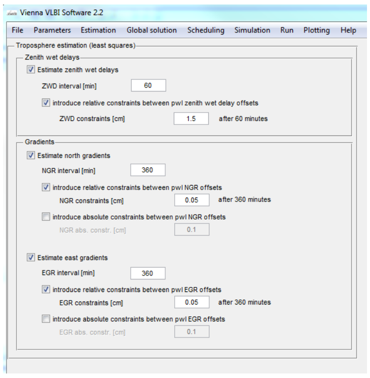

Figure 3.15: Estimation parameters for the troposphere

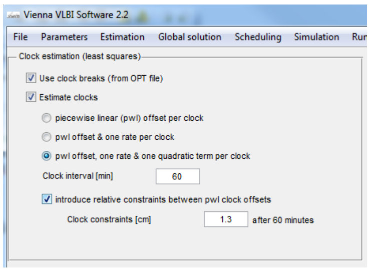

Figure 3.16: Estimation parameters for clocks

3.5.3 Clock

Estimation settings for clock parameters can be found in *Estimation - Least squares - Clock*. A screen shot of the GUI is depicted in Figure 3.16. One can specify if clock breaks from an OPT file (see Chapter 3.3.5) should be used.

In order to estimate clock errors a reference clock has to be selected. The clock of the first station in the *_antenna* file is chosen as default. One can specify any other clock as reference in the OPT file, see Chapter 3.3.5. The deviation of the other clocks w. r. t. the reference clock is then modeled according to the selection of the user. The CPWLO for each clock at each UTC integer hour or any other user defined interval (t_1 and t_2) is modeled according to:

$$\Delta\tau_{clk}^{CPWLO}(t) = x_1 + \frac{t - t_1}{t_2 - t_1}(x_2 - x_1) \tag{3.8}$$

and the quadratic polynomial term is estimated with:

$$\Delta\tau_{clk}^{poly}(t) = \beta_0 + \beta_1(t - t_0) + \beta_2(t - t_0)^2. \tag{3.9}$$

The total clock error at the epoch t is the summation of the CPWLO for each clock and the quadratic polynomial term for each clock:

$$\Delta\tau_{clk}(t) = \Delta\tau_{clk}^{CPWLO}(t) + \Delta\tau_{clk}^{poly}(t). \tag{3.10}$$

Relative constraints can be introduced by the user.

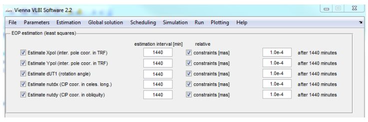

Figure 3.17: Estimation parameters for EOP

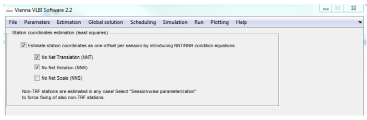

Figure 3.18: Estimation parameters for station coordinates

3.5.4 Earth orientation parameters

The settings of the EOP estimation can be changed in *Estimation - Least squares - EOP*. A screen shot of the GUI is depicted in Figure 3.17 It is possible to estimate EOP (with the CPWLO method) in any given interval with specified constraints. One can fix the EOP to the a priori values by ticking off the parameters respectively.

3.5.5 Station coordinates

The settings for station coordinate estimation can be found in *Estimation - Least squares - Station coordinates*.

To specify the datum of the network one has to define the origin and orientation of the coordinate system. This can either be done by fixing station coordinates to their a priori (TRF) values or by introducing the no-net-translation (NNT) and no-net-rotation (NNR) conditions. To fulfill the NNT condition the three translations are constrained to zero. The NNR condition is fulfilled when all three rotations are constraint to zero. The common approach for VLBI estimation is to use the NNR and NNT approach, as depicted in Figure 3.18. The no-net-scale (NNS) condition (constraining the scale to 1) is usually not used for VLBI parameter estimation.

Coordinates are estimated daily. The Estimation of sub-daily antenna TRF CPWLO coordinates with NNR/NNT conditions is not yet implementes in VIE_LSM.

3.5.6 Source coordinates

VieVS is able to estimate source coordinates. The settings can be found in *Estimation - Least squares - Source coordinates*. Estimation interval and relative constraints can be selected in the GUI, see Figure 3.19. By default the estimation of source coordinates is not selected.

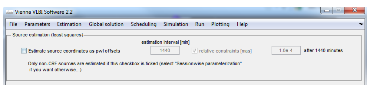

Figure 3.19: Estimation parameters for source coordinates

3.6 Global parameter estimation (vie_glob)

3.6.1 Introduction

Module Vie_GLOB has been designed and written by Hana Krásná in connection to her Ph.D. thesis. It has the capability to estimate parameters which are common to all VLBI sessions from a so-called global solution, i.e. from a common adjustment of many VLBI sessions. The input data for Vie_GLOB are datum-free normal equations (NEQ) prepared by the module Vie_LSM. The global solution is typically used to determine TRF in terms of station positions and velocities, and the CRF in terms of radio source coordinates.

3.6.2 Input data

For each session there are 3 files: (* denotes name of the session, i.e. 10JAN04XA_N004)

- *_an_glob.mat (in Vie_GLOB the name of this matlab structure is glob1) a priori station coordinates and velocities used for analysis in this session + information about discontinuities
- *_Nb_glob.mat (glob3) datum free normal matrix $N = A^TPA$ and right-hand side vector $b = A^TPl$
- *_par_glob.mat (glob2) glob2.x - information about columns, where the parameters are stored. It also contains estimates from the single session adjustment with Vie_LSM. glob2.opt - information about options, which were chosen for the analysis with VieVS and for preparation of the LEVEL2 data.

3.6.3 Program

The computational strategy of Vie_GLOB follows several steps. First, information from all sessions is read to detect all parameters which are contained in the input normal equations. Because of limited computer memory capacity, and due to time consumption, it is essential to keep the equation system small. Therefore only parameters of interest for the global solution are kept in the session-wise NEQ and the remaining parameters are either fixed to their a priori values or reduced from the equations. This can be specified in the GUI, see Figure 3.21. The reduction takes place for parameters which appear in only a single session and are dependent on a finite amount of time. These are, for example, the clock parameters, zenith wet delays or tropospheric gradients which can vary by several hours. The reduction means an implicit estimation of such parameters from the session-wise NEQ by a least squares adjustment. The global parameters are detected in the NEQ taken from single sessions, and a new reference number is assigned to each parameter. In the second step of Vie_GLOB the NEQ are reorganized following the new order of parameters (columns/rows in normal matrix and rows in normal vector) and stacked together with the reorganized NEQ from other sessions. This leads to one common global normal matrix which consists of the global parameters only. In the third step conditions (like no-net-rotation and no-net-translation on TRF or no-net-rotation on CRF) and eventually constraints are applied (see Figure 3.22 for GUI settings), and by a final inversion of the NEQ system the estimates of the global parameters are obtained. In a usual run of Vie_GLOB where we are only interested in the global parameters (e.g. in a new reference frame) the analysis stops at this stage. However, if we are also interested in the solution for parameters which have been session-wise reduced, a backward solution has to be carried out. This means that the residuals estimated for the global parameters are taken and substituted into the reduced equation going step by step always one level up.

Directory	Description
VDG/CRF/DATUM/	arbitraryname.txt files with source names, which will be used for an NNR condition
VDG/CRF/FIXED_SOURCES/	arbitraryname.txt files with source names, which will be fixed to their a priori coordinates (i.e. they will be not involved in the adjustment)
VDG/CRF/REDUCE/	arbitraryname.txt files with source names, which position will be session-wise reduced
VDG/TRF/DATUM/	arbitraryname.txt files with station names, which will be used for an NNT/NNR condition
VDG/TRF/DISCONT/	arbitraryname.mat files with station names describing the VLBI position discontinuities. The original VLBI-DISCONT.txt file is provided at the web site http://vlbi.geod.uni-bonn.de/IVS-AC/data/VLBI-DISCONT.txt (vlbi_discont.mat is provided within vie_glob and at least one file must be in the ../DISCONT/ directory (also if station coordinates are not estimated))
VDG/TRF/REDUCE/	arbitraryname.txt files with station names, which position will be session-wise reduced. Their velocity will be fixed to the a priori value
VDG/TRF/VELOC/	arbitraryname.txt files with station names, at which a position discontinuity happened, but we want to estimate a constant velocity for all intervals
VDG/TRF/VELOC/TIES/	arbitraryname.txt files with station names in a special format: names of antennas (8 character for each), the line has to end with "\\". Velocity ties will be introduced to stations at one line and the same velocity will be estimated for them.
VieVS/OUT/GLOB/*.m	Matlab function backward_solution.m estimates after the global adjustment the session-wise reduced parameters. The plot_backward_*.m functions plot the time series of the session-wise estimated parameters (= output of backward_solution.m)
VieVS/OUT/GLOB/	directories / mat. files are for outputs - data will be automatically written into them

Table 3.1: Description of the external files needed for Vie_GLOB. VDG = VieVS/DATA/GLOB

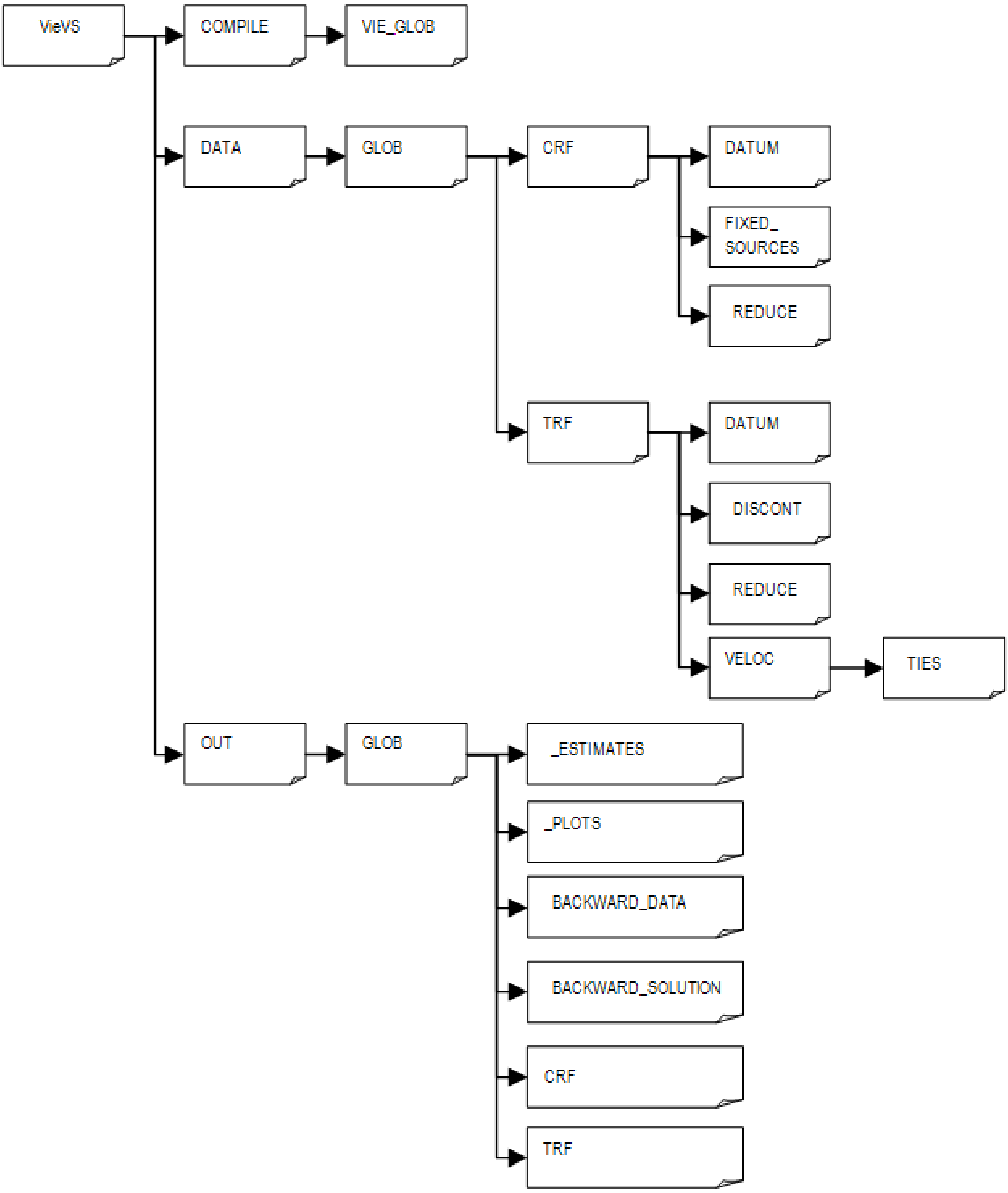

Figure 3.20: Structure of Vie_GLOB in VieVS directories.

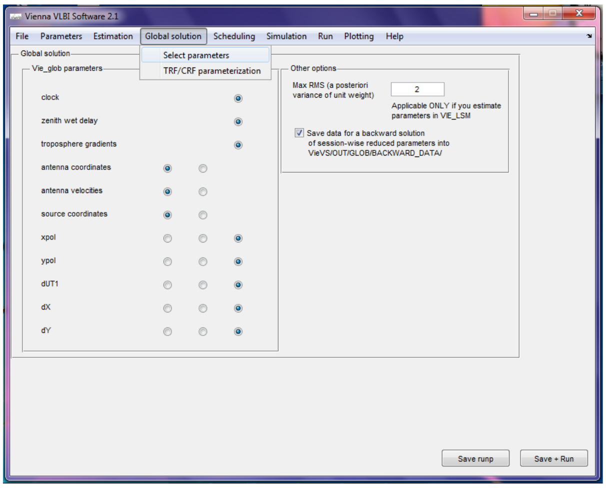

Figure 3.21: GUI of Vie_GLOB - reduction of parameters.

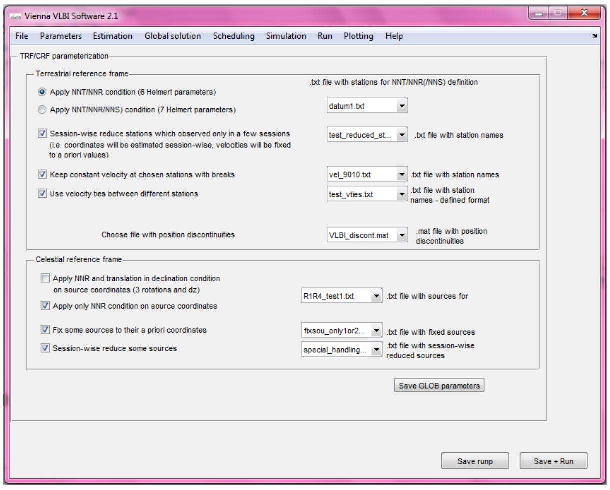

Figure 3.22: GUI of Vie_GLOB - TRF/CRF settings.

Reduction and stacking of parameters

The reduction of parameters is based on a division of the normal equation system into two parts. In the first part those parameters are concentrated, which will be kept in the global matrix, and in the second part parameters are ordered, which will be estimated only from a single session:

$$\begin{bmatrix} N_{11} & N_{12} \\ N_{21} & N_{22} \end{bmatrix} \cdot \begin{bmatrix} dx_1 \\ dx_2 \end{bmatrix} = \begin{bmatrix} b_1 \\ b_2 \end{bmatrix}. \tag{3.11}$$

The matrix equation (3.11) corresponds to the following two coupled equations:

$$N_{11} \cdot dx_1 + N_{12} \cdot dx_2 = b_1, \tag{3.12}$$

$$N_{21} \cdot dx_1 + N_{22} \cdot dx_2 = b_2. \tag{3.13}$$

From equation (3.13) vector dx_2 can be expressed containing the reduced parameters:

$$dx_2 = N_{22}^{-1} \cdot b_2 - N_{22}^{-1} N_{21} \cdot dx_1 \tag{3.14}$$

and substituted into equation (3.12):

$$N_{11} \cdot dx_1 + N_{12} N_{22}^{-1} \cdot b_2 - N_{12} N_{22}^{-1} N_{21} \cdot dx_1 = b_1, \tag{3.15}$$

$$(N_{11} - N_{12} N_{22}^{-1} N_{21}) \cdot dx_1 = b_1 - N_{12} N_{22}^{-1} \cdot b_2, \tag{3.16}$$

$$N_R \cdot dx_1 = b_R. \tag{3.17}$$

The reduced N matrix N_R and the reduced b vector b_R are than "stacked" with reduced normal equation systems from other sessions and a global N matrix N_G and a global b vector b_G is created. Attention has to be paid so that the order of parameters is identical in the reduced normal equation systems:

$$\begin{aligned} N_G &= N_{R1} + N_{R2} + N_{R3} + \cdots, \\ b_G &= b_{R1} + b_{R2} + b_{R3} + \cdots. \end{aligned} \tag{3.18}$$

The final solution for the global parameters is done using an inversion of the global normal equation system:

$$dx_G = N_G^{-1} \cdot b_G. \tag{3.19}$$

The estimates of the session-wise reduced parameters can be obtained by substituting the vector dx_G into the equation (3.14), where $dx_1 = dx_G$ and thus contains the globally adjusted parameters. It is obvious that one has to store the matrices N_{22}, N_{21} and vectors b_2 of each session. To obtain the time series of the reduced parameters from all sessions it should be started with the reduced normal equation of the last session and then continued in a "backward direction" always one level up (Gipson, 1998).

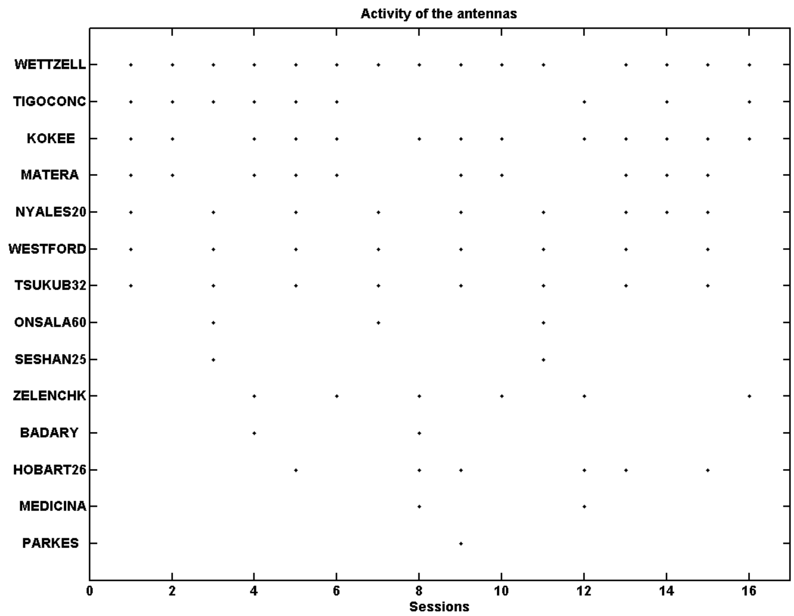

Figure 3.23: Stations in sessions included in the global adjustment.

3.6.4 Output data

Output figures

saved in VieVS/OUT/GLOB/_PLOTS/TEST_OUT (source code for saving the figures is at the very end of the main program Vie_GLOB.m)

Figure 3.23 shows stations in sessions included in the global adjustment. It is created with the function plot_antactiv.m. It is stored in
VieVS/OUT/GLOB/_PLOTS/TEST_OUT/ant_activity_TEST_LEVEL2.eps

Figure 3.24 shows the map with all stations included in the global adjustment. Blue circles denote stations included in the NNT/NNR condition, red circles show stations excluded from the NNT/NNR condition. It is created with the function plot_ant.m. It is stored in
VieVS/OUT/GLOB/_PLOTS/TEST_OUT/ant_map_TEST_LEVEL2.eps

Figure 3.25 shows sources in sessions included in the global adjustment. It is created with the function plot_souactiv.m. It is stored in
VieVS/OUT/GLOB/_PLOTS/TEST_OUT/sou_activity_TEST_LEVEL2.eps

Figure 3.26 shows the map with all sources included in the global adjustment. Blue circles denote sources included in the NNR condition, red circles are sources excluded from the NNR condition. Sources which were fixed to their a priori coordinates are not shown. It is created with the function plot_sou.m. It is stored in
VieVS/OUT/GLOB/_PLOTS/TEST_OUT/sou_map_TEST_LEVEL2.eps

Results

Estimates are stored in VieVS/OUT/GLOB/_ESTIMATES/TEST_OUT/
- in Matlab format: globsol_TEST_LEVEL2.mat
- in TXT format: glob_results_TEST_LEVEL2.txt

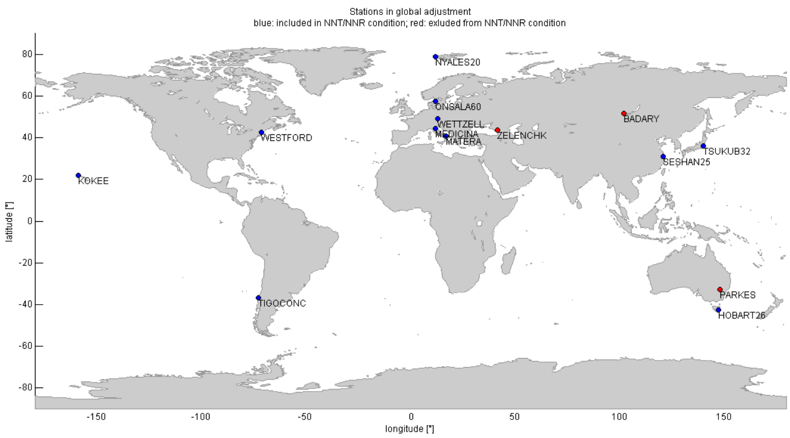

Figure 3.24: Map of stations included in the global adjustment.

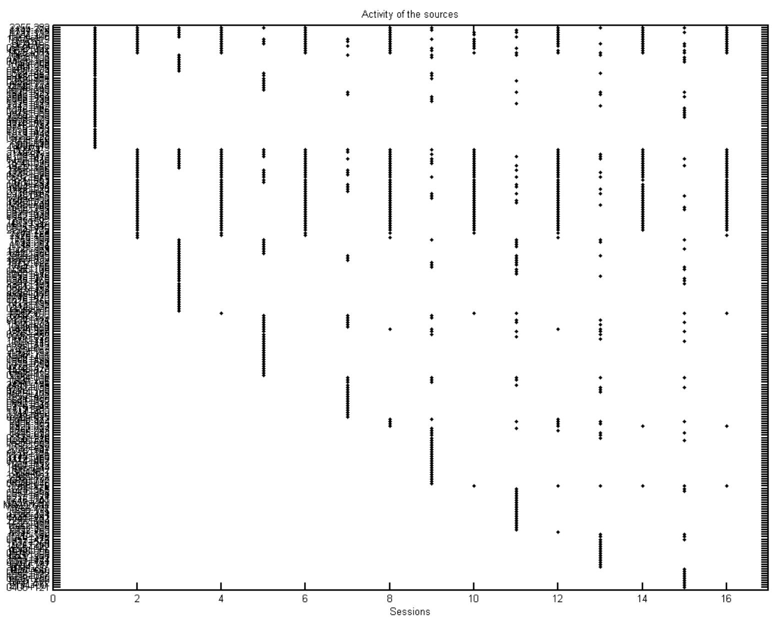

Figure 3.25: Sources in sessions included in the global adjustment.

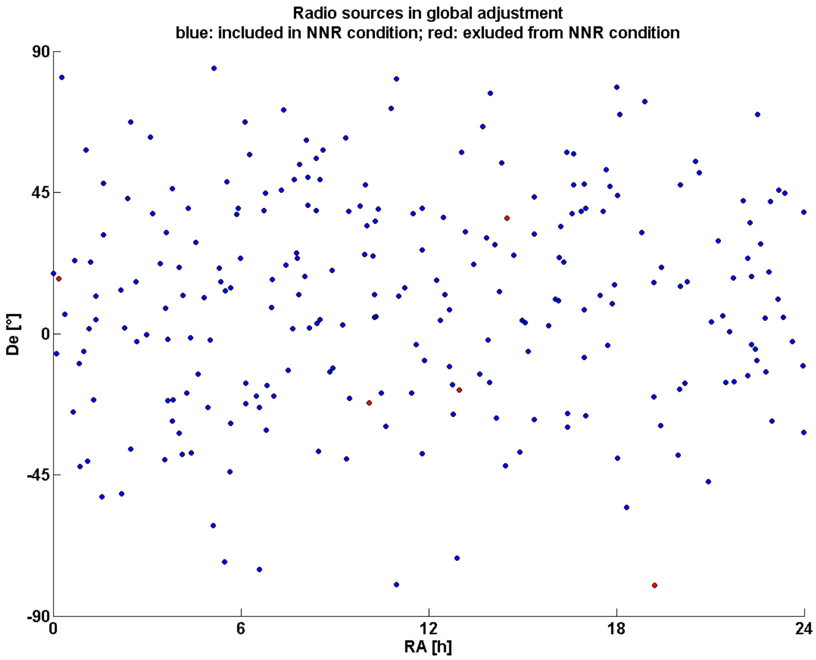

Figure 3.26: Map of sources included in the global adjustment.

3.7 Scheduling

3.7.1 Overview of VIE_SCHED

Scheduling is the first step in preparation for a VLBI experiment. VIE_SCHED is a module in VieVS which helps you to prepare schedules for VLBI observing sessions automatically. VIE_SCHED is normally used for geodetic VLBI sessions.

The structure of VIE_SCHED within VieVS is shown in Figure 3.27. In the *VieVS/CATALOGS/* directory, all input files consisting of catalog system files and local control files are located. The source code of VIE_SCHED is saved in the *VieVS/COMPILE/VIE_SCHED_V21/* folder. The 'V21' indicates the version of VIE_SCHED. During the scheduling some temporary files are created and stored in the *VieVS/DATA/LEVEL5/* folder, which can be used for troubleshooting when an error occurs. The output scheduling files are written into the *VieVS/DATA/SCHED/* folder. To keep the station position consistent for the scheduling, simulation and estimation process, a *trf_sched.txt* file is created by copying the station positions out of the *position.cat* file. The file is saved into the *VieVS/TRF/* directory.

3.7.2 Input files

All the input files of VIE_SCHED are located in the *VieVS/CATALOGS/* directory, which consist of catalog system files (*.cat* files) and local control files (*.txt* files). The directory (path for the input files) and file names are fixed in VIE_SCHED and should not be changed.

Catalog system files

VIE_SCHED reads catalog system files for the selection of sources, stations, and observing modes when creating a schedule for a VLBI experiment. The catalog system files are ASCII files con-

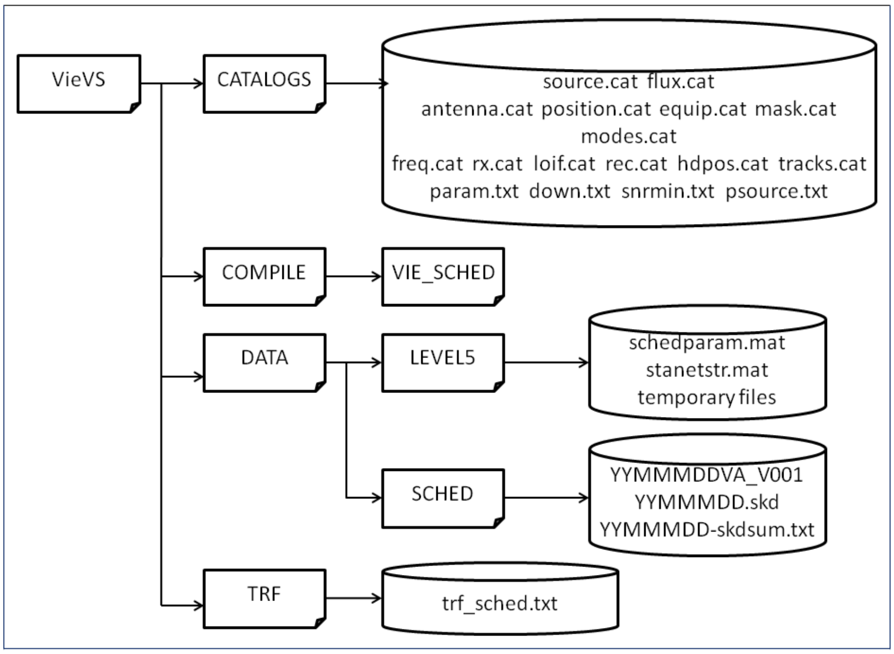

Figure 3.27: The structure of VIE_SCHED within VieVS.

trolled and maintained at the Goddard Space Flight Center (GSFC) and are available via an anonymous ftp (*ftp://gemini.gsfc.nasa.gov/pub/sked/catalogs/*). The catalog files on the server contain only up-to-date information on sources, antennas, and equipments. These files should be updated by copying the latest versions via ftp to your local *VieVS/CATALOGS/* directory whenever a change is announced. The information on the catalog files and the fields therein are described in the documentation which can be found at: *ftp://gemini.gsfc.nasa.gov/pub/sked/docs/*. Table 3.2 lists all the catalog files and their contents. The VIE_SCHED program can be either run for simulation research or real VLBI experiment. The last column in Table 3.2 lists the designated use of each catalog file.

For simulation studies, the catalog files might need to be extended by virtual stations at different locations and of different quality (station specifications). The task of editing the catalog file should be given great care, since the catalog file are connected and there are cross references to other catalogs within some of the catalog files. Matching is done by name or by code which is required to be unique within a file. Therefore the order of the entries is not relevant. To change some catalog entries for real VLBI experiments, we refer to the catalogs manual for detailed format descriptions.

The next section outlines how to change information on sources, stations, and observing modes for simulation research.

(1) How to change information on sources.

The IAU names (and other common names) in the *source.cat* file are used to find matching entries in the *flux.cat* file. To change the list of available sources, one has to edit the *source.cat* file. Source names refer to the given IAU names (and other common names) and positions are defined in right ascension and declination. Then edit the *flux.cat* file to enter the source fluxes and models with matching names. If you make a change in the *source.cat* file or the *flux.cat* file, you must delete the current source.mat file (located in *VieVS/DATA/LEVEL5/*) before running VIE_SCHED. Then the new information on sources can be read and used by

Table 3.2: Catalog system files.

Type	File Name	Contents	Used for
Sources:			
	source.cat	source positions	simu + real
	flux.cat	source fluxes	simu + real
Stations:			
	antenna.cat	antenna information	simu + real
	position.cat	station x,y,z locations	simu + real
	equip.cat	equipment IDs	simu + real
	mask.cat	horizon and coordinate masks	simu + real
Observing modes:			
	modes.cat	observing modes	simu + real
	freq.cat	frequency sequences	real
	rx.cat	receiver setups	real
	loif.cat	station LO and IF setups	real
	rec.cat	recording modes	real
	hdpos.cat	head offsets	real
	tracks.cat	standard recorded tracks	real

VIE_SCHED, otherwise the old information on sources saved in the *source.mat* file will be loaded into VIE_SCHED. If no flux value is available for a given source, the source will not be used for the schedule.

(2) How to change information on stations.

VIE_SCHED reads the antenna names in the *antenna.cat* file to find the corresponding entries in the *position.cat*, *equip.cat*, and *mask.cat* catalog files. Since the four catalogs are linked by the antenna name it must be unique in each catalog. You can edit the ASCII catalog files and change the parameters following the original version. If you want to comment (e.g. before or after your new/revised entry to indicate what you changed and why) use '*' at the beginning of the line. To add a new station locally, you need the steps below to make sure all of the necessary catalogs and important parameters are updated.

Step 1: Edit the *antenna.cat* file to add the new antenna information including the 8-character antenna name, axis type, slewing rate, constant, and limits for axis. In the current version, two kinds of axis type (AZEL and HADC) can be processed in VIE_SCHED. For the other axis types the user has to transform the antenna parameters correspondingly.

Step 2: Edit the *position.cat* file to enter the new position using the same antenna name. Geocentric XYZ coordinates of the site will be used in VIE_SCHED, while latitude and longitude are ignored.

Step 3: Create a new entry in the *equip.cat* file. The SEFD information of stations will be used to calculate the scan length automatically.

Step 4: Create a new entry in the *mask.cat* file if the station has a horizon mask. This step is not necessary for the scheduling procedure.

If there are missing values for an antenna, this antenna will be excluded from the schedule and VIE_SCHED will issue a warning message and proceed. Hence care has to be taken to ensure that the antenna parameters are complete.

(3) How to change information on observing modes.

All the possible observing modes for scheduling are listed in the *modes.cat* file. You can edit an existing entry or insert a new observing mode, but the mode name is fixed to be 'VLBI2010obsmodes' in VIE_SCHED. Be careful that the number of channels, sample rate, and 1 or 2 bit quantification are specified for this observing mode, which will be used for the calculation of the scan length. The completeness of the information on observing modes is checked at the beginning of the scheduling. VIE_SCHED will not continue if the observing mode is not complete.

Local control files

Besides the catalog system files, four local control files are read and used by VIE_SCHED. Out of the four files described below, only the *param.txt* file is a required input for VIE_SCHED, while the other three are optional and are only included if they are needed.

(1) *param.txt* file

VIE_SCHED automatically chooses scans using a rule-based approach. The major selecting options such as the network, session time, scheduling strategy (source-based strategy or station-based strategy) can be specified in GUI of VIE_SCHED. The various minor scheduling parameters are listed and set by the user in the *param.txt* file. For example, generally speaking, you do not want to observe the same source twice in a short interval. This leads to a rule saying "don't observe a source if it has been observed in the last X minutes", where X can be set by the user in the *param.txt* file. Table 3.3 presents an overview of each of the minor scheduling options and a brief description.

(2) *down.txt* file

Frequently a station is unavailable for some part of the session. The most common, although not the only, reason is that it is participating in an intensive session. The *down.txt* file is used to indicate when some stations are unavailable for observing during a session. The scheduler specifies an interval when a station or subnet is unavailable ("down"), and VIE_SCHED will automatically ignore these stations during this interval. A station can have multiple downtimes in a schedule.

(3) *snrmin.txt* file

The minimum SNR targets for all stations are specified on the GUI of VIE_SCHED. In practice, some antennas are weaker, i.e. larger SEFD, so they will be given a lower minimum SNR target on all baselines involving this single station by band. The *snrmin.txt* file, if present, overrides the values from the GUI.

(4) psource.txt file

As it is said above, VIE_SCHED is developed for geodetic VLBI experiments. On the other side, we are always observing new sources or particular sources with the VLBI technique. The *psource.txt* file is used to list the astrometric sources and set the observation density target.

3.7.3 Output files

The output of VIE_SCHED, can generate standard NGS files for simulation and schedule files (.skd) for real VLBI experiment, which can be found in VieVS/DATA/SCHED/. You can create the different types of outputs by setting the options on the GUI to meet your requirements. Additionally, a summary file (*skdsum.txt*) can be created, it is written in the *VieVS/DATA/SCHED/* directory where you can get a preliminary evaluation of many aspects of the schedule. In *VieVS/TRF/*, the *trf_sched.txt* file is saved. It contains the station positions used for scheduling.

Table 3.3: Minor scheduling options.

Option	**Description**
PARA.WAVEL(1)	Wavelength of the X band [meter]
PARA.WAVEL(2)	Wavelength of the S band [meter]
PARA.RATE1A	Acceleration of the AZ/HA axis [deg/s^2]
PARA.RATE2A	Acceleration of the EL/DC axis [deg/s^2]
PARA.MARGEL1	Marge for the AZ/HA axis [deg]
PARA.MARGEL2	Marge for the EL/DC axis [deg]
PARA.MIN_SRCRP	The interval which specifies that the same source will not be observed twice [min]
PARA.SOURCE	Time for the antenna to settle down after slewing and before observation start time [sec]
PARA.TAPETM	Time for the tape after slewing and before observation start time [sec]
PARA.IDLE	Time allowed for idling after slewing and before observation start time [sec]
PARA.CALIBRATION	Time allowed for calibration after slewing and before observation start time [sec]
PARA.MAXSLEWTIME	Maximum time to allow an antenna to slew [sec]
PARA.MAX_WAIT	Maximum time to wait for a slow antenna [min]
PARA.CORSYNCH	Time to allow the correlator to synchronize tapes [sec]
PARA.MAX_SCAN	Maximum allowable scan time [sec]
PARA.MIN_SCAN	Minimum allowable scan time [sec]
PARA.FILLINMODE	Use fill-in mode (1/0)
PARA.FILLENDT	Maximum time for the end time of fill-in scan [min]
PARA.SCREEN	Print processing information on screen (1/0)
PARA.MIN_STANUM	Minimum subnet scheduled at one time
PARA.MIN_SRC2ANG	Minimum angle between two sources observed simultaneously [deg]
PARA.SKYDT	The interval for calculation of sky coverage [min]
PARA.EXPER	Experiment code
PARA.DESCRIPTION	Description of the experiment
PARA.SCANDURA	The default scan length [sec]
PARA.TRACKSMODE	The formatter mode

(1) In the output NGS file, the delay observations are set to zero in the data cards. The VieVS simulation package (VIE_SIM) is able to read the empty NGS file directly, which provides a convenient way to connect scheduling with simulation and provides feedback on the quality of the schedule.

(2) The schedule file with a *.skd* extension is simply an ASCII file with different labeled sections. It contains a complete description of the session, the schedule, and the additional information needed to conduct the experiment for the complete network of stations and correlators. The naming convention for IVS schedule files is 'experiment code.skd'. The experiment code is listed in the master file (*DATA/MASTER*). After you generate your schedule, the *.skd* file is copied to a central server location where the participating stations can access it electron-

ically. The stations download the file and then run the Field System program drudg to create control files and listings for the experiment.

3.7.4 Create schedules

After starting Matlab you should make the *VieVS/WORK/* directory your current folder. Typing “VieVS”in the Matlab command window starts the interface of the latest version of VieVS. After you select the *Scheduling* menu label on the top of the interface, the interface of VIE_SCHED appears (see Figure 3.28).

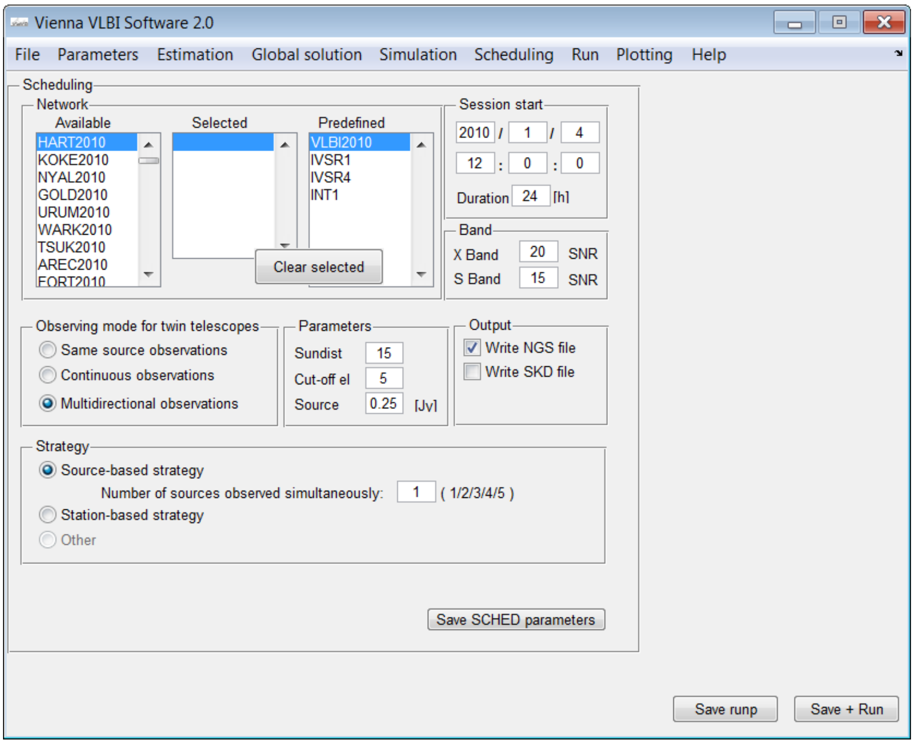

Figure 3.28: VIE_SCHED graphical user interface (GUI).

Here you can:

- Select the stations or use a predefined network. VIE_SCHED put the station names of all the entries in *antenna.cat* into the listbox of *Available*. During the process of selecting stations you can add or remove stations from this list.
- Change the start times of the session and its duration.
- Set the SNR targets.
- Specify the observing mode for twin telescopes if there are twin telescopes in the network.
- Give the three basic parameters for scheduling (minimum angle distance to the Sun, cut-off elevation angle, minimum flux of source over all baselines).
- Specify the type of output file (NGS file or SKD file).
- Specify the strategy used for scheduling.

For a real VLBI experiment, the master file is the usual starting point for setting up a schedule. The master file (*DATA/MASTER*) is a table that lists all geodetic and astrometric sessions within the IVS. All IVS sessions have a unique experiment code associated with it. In addition to the session code, it includes the date of the session, the duration, the institution responsible for scheduling the session, the correlator, and other information.

To create the schedule go to *Run - Run options* and select the *Run vie_sched* checkbox. Make sure that every other checkbox is deselected if you don't want the corresponding module to run. Pushing the *Save+Run* button starts VIE_SCHED.

After announcing itself, VIE_SCHED reads all the input files and summarizes what it finds. VIE_SCHED will automatically select scans to fill up the schedule from the start time to the end time. One can find detailed information on the scheduled scans in the command window when VIE_SCHED is running. Experienced users can use those messages for judging its running status or for debugging purposes. At the very end VIE_SCHED finishes with the ending time information.

3.8 Simulation

3.8.1 Overview of VIE_SIM

With the VieVS simulation module (VIE_SIM) simulated VLBI observables are generated, taking into account the three most important stochastic error sources in VLBI (additionally the simulation of source structure was added later on). VIE_SIM sets up the o-c vector (observed minus computed) of the least-squares adjustment at each epoch. The artificial observations from the VieVS simulator (VIE_SIM) are then transformed to databases in NGS format.

Group delay observables are calculated containing the following four main stochastic error sources in VLBI: The wet troposphere delay, the station clock error, the measurement noise and the source structure (see Equation 3.20). The wet troposphere delay has the largest impact on the error.

$$o - c = (wzd_2 \times mfw_2(el) + clock_2) - (wzd_1 \times mfw_1(el) + clock_1) + ss + wn. \tag{3.20}$$

$wzd_{1,2}$ and $clock_{1,2}$ are the simulated zenith wet delays and clock values at the station 1 and 2 and $mfw_{1,2}(el)$ are the corresponding wet mapping functions for the elevation angles el which are assumed to be error-free. The source structure (ss) and the white noise (wn) is added per baseline.

3.8.2 Input files

NGS file

You can select the sessions to be simulated in the GUI (*File - Set input files*), e.g. from the *VieVS/DATA/SCHED*, *VieVS/DATA/NGS* or *VieVS/DATA/SIM* folder.

Simulation parameters file

The input simulation parameters file is located in the *VieVS/DATA/TURB* folder. It contains station names (8 characters), the refractive index structure constant [10^{-7}m$^{-1/3}$], the effective height of wet troposphere [m], components of the wind vector [m/s], the a priori zenith wet delay [mm], the correlation interval [m], the step width for the numerical integration [m], the clock Allan Standard Deviation and the white noise [ps].

3.8.3 Output files

The simulated NGS files are stored in the *VieVS/DATA/SIM/year* directory. In *DATA/LEVEL4/your_dir* you find the corresponding Matlab structure files.

3.8.4 Perform simulations

After starting Matlab you should select the *VieVS/WORK/* directory as current folder. Typing "VieVS"in the Matlab command window starts the interface of the latest version of VieVS.

- In the GUI (*File - Set input files*) you can choose the sessions to be simulated. Do not use outlier files and, if OPT files exist, create an empty OPT directory (e.g. 'SIM'). Select this directory in the GUI before starting the simulator.
- In the GUI (*Parameters - observation restrictions*) set the quality code limit to a large number (> 9).
- After you select the *Simulation* menu label on the top of the interface, the interface of VIE_SIM appears (as shown in Figure 3.29). You can choose the parameters to be simulated and enter the number of days and a starting point for the running number of the NGS files. The additional options include 'set reference clock to zero' and 'write ngs file'. You can choose a file containing the simulation parameters (stored in *VieVS/DATA/TURB/* folder). An alternative option is to directly enter the values, these will then be applied to all stations. If you want to simulate source structure as well you have to select a predefined catalog which contains the source structure of every source. It shall be noted here, that while clk, trp and wn have a stochastic component that chages for each simulation run, source structure is a geometrical quantity and is identical for the individual observations in repeated simulation runs. Hence it is a systematic effect.
- In the menu (*Run - Run options*) the checkboxes VIE_INIT, VIE_MOD and VIE_SIM have to be selected to run the simulation.

3.9 Run

3.9.1 Sinex output

The SINEX file format is a standardized output ASCII format used by the International Earth Rotation and Reference Systemsn Service (IERS). It is used for the distribution of products and estimates. VieVS is capable of writing SINEX files as output. This option is given in '*Run - Sinex output*'. Only values which are estimated can be chosen. The option 'include' writes the chosen parameters to the SINEX files. Zenith wet delays are usually estimated every hour. Therefore the normal equation matrix (and also the SINEX file) would become very large. The option 'reduce from N matrix', removes the entries for the chosen parameters (e.g. zenith wet delays) from the normal equation matrix and makes the SINEX files considerably smaller. However, the parameters can be derived from the 'reduced' N matrix as well.

3.9.2 VieVS estimation settings

In the VieVS processing settings (*Run - VieVS processing settings*) the user can select the clock parametrization in the first solution (in which only one zenith wet delay per station and one linear clock function per station is estimated) and the outlier test in the main solution (in which all parameters are estimated). Furthermore the user can (de-)select to actually estimate

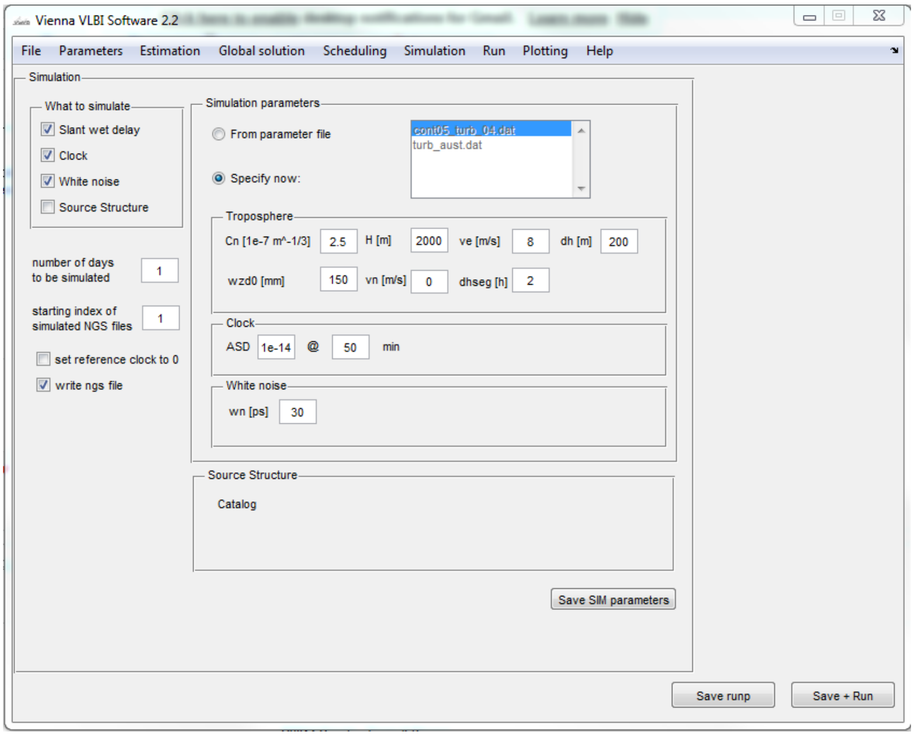

Figure 3.29: VIE_SIM graphical user interface (GUI).

parameters (otherwise only the normal equation matrix is set up) and start a station- and source wise parametrization for each session chosen in *File - Set input files*.

There is a button to save a current parametrization to an ASCII file in this panel as well.

3.9.3 Run options

In *Run - Run options* the user can basically chose which modules should be run and to which subfolders the (intermediate) results should be saved to. The results are saved in the *VieVS/DATA/LEVELx/ subfolder/*.

3.10 Plotting tool

3.10.1 Residuals

The residual plotting tool is shown in Figure 3.30. It allows the user to plot residuals from first (only clock functions and one zenith wet delay per station estimated) and main (all parameters estimated) solutions. Those can furthermore be visualized per station, per baseline and per source to e.g. detect problematic sources, stations or baselines.

By clicking *Load* all sessions in the chosen folder ('/' corresponds to */DATA/LEVEL3/* are loaded by the program and shown in the second popupmenu. If nothing seems to happen there are probably no sessions in the desired folder which have been analysed with version 2.1 or later (only then the *res_* files are written).

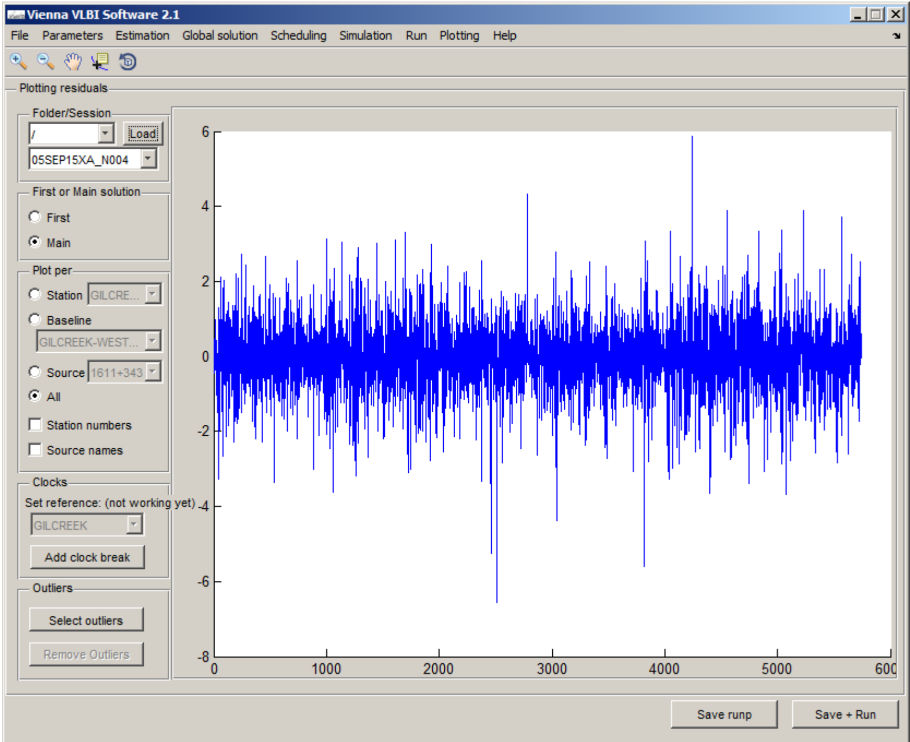

Figure 3.30: Screenshot of the residual plot tool.

Adding clock break information

If a session contains a clock break, a jump in the residuals at the epoch of the clock break might be observed. This can be removed interactively when station-wise residuals are plotted. The user has to click *Add clock break*, select the time epoch of the clock break (simply click with the white cross on the plot; the y-value is not important) and confirm that the information is written to the OPT-file. The OPT-folder will be the same as chosen in *File - Set input files*. The clock-break will be applied the next time this session is analyzed with VieVS.

Removing outliers manually

Outliers can be removed by clicking *Select outliers* in the residual plot window. The user can either click on one value or drag-open a box containing the outlier values. All values will be marked with black crosses. To write all those values to the OUTLIER file, the button *Remove Outliers* must be pushed. Similar to the clock break information, the outlier information is written to the outlier folder selected in *File - Set input files*. The outliers will be removed right at the beginning in all following VieVS runs.

3.10.2 Parameters

To visualize estimated parameters, VieVS includes a plotting window (*Plotting - parameters*. Besides the axes on the right, there are three panels where you can load data separately - the three panels plot the data in different colors (panel1: black, panel2: red, panel3: blue) for e.g. comparison. To load data, select the subfolder you chose before processing (if you did not select any, leave '/') and click on *Load*. All the sessions which are in the selected directory appear in the popupmenu *One session*. Select this radiobutton to plot single session, otherwise (if you want to plot parameters from all those sessions) click *All sessions*. Select the parameter and station (only needed for station dependent parameters, such as station coordinates, zenith wet delays or tropospheric gradients) and select *Plot* below. If nothing appears on the axes, the parameter you selected may not have been estimated for the chosen session.

3.10.3 Session analysis

In *Plotting - Session analysis* three session related informations can be plotted: (1) The station network of one session, (2) the baseline length repeatability (standard deviations of baselines from all sessions in the chosen folder) and (3) correlation matrix values of the chosen session. Up to four sessions can be selected and visualized for network and baseline length repeatability plots (do not forget to check *Add network/BLR* below each session).

3.11 Output

VieVS creates a number of information/data by default, such as session information, estimated parameters and statistics which are described in this chapter.

3.11.1 Command window

In a single-session analysis several informations are provided in the Matlab command window. Those include:

- Name of the session
- Information about excluded sources, baselines or stations
- Participating stations
- A priori models used for the theoretical delay
- Reference clock station
- Statistics
  - Number of scans, antennas, sources and observations (also per station)
  - A priori and a posteriori stdandard deviation of unit weight
  - χ^2 of the first and main solution $\left(\frac{v^T P v}{n-u+n_C}\right)$, also per antenna and baseline (v...residuals, P...weight matrix, n...number of observations, u...number of unknown parameters, n_C...number of constraint equations)
  - Number of automatically detected outliers
  - Number of estimated parameters
- Path of saved output files
- Program error/crash information

3.11.2 Residuals plot

After a processing run, a plot appears showing the residuals of the last session (if only one session was processed, the residuals of this session are shown). The residuals can also be (at a later stage) visualized in *Plotting - Residuals*.

3.11.3 SINEX

SINEX is a standard output format for geodetic parameters. If you want to write these textfiles, go to *Run - Sinex output* and tick the checkbox *write SINEX file*. The user can select the parameters to be included (=write parameter) in the SINEX file. This might be useful, since the SINEX file could become very large when all parameters are written to the SINEX file.

3.11.4 Parameter logfile

VieVS writes automatically all selected parameters to a textfile, which is overwritten in every new run. The output file is */VieVS/WORK/input_protocol.txt*. If you want to write that file to a different directory, click on the button *Save as...* in *Run - VieVS estimation settings*.

3.11.5 Saved files

- Estimated parameters are saved in VieVS/DATA/LEVEL3/*subfolder*/x_ *sessionname.mat*.
- Estimation options
- Normal equation matrix
- Right hand side vector

Chapter 4

Data

This Chapter provides some details about different data being used in VLBI analysis and how they are used in VieVS. For data used in VIE_GLOB, VIE_SCHED and VIE_SIM we refer to the Chapters 3.6, 3.7 and 3.8 respectively.

Time-dependent correction and coefficients of periodic time dependencies are stored in the superstation file which can be found in *VieVS/TRF/superstation.mat*. Files used for the superstion file are stored in *VieVS/TRF/create/superstation/neededFiles*.

Corrections without periodic time dependencies are saved as time series. The corresponding files can be found in folders located the VieVS root directory (e.g. non-tidal atmosphere loading is saved at *VieVS/ATM/*).

Similar folders can still be found for corrections that are now saved in the superstation file. Those folders are used with older VieVS versions and are obsolete if the newest VieVS version is used.

4.1 NGS files

The observations are stored in the NGS file which is the main input file for VieVS.

1. NGS header

   The NGS header consists more or less of stations and sources of the session, including their rough coordinates - x,y,z for stations, right ascension and declination for sources. The mounting type of the telescope is given as well.

2. NGS data cards

   This is the main part, all observation information is stored in here.

A full description of the NGS files can be found at *http://lacerta.gsfc.nasa.gov /mk5/help/dbngs_format.txt*.

To select one or more sessions (NGS files) go to *File - Set input files* (see Fig. 3.2) and click on *Browse for sessions*. Multiple selections (press and hold down *Ctrl*) are possible. Process lists can be loaded using the button *Browse for process lists* (for details on process lists see Chapter 3.3.3). All selected sessions (single sessions and sessions from process lists) appear in the listbox in the GUI.

4.2 Atmospheric loading

4.2.1 Tidal atmosphere loading

Tidal atmosphere loading is caused by diurnal heating of the atmosphere. Two models are currently implemented in VieVS:

- GSFC VLBI group (Petrov & Boy, 2004)
- University of Luxembourg (GGFC) (van Dam, 2010)

The tidal atmospheric loading effect can be found in the superstation file and the corresponding source folder. We refer to the given references for more detail on the implemented models.

4.2.2 Non-tidal atmosphere loading

Non-tidal atmosphere loading is caused by pressure changes due to air mass movements. At mid-latitude stations experience a vertical crustal displacements of up to 25 mm. Two models are currently implemented in VieVS:

- GSFC VLBI group (Petrov & Boy, 2004)
- University of Luxembourg (GGFC) (van Dam, 2010)

Files used for the non-tidal atmospheric loading effect can be found in the *ATM* folder. We refer to the given references for more detail on the implemented models.

4.3 Hydrology loading

Hydrology loading is caused by non ocean water bodies (e.g. canopy water, soil moisture, snow etc.) which cause a load on the crust. The corrections are provided by the NASA GSFC VLBI group (Eriksson & MacMillan, 2012). Files used for the hydrology loading can be found in the *HYDLO* folder. We refer to the given reference for more detail on the implemented models.

4.4 Ocean tide loading

Ocean tide loading is caused by the redistribute of water mass due to tides. The water causes a load on the crust and therefor a deformation of up to 10 cm. 5 ocean tide loading model are implemented in VieVS:

- TPX07.2 (Egbert & Erofeeva, 2002)
- GOT00 (Ray, 1999)
- FES2004 (Letellier, 2004)
- EOT08a (Savcenko & Bosch, 2008)
- AG06 (Andersen, 2006)

The ocean tide loading effect can be found in the superstation file and the corresponding source folder. We refer to the given references for more detail on the implemented models.

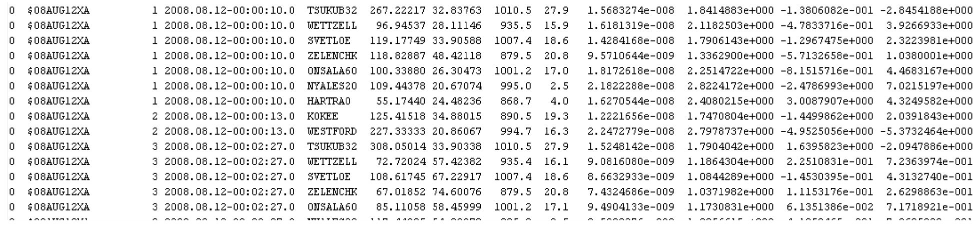

```
0  $08AUG12XA      1 2008.08.12-00:00:10.0  TSUKUB32  267.22217 32.83763  1010.5  27.9  1.5683274e-008  1.8414883e+000 -1.3806082e-001 -2.8454188e+000
0  $08AUG12XA      1 2008.08.12-00:00:10.0  WETTZELL   96.94537 28.11146   935.5  15.9  1.6181319e-008  2.1182503e+000 -4.7833716e-001  3.9266933e+000
0  $08AUG12XA      1 2008.08.12-00:00:10.0  SVETLOE   119.17749 33.90588  1007.4  18.6  1.4284168e-008  1.7906143e+000 -1.2967475e+000  2.3223981e+000
0  $08AUG12XA      1 2008.08.12-00:00:10.0  ZELENCHK  118.82887 48.42118   879.5  20.8  9.5710644e-009  1.3362900e+000 -5.7132658e-001  1.0380001e+000
0  $08AUG12XA      1 2008.08.12-00:00:10.0  ONSALA60  100.33880 26.30473  1001.2  17.0  1.8172618e-008  2.2514722e+000 -8.1515716e-001  4.4683167e+000
0  $08AUG12XA      1 2008.08.12-00:00:10.0  NYALES20  109.44378 20.67074   995.0   2.5  2.1822288e-008  2.8224172e+000 -2.4786993e+000  7.0215197e+000
0  $08AUG12XA      1 2008.08.12-00:00:10.0  HARTRAO    55.17440 24.48236   868.7   4.0  1.6270544e-008  2.4080215e+000  3.0087907e+000  4.3249582e+000
0  $08AUG12XA      2 2008.08.12-00:00:13.0  KOKEE     125.41518 34.88015   890.5  19.3  1.2221656e-008  1.7470804e+000 -1.4499862e+000  2.0391843e+000
0  $08AUG12XA      2 2008.08.12-00:00:13.0  WESTFORD  227.33333 20.86067   994.7  16.3  2.2472779e-008  2.7978737e+000 -4.9525056e+000 -5.3732464e+000
0  $08AUG12XA      3 2008.08.12-00:02:27.0  TSUKUB32  308.05014 33.90338  1010.5  27.9  1.5248142e-008  1.7904042e+000  1.6395823e+000 -2.0947886e+000
0  $08AUG12XA      3 2008.08.12-00:02:27.0  WETTZELL   72.72024 57.42382   935.4  16.1  9.0816080e-009  1.1864304e+000  2.2510831e-001  7.2363974e-001
0  $08AUG12XA      3 2008.08.12-00:02:27.0  SVETLOE   108.61745 67.22917  1007.4  18.6  8.6632933e-009  1.0844289e+000 -1.4530395e-001  4.3132740e-001
0  $08AUG12XA      3 2008.08.12-00:02:27.0  ZELENCHK   67.01852 74.60076   879.5  20.8  7.4324686e-009  1.0371982e+000  1.1153176e-001  2.6298863e-001
0  $08AUG12XA      3 2008.08.12-00:02:27.0  ONSALA60   85.11058 58.45999  1001.2  17.1  9.4904133e-009  1.1730831e+000  6.1351386e-002  7.1718921e-001
```

Figure 4.1: Screenshot of the external tropospheric file

4.5 Ocean pole tide loading

Ocean pole tide loading is generated by the centrifugal effect of polar motion on the oceans. The IERS Conv. 2010 recommends the ocean pole tide model of (Desai, 2002) which provides the ocean pole load tide coefficients. The ocean pole tide loading effect can be found in the superstation file and the corresponding source folder. We refer to the given reference for more detail on the implemented models.

4.6 External tropospheric files

External tropospheric files contain the path delay through the troposphere and the partial derivatives needed for the estimation of VLBI observations in a standardized format. They provide an easy way of using different models for the delay for different stations.

The *.trp* files have to be created prior to VLBI analyses. The delays are read in during the calculation of the theoretical delay.

Two files have to exist. For all sessions these tropospheric files should be created:

- Tropospheric parameter files (must be in */VieVS/TRP/* or in a subfolder)
- - Azel-file (must be in */VieVS/VieVS/OUT/AZEL/year/*)

A screenshot of the external tropospheric file is depicted in Figure 4.1. The file contains the following information (sorted by column):

1. Session name,
2. date and time,
3. station name,
4. azimuth,
5. elevation,
6. surface pressure,
7. temperature,
8. slant delay and
9. partial derivatives

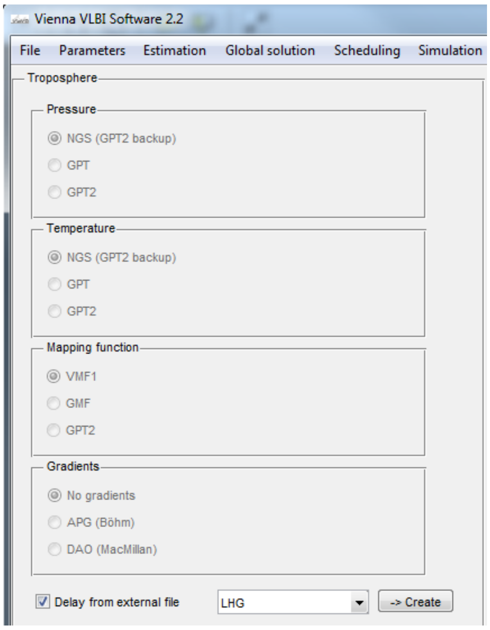

Figure 4.2: Open GUI for the creation of an external tropospheric file

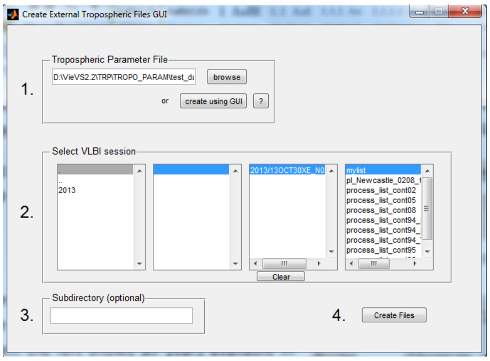

Figure 4.3: Create external troposheric files GUI

4.6.1 Create an external tropospheric file

Start the GUI by selecting *Parameters - Troposphere* in the VieVS GUI. Then click the last check box with the caption *Delay from external file* and push the button *Create*. A screenshot of this procedure is provided in Figure 4.2.

In Figure 4.3 the GUI is depicted.

In the first (1.) part of the GUI the tropospheric parameter file has to be specified. See Chapter 4.6.2 if you want to create a tropospheric parameter file.

In a second step (2.) the sessions, for which *.trp* files should be created, have to be chosen. The first listbox from the left shows all years available in the folder *VieVS/NGS*. After selecting one year, all files from the folder are depicted in the second listbox. If a session is selected, it appears in the third listbox which specifies the used sessions (multiple selections are possible). There is also the option of using predefined process lists (fourth listbox).

A subdirectory where *.trp* files are saved can be selected in (3.). Pushing the *Create Files* button (4.) will create the *.trp* files.

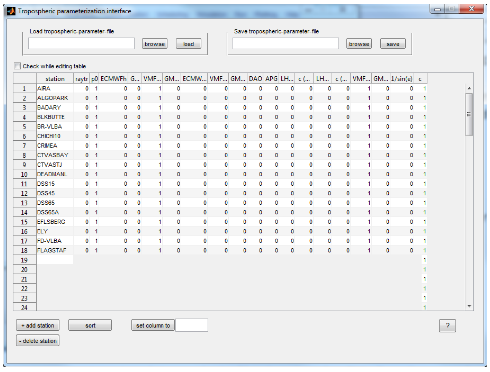

Figure 4.4: Create a tropospheric parameter file GUI

Writing one file successfully takes a few seconds. If an error occurs, the error log message should appear in the matlab command window. Following errors messages can be found:

- No *.azel* file found; solution: Create the *.azel* file first.
- No antenna struct found; solution: Run VieVS with the current session.
- A station in the *.azel* file was not found in antenna struct; solution: change the quality code limit, or any other parameter that excludes observations (for example when the *.azel* file was written using all observations, the antenna struct only consists of good-quality-observations).
- Tropospheric parameter file not found; solution: Create it first (see Chapter 4.6.2).
- Name of chosen subdirectory not allowed; solution: The following names of subfolders for *.trp* files are not allowed: *PROGRAMM*, *LHG*, *TROPO_PARAM*.
- Tropospheric parameter file was not correctly defined, solution: Edit the tropospheric parameter file in the GUI.
- VMF1 file not found; solution: Download the latest version of the yearly file of the Vienna Mapping Function to your *VieVS/VM1/temp/* directory.
- A station was not found in tropospheric parameter file; solution: A station which takes part in the session is not included in the tropospheric parameter file. Use the GUI to add the station and the favored parametrization.

4.6.2 Create an tropospheric parameter file

The tropospheric parameter file is a simple text file which contains the parametrization for all stations. A different parametrization for each station can be selected, for example:

Wettzell:	Raytracing (only possible if available)
Westford:	p0+Saastamoinen, no Gradients
All others:	ECMWFh+VMF1h, LHG gradients

The tropospheric parameter file can be created using the VieVS GUI by pushing the button *create using GUI* depicted in Figure 4.2 (1.). Another GUI should appear, see Figure 4.4.

Parameter	A priori model
Hydrostatic zenith delay	Pressure at the site with model from Saastamoinen
Hydrostatic mapping function	$VMF1_h$
Wet delay	None
Gradients	None
Partial derivatives:	
Direction of atmosph. asymmetry	$VMF1_w$
North Gradient	$\frac{\cos\alpha}{\sin\epsilon\cdot\tan\epsilon+c'}$, $c = 0.0032$
East Gradient	$\frac{\sin\alpha}{\sin\epsilon\cdot\tan\epsilon+c'}$, $c = 0.0032$

Table 4.1: Default parametrization for the tropospheric parameter file

All ITRF stations should appear, their default parametrization is listed in Table 4.1. A more detailed description of the columns is given in Figure 4.5.

In general a 1 indicates that this specific model should be used for this station. If a 0 is written into the cell the program wont use the corresponding model. If there is more than one model available (e.g. p_0, ECMWFh and GPT for the hydrostatic zenith delay model), their sum has to be <= 1 (only one or no model can be used). Mapping functions are only used when there is a "main" model chosen (for example: $ECMWF_w = 0$, $VMF1_w = 1$: The wet part of the atmosphere is NOT considered). If all mapping functions are set to zero (e.g. $VMF1_h$ and GMF_h) but one model is chosen (e.g. $p0 = 1$), then the correction is NOT applied. There is one exception: If the c coefficient is set to zero and one model is used (e.g. $DAO = 1$) the correction is applied with a c coefficient of zero. Partial derivatives are mandatory which means that either the $VMF1_w$, GMF_w of $1/sin(e)$ in the partials block has to be 1. Such problems can be prevented by selecting the check box *check while editing table* which checks the input for errors.

One can now edit the parametrization by hand. It is possible to set a whole column to one value by simply clicking into this column and pressing the button *set column to* (the desired value can be specified next to the button).

Stations can be deleted (button - *delete station*) or added (button + *add station*) to the list. An option to sort the list (button *sort*) is also included in the GUI.

A previously created tropospheric parameter file can be loaded into the GUI in the *Load tropospheric-parameter-file* section.

The output file can be specified in the *Save tropospheric-parameter-file* section. By clicking the *save* button the created/edited file is saved to the given location.

4.6.3 Azel Files

Azel files are text-files which are created automatically as part of the daily automatic processing. For each session one *.azel* file is created. It contains one line for each observation and each station. The parameters written to these files are:

- Number of scan
- Mjd of observation
- Year of observation
- Day of year of observation
- Hour, minute and second of observation

	#	Name of column	Description	Possible values	Default values
	1	station	Name of the station		
	2	raytr	Delays derived from raytracing	1 | 0	0
Hydrostatic zenith delay	3	p0	Pressure at site, model Saastamoinen	1 | 0	1
	4	ECMWFh	Delay from numerical weather model (NWM)	1 | 0	0
	5	GPT	Pressure from empirical model, model Saastamoinen	1 | 0	0
Hydrostatic mapping function	6	VMF1h	From NWM	1 | 0	1
	7	GMFh	Empirical hydro mf, includes bending	1 | 0	0
Wet zenith delay	8	ECMWFw	Wet zenith delay from NWM	1 | 0	0
Wet mapping function	9	VMF1w	From NWM	1 | 0	0
	10	GMFw	Empirical wet mapping function	1 | 0	0
Hydrostatic gradients	11	DAO	Gradient model (MacMillan)	1 | 0	0
	12	APG	Gradient model (Böhm)	1 | 0	0
	13	LHGh	Gradient model (IGG, GGOS)	1 | 0	0
Coefficient for "gradient mf"	14	c (mf)	c in formula for gradient (if set to one: default value of 0.0032)	numeric	0
Wet gradients	15	LHGw	Gradient model wet (IGG, GGOS)	1 | 0	0
Coefficient for "gradient wet mf"	16	c (mf)	c in formula for gradient (if set to one: default value of 0.0007)	numeric	0
Partial derivative w.r.t. zenith direction	17	VMF1w	Wet mapping function from NWM	1 | 0	1
	18	GMFw	From empirical mapping function	1 | 0	0
	19	1/sin(e)	Simple approach	1 | 0	0
Coefficient for mf of north, east partial	20	c		numeric	1

Figure 4.5: Description of all columns in the tropospheric parameter files

- Stationname
- Azimuth [rad]
- Elevation [rad]
- Source
- Temperature [°C]
- Pressure [hPa]

On the basis of the azel-files the *.trp* (external tropospheric files) are created. The number of rows in the *.azel* file is therefore the same for the *.trp* file. This is important because the azel-files specifies if all observations are used (even those with a quality flag not equal 0).

4.7 External ionospheric files

Introduction Taken from: 'Use of GNSS-derived TEC maps for VLBI observations', Tierno Ros, C., J. Böhm, H. Schuh. In: Proceedings of the 20th Meeting of the European VLBI group for Geodesy and Astronomy. Schriftenreihe 22, Institut für Geodäsie und Geoinformation, Universität Bonn, 2011.

The ionosphere is a portion of the upper atmosphere; it is extended from about 60 km to 2000 km and has the characteristics that the particles there can be easily ionized by solar radiation resulting in a positive ion and a free electron. The ionospheric delay makes up a large fraction of observed VLBI group delays and it depends on the number of free electron (TEC) along the ray path. Usually, a correction can be applied by making simultaneous observations in both S- and X-band. However, this is not always possible. For such cases, there is the alternative of calculating the ionospheric correction from Global Navigation Satellite Systems (GNSS) TEC maps. (Please note that it is only recommended to use the GNSS corrections in case of not having observations in both S- and X-band, since the X/S ionosphere values are instantaneous direct measurements while the GNSS values suffer from low spatial and temporal resolution, Gordon, 2010).

GNSS TEC maps are representing the TEC values over the whole globe determined from GNSS observations. The routine generation of these Global Ionosphere maps (GIMs) is currently done at four analysis centers of the International GNSS Service (IGS), more details about the different techniques they use can be found in Schaer (1999); Feltens (1998); Mannucci et al. (1998) and HernÃ¡ndez-Pajares et al. (1999). The analysis centers transmit their products to the IGS Ionosphere Product Coordinator, who produces a weighted combined product (HernÃ¡ndez-Pajares et al.,2009). The accuracy of the maps is between 2 to 8 TECU. Such maps exist since 1998 and have a latitude/longitude resolution of 2.5/5.0 degrees.

External ionospheric file

Figure 4.6 shows how an external ionospheric file looks like. The header contains information about the creation date of the file, the VLBI-session which corresponds to the file, the type of GIM used and the coordinates of the stations participating in the session.

The file body is divided in columns:

1. VLBI-Session that corresponds with the file
2. Number of scan
3. Date and time of the observation in YYY.MM.DD-hh:mm:ss.s

```
# IONOSPHERIC DELAY
#
# This file was created on: 07.11.2012 (13:39:59)
#
# Session: 11SEP29XA_N004
# IONEX-Map used: IGS
#
#
#              X[m]          Y[m]          Z[m]     geocLat(°) long(°)   ellHeight[m]
#  FORTLEZA   4985370.0380 -3955020.3430  -428472.2470   -3.8779 321.5741   23.5
#  WESTFORD   1492206.5410 -4458130.5150  4296015.5480   42.6129 288.5062   87.2
#  BADARY     -838200.7240  3865751.5880  4987670.9770   51.7703 102.2339  822.1
#  YEBES40M   4848762.1000  -261484.5000  4123084.9000   40.5247 356.9131  989.5
#  WETTZELL   4075539.8360   931735.3120  4801629.4000   49.1450  12.8775  669.6
#  TSUKUB32  -3957409.3290  3310228.8070  3737494.6900   36.1031 140.0887   85.1
#  HARTRAO    5085442.7760  2668263.5400 -2768696.9610  -25.8898  27.6854 1416.1
#  HOBART12  -3949990.7000  2522421.2000 -4311708.2000  -42.8056 147.4381   41.4
#  KOKEE     -5543837.6560 -2054567.6730  2387852.0420   22.1266 200.3349 1177.0
#  ONSALA60   3370605.9840   711917.5280  5349830.7710   57.3958  11.9264   59.7
#  TIGOCONC   1492051.3691 -4887961.4981 -3803541.7545  -36.8427 286.9748  171.3
#  ZELENCHK   3451207.7810  3060375.2080  4391914.9190   43.7878  41.5652 1175.4
#
#
#
#                  TAI in YYYY.MM.DD-hh:mm:ss.s          Azi(°)  Elev(°) SurfAtmPres(mbars)  SlantPathDel(sec)
O  $11SEP29XA_N004     1 2011.09.29-00:01:50.0  FORTLEZA  213.79693 45.90472  1007.9  27.1   8.41101950e-10
O  $11SEP29XA_N004     1 2011.09.29-00:01:50.0  WESTFORD  177.37658  8.61136  1003.9  17.4   8.71857831e-10
O  $11SEP29XA_N004     2 2011.09.29-00:02:34.0  BADARY    216.74682 58.11636   931.2  -3.1   2.57794152e-10
O  $11SEP29XA_N004     2 2011.09.29-00:02:34.0  YEBES40M   74.23363 18.81992   919.0  16.0   3.70893038e-10
O  $11SEP29XA_N004     2 2011.09.29-00:02:34.0  WETTZELL   88.74546 31.29329   958.6  12.6   2.18460132e-10
O  $11SEP29XA_N004     2 2011.09.29-00:02:34.0  TSUKUB32  273.13028 39.00029  1014.7  22.1   6.27031180e-10
O  $11SEP29XA_N004     3 2011.09.29-00:03:02.0  HARTRAO   138.16893 69.45971   865.0  15.5   2.08553795e-10
O  $11SEP29XA_N004     3 2011.09.29-00:03:02.0  HOBART12  232.22131 18.75657   982.8  11.5   6.38495386e-10
O  $11SEP29XA_N004     4 2011.09.29-00:03:24.0  KOKEE     310.84661 57.79776   890.3  23.4   1.07515241e-09
O  $11SEP29XA_N004     4 2011.09.29-00:03:24.0  ONSALA60   17.90093  9.25740  1025.9  14.9   2.75742947e-10
```

Figure 4.6: Fragment of an external ionospheric file

4. VLBI-station observing
5. Azimut (in degrees) of the observation
6. Elevation angle (in degrees) of the observation
7. Atmospheric pressure at surface (mbars)
8. Temperature
9. Ionospheric slant path delay (in seconds)

How to create an external ionospheric file

In order to create an external ionospheric file you should follow these instructions: (Please note that before creating it, VIE_INIT and VIE_MOD should have been executed for the sessions for which you want to create the external files)

1. Open VieVS and go to *Parameters - Ionosphere* (Fig. 3.10), select the external file and click the button *create*.
2. A new GUI should open (Figure 4.7). Here you can specify which ionospheric map you want to use (CODE or IGS), for which sessions you want to create the external ionospheric file and optionally the name of the directory where the external file will be saved (default is VIEVS/ION/FILES). In Figure 4.8 you can see an example of how the GUI looks after you selected the parameters.
3. Click on the button *create files*
4. Now the creation of the external file starts, first the CODE/IGS ionospheric maps will be automatically downloaded from the corresponding CODE/IGS server (depending on the session 1 or 2 maps are needed). Then the files are uncompressed (depending on your computer it might be automatic). Finally, the ionospheric delays are calculated and saved in an *.ION* file.
5. If no problems occurred during the process, in your command window should appear this message Figure 4.9.

4.8 Ephemerides

The files containing the ephemerides are already described in Chapter 3.4.4.

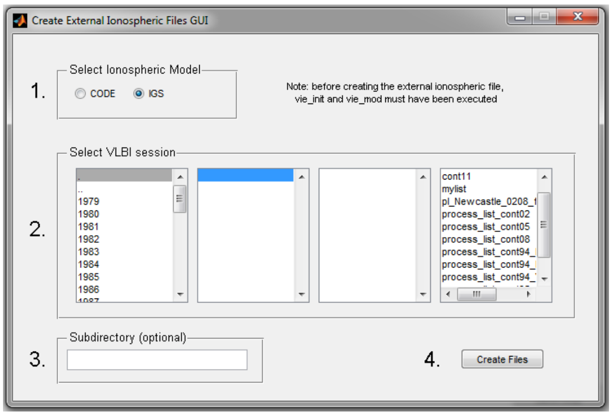

Figure 4.7: Screenshot GUI creating external ionospheric file

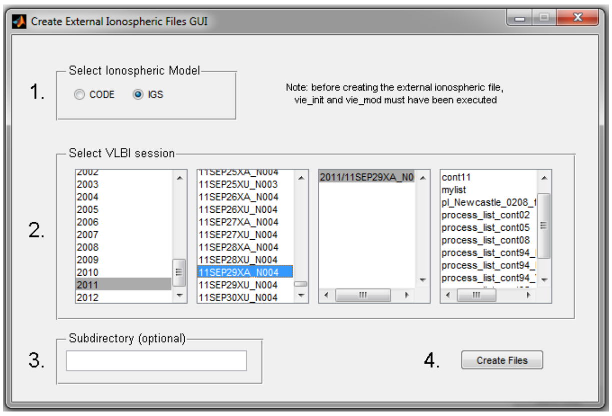

Figure 4.8: Example of screenshot GUI creating external ionospheric file

Figure 4.9: Command window after external ionospheric file is created

Type of data	Included	Own
TRF	ITRF2005, ITRF2008, VTRF2008, VieTRF10a, vievsTrf (Backup)	x
Tidal ocean loading	FES2004, GOT00, EOT08a, TPXO72, AG06	x
Ocean pole tide loading	by S. Desai	x
Tidal atmosphere loading	GSFC ('leonid' - remove that!), VanDam	x
Additional	Antenna information, eccentricities, equipment, horizon mask, discontinuities	-

Table 4.2: Content of the superstation file

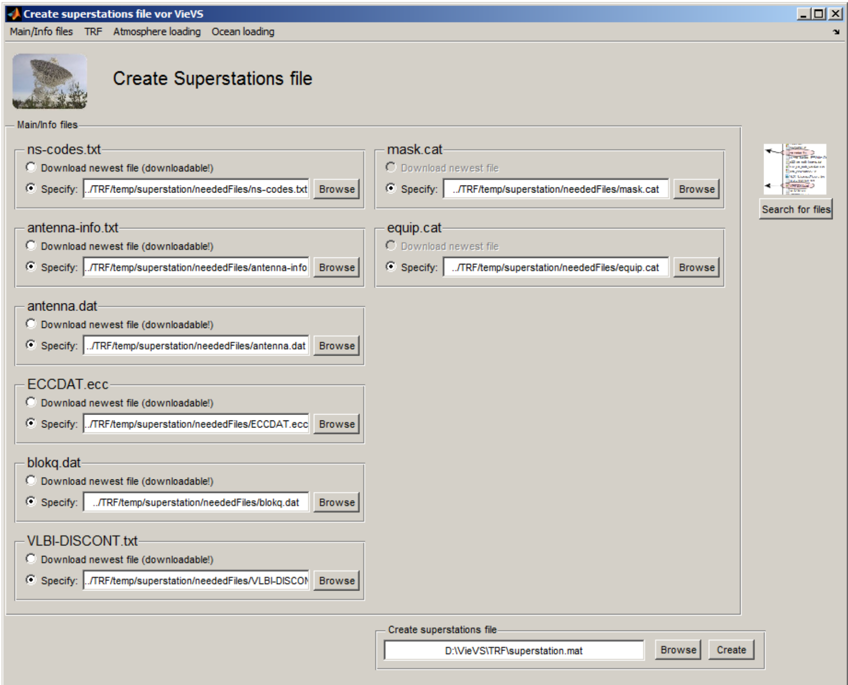

Figure 4.10: Screenshot GUI creating superstation files

4.9 Terrestrial reference frames - Superstation file

The superstation file is a *.mat* file containing all static station-dependent data, e.g. TRF, loading data, discontinuities, eccentricities, furhter antenna information. Table 4.2 provides a summary of all realizations/models which are included by default.

4.9.1 Create a superstation file

In *Parameters - Reference frames* there is a button *Create file.* This button runs the *createsuperstationsFile.m* function which is a interface for creating the superstation file (Fig. 4.10). This function as well as all needed data for the superstation file are located in */TRF/temp/superstation/.*

The four menu buttons in the GUI let you specify filenames of the shown textfiles. In *Main/Info files* data like general antenna information, horizon masks and equipment data can be found. The menu button *TRF* lets the user specify up to six different terrestrial reference frames. The two most-right menu items ask the user to input loading correction data. If the files are located in */TRF/temp/superstation/neededFiles/*, the button *Search for files* on the right

```
% User Own TRF
% station              x [m]          y [m]          z [m]          vx [m/y]   vy [m/y]   vz [m/y]    epoch  start    end
FORTLEZA        4985370.0378  -3955020.3431   -428472.2433        -0.0021    -0.0038     0.0124    51544      0  99999
KOKEE          -5543837.6553  -2054567.6727   2387852.0407        -0.0090     0.0633     0.0322    51544      0  99999
NRAO20           883772.7035  -4924385.5990   3944042.5057        -0.0143    -0.0029     0.0041    51544      0  99999
WETTZELL        4075539.8364    931735.3129   4801629.4022        -0.0158     0.0168     0.0101    51544      0  99999
NYALES20        1202462.7131    252734.4198   6237766.0788        -0.0143     0.0074     0.0103    51544      0  99999
GILCREEK       -2281547.3705  -1453645.0928   5756993.1398        -0.0215    -0.0035    -0.0075    51544      0  52581
GILCREEK       -2281547.3464  -1453645.0583   5756993.3265        -0.0412    -0.0333    -0.0740    51544  52581  52669
GILCREEK       -2281547.3814  -1453645.1303   5756993.0945        -0.0299    -0.0101     0.0009    51544  52669  52758
```

Figure 4.11: Format of the user own TRF file

```
AIRA        31.82  130.60  322.39   -0.34    0.41   -0.76   -0.45    0.13   -0.11    0.05    0.03    0.25    0.29   -0.06    0.19
ALGOPARK    45.96  281.93  224.00    0.40    0.08   -0.06   -0.56   -0.23    0.05   -0.04    0.13   -0.09   -0.36   -0.21   -0.01
AUSTINTX    30.34  262.30  189.63    0.72    0.29    0.62   -0.77   -0.16   -0.02   -0.10    0.07    0.04   -0.32   -0.18   -0.16
AZORES      37.74  334.34   58.57    0.16   -0.12   -0.70    0.14   -0.08    0.18    0.06   -0.00   -0.38   -0.21    0.04    0.21
BERMUDA     32.36  295.33  -30.69    0.41    0.04   -0.39   -0.84   -0.14    0.06   -0.00    0.10   -0.16   -0.35   -0.22    0.09
BLKBUTTE    33.66  244.28  489.40    0.42    0.45    0.85   -0.24   -0.16   -0.05   -0.14    0.03    0.12   -0.31   -0.07   -0.23
BLOOMIND    39.18  273.50  217.94    0.56    0.18    0.19   -0.71   -0.19    0.02   -0.07    0.12   -0.03   -0.34   -0.21   -0.07
BR-VLBA     48.13  240.32  250.50    0.23    0.33    0.43   -0.07   -0.23   -0.10   -0.17    0.02    0.16   -0.31   -0.04   -0.21
BREST       48.41  355.50  104.48    0.07   -0.14   -0.36    0.41   -0.00    0.27    0.04   -0.08   -0.41   -0.05    0.12    0.10
```

Figure 4.12: Format of the user own atmosphere loading file

of the interface searches for those files and writes the correct file names (including paths) to the textboxes. The textbox at the bottom specifies the output file name (requires a *.mat* file), the button *Create* runs the program and creates the superstation file.

4.9.2 Datum definition

If station coordinates are estimated, some conditions need to be applied in order to avoid singularity - e.g. No net translation (NNT) and No net rotation (NNR). If a station has bad a priori coordinates (or after an earthquake, when coordinates are wrong), this antenna should be removed from the NNTR/NNR(/NNS) condition. The rest of the paragraph gives instructions on how to exclude a station from the given conditions. If an official TRF (i.e. all but *vievsTrf*) is chosen in *Parameters - Reference frames* and a station is found there (coordinates exist for an appropriate break), this station is taken as datum station. If the station does not exist or has no appropriate break (i.e. backup coordinates are taken from *vievsTrf*), the station is excluded from NNT/NNR. If *vievsTrf* is chosen as a priori reference frame (and only then), the ones and zeros in the vievsTrf-textfile indicate if a station is treated as datum station.

4.9.3 Own data

For the TRF, tidal ocean loading, ocean pole tide loading and tidal atmosphere loading the user can add a desired model to the superstation file. Each file has to be specified in the proper panel. The format of the user own TRF file is shown in Fig. 4.11. Comment lines start with '%', data lines start with a station name, followed by x, y and z coordinates and the velocities in x, y and z direction. The three last columns are epoch, start- and end-break (this specifies the time for which the coordinates and velocities are valid). Each column has to be separated by at least one blank; the columns don't have to be aligned with each other.

The user defined atmosphere loading file should have the same format as the 'original' files given by the corresponding models (see Fig. 4.12). A data line starts with an eight-character station name. The required twelve values must start from position (column) 35 (more blank is allowed).

The user defined ocean pole tide loading file should have the same format as the 'original'

```
Ocean Pole Load Tide Deformation Parameters from Self-Consistent
Equilibrium Model of Ocean Pole Tide (Desai, 2002)
Deformation Parameters Generated by S. Desai on March 28, 2006: CM correction applied
Number_longitude_Grid_Points =       720
First_longitude_degrees      =      0.25
Last_longitude_degrees       =    359.75
Longitude_step_degrees       =      0.50
Number_latitude_grid_points  =       360
First_latitude_degrees       =    -89.75
Last_latitude_degrees        =     89.75
Latitude_step_degrees        =      0.50
Longitude   Latitude   u_r^R       u_r^I       u_n^R       u_n^I       u_e^R       u_e^I
(degrees)  (degrees)  (         )  (         )  (         )  (         )  (         )  (         )
---------  ---------  ----------  ----------  ----------  ----------  ----------  ----------
     0.25     -89.75    0.022015    0.040741   -0.021861   -0.029058   -0.025845   -0.055643
     0.75     -89.75    0.022014    0.040728   -0.022086   -0.029542   -0.025654   -0.055389
     1.25     -89.75    0.022013    0.040716   -0.022309   -0.030024   -0.025461   -0.055131
     1.75     -89.75    0.022013    0.040703   -0.022531   -0.030504   -0.025266   -0.054868
     2.25     -89.75    0.022012    0.040690   -0.022751   -0.030982   -0.025069   -0.054601
     2.75     -89.75    0.022011    0.040678   -0.022969   -0.031457   -0.024870   -0.054331
     3.25     -89.75    0.022011    0.040665   -0.023186   -0.031930   -0.024670   -0.054056
```

Figure 4.13: Format of the user own ocean pole tide loading file

file. The file provides all values on a longitude/latitude grid. A screenshot of this structure is shown in Fig. 4.13.

4.10 Celestial reference frames - Supersource file

Similar to the superstation file, there is also one file containing all static information about sources (i.e. name representations and catalog positions). The *.mat* file can be found in *VieVS/CRF/supersource.mat*. The most complete list of sources can be found in the ASCII file *VieVS/CRF/create/neededFiles/vievsCrf.txt*. There, the user can also add new/own sources.

4.10.1 Create supersource file

To create a supersource file, go to *Parameters - Reference frames* and click on *Create file* in the Celestial reference frame panel. In the appearing GUI set the paths to all required files (all but user crf are required) and save the supersource file.

VieVS automatically reads the default file (*supersource.mat* in *VieVS/CRF/*) at the start of VieVS. If you want to load another one, select *Chose file* in *Parameters - Reference frames* in the CRF panel.

Chapter 5

Exercises

5.1 Process your first session

Run VieVS

Start matlab and change the *Current folder* to your VieVS-WORK directory, e.g. *D:/VieVS/WORK/*. Run the GUI by writing *vievs* in the command window and press Enter.

Load file

Go to *File - Set input files*, click on *Browse for sessions* and select your desired NGS file. The session should appear in the listbox, similar to Figure 5.1.

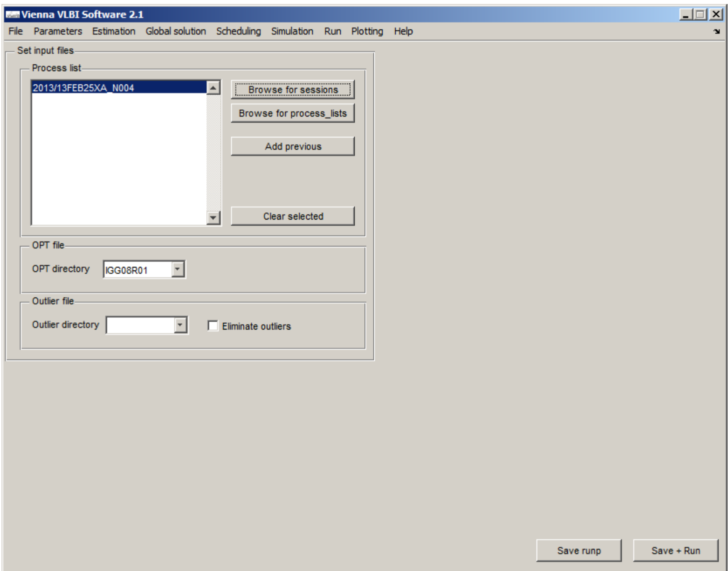

Figure 5.1: Session was selected and appears in the listbox

Change output subfolder

The default parametrization can be used, but we will change the output subfolder to find the results more easily: As depicted in Figure 5.2, we go to *Run - Run options* and write e.g. *myFirstSession* into *one subdirectory*. The results will then be saved in *VieVS/DATA/LEVELx/*

myFirstSession/.mat* where x stands for a number (1 to 5). The estimated parameters, f3.3.3or example, will be saved in folder *LEVEL3*.

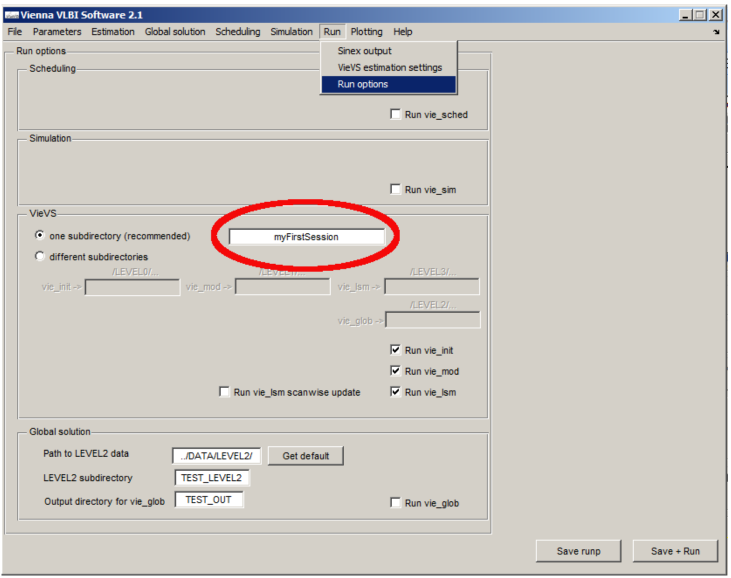

Figure 5.2: Selecting an output subfolder

Run VieVS

To start the processing, simply click on *Save + Run*. The processing of one session takes roughly between ten seconds and one minute, depending on the nubmer of observations and estimated paramters. If the processing was successfull, a residual plot should appear (Figure 5.3).

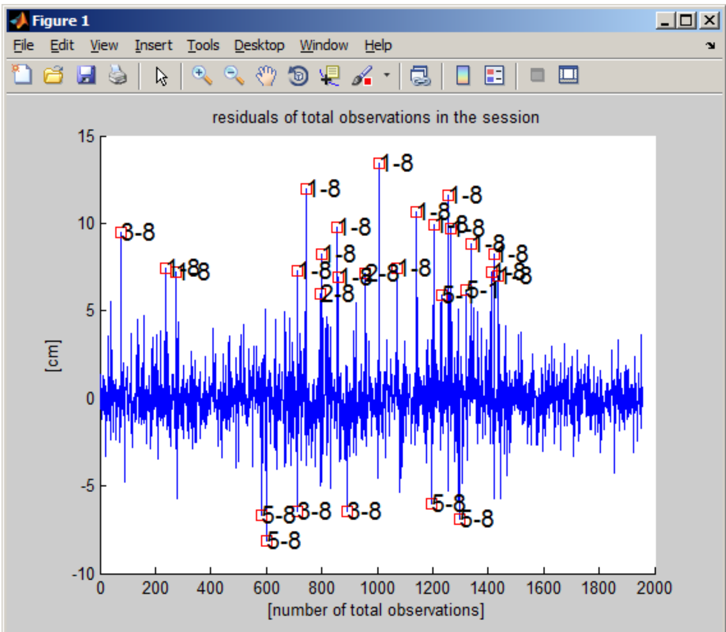

Figure 5.3: Automatic residual plot of the last session in the current processing

The estimated parameters are saved in a matlab binary file in *VieVS/DATA/LEVEL3/ subfolder/x_sessionname*, e.g. *VieVS/DATA/LEVEL3/myFirstSession/x_13FEB25XA_N004.mat*.

More information about the output and results can be found in Chapters 3.11 and 3.10.

5.2 Clock break

In this exercise a clock break at a station clock has to be corrected by the user (Information about clock breaks can also be found in Chapter 3.10.1). The station at which a clock break occurs should not be taken as a reference clock (see Chapter 3.3.5 on how to change the reference clock).

A typical residual plot of a session with a clock break is depicted in Figure 5.4: Large residuals are close together at a certain epoch.

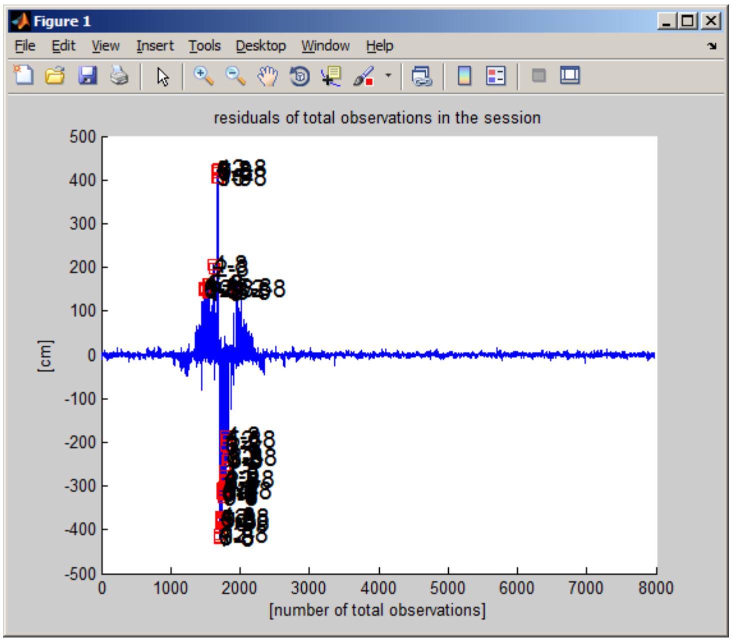

Figure 5.4: Typical residual plot with a clock break

To find the station and epoch of the clock break, the user can go to *Plotting - Residuals*, select the output subfolder of the processed session and click *Load*. When the session is selected in the second popupmenu, the residuals appear in the plot window. Select *First* to show only the first-solution (only one zenith wet delay and one clock function per station is estimated) and *Station* to see only the residuals of one station. Figures 5.5 and 5.6 depict the residuals of two different stations for a session with a clock break. The clock break occurs at ZELENCHK (right figure) since the jump in residuals can be seen in all observations (to all other stations).

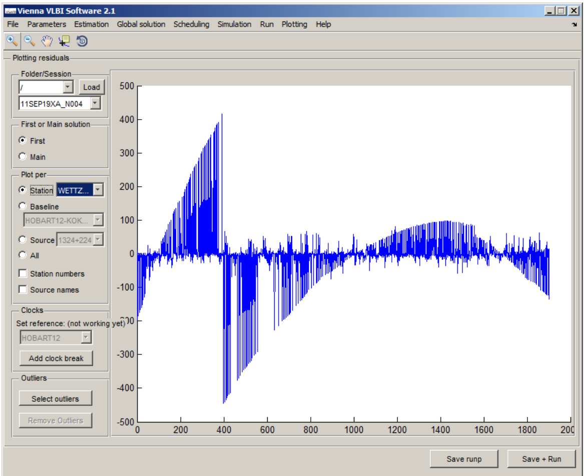

Figure 5.5: Residuals with clock break NOT at the chosen station (WETTZELL)

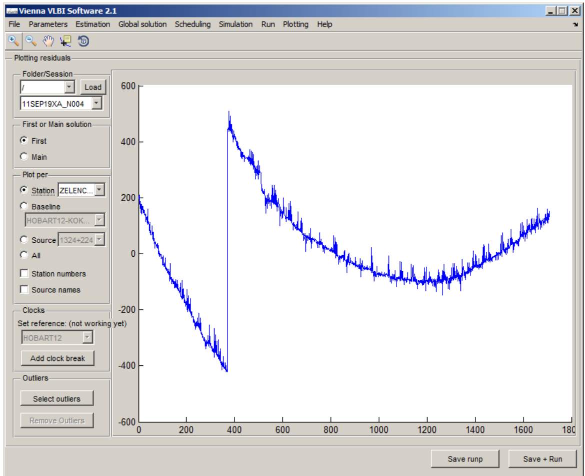

Figure 5.6: Residuals with clock break at the chosen station (ZELENCHK)

To remove the clock break (or in other words: add clock break information) we click on the button *Add clock break* – a grey cross-wire appears – and the user clicks on the epoch of the 'vertical' line of the clock break (the y–value is not important). To make it easier, the user can zoom in before clicking on *Add clock break* (see Figure 5.7). When zooming is finished, deselect the zooming again!

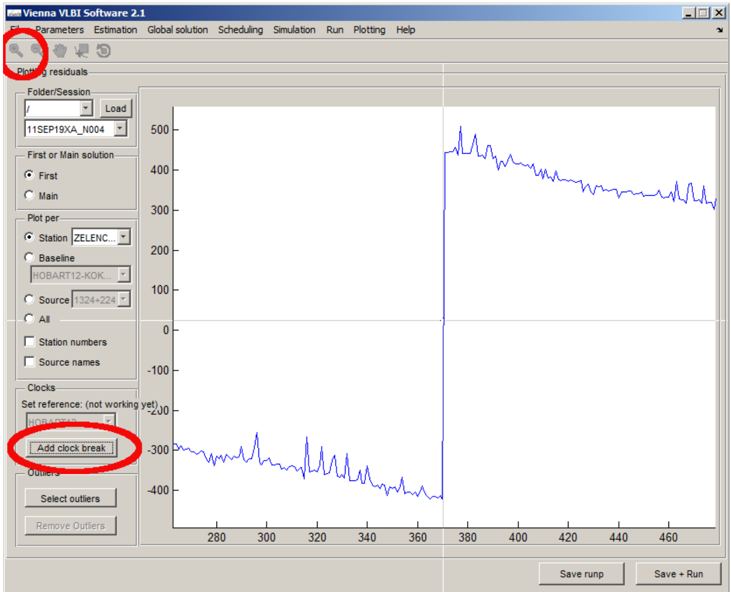

Figure 5.7: Add clock break information

The clock break information will be written to the OPT file in the folder selected in *File - Set input files*. The clock break information will be applied the next time VieVS processes this session (when the same OPT-folder is selected).

5.3 Intensive sessions

Intensive sessions are 1- or 2-hour VLBI experiments which are carried out (nearly) every day with the goal of near-real time estimation of Universal Time (UT1). The stations taking part in Intensive sessions are Kokee Park, NyÅlesund, Tsukuba and Wettzell (see plot of baseline in Fig. 5.8).

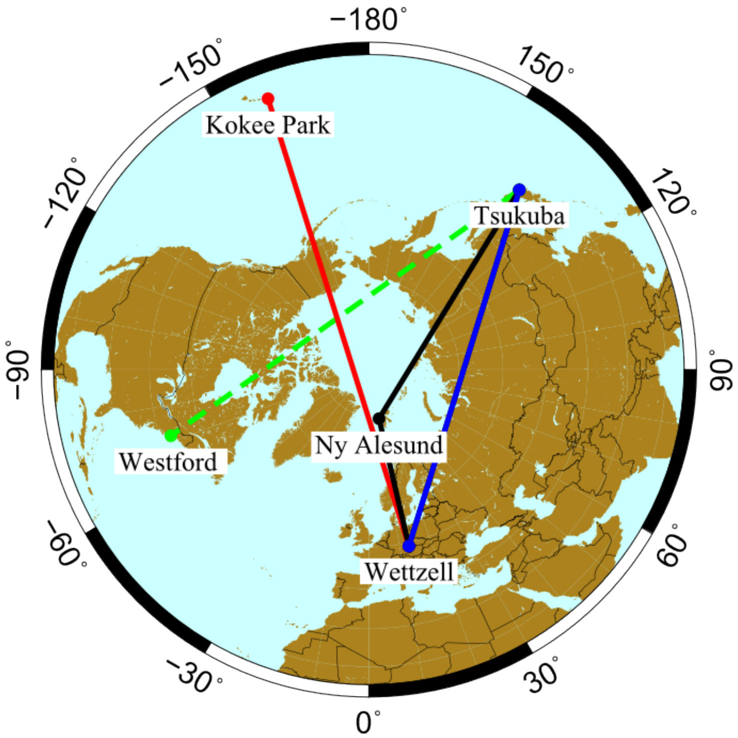

Figure 5.8: Station network for Intensive sessions

Intensive sessions in NGS format usually have the suffix *XK* or *XU*. In *File - Set Input Files* you can select session/s using the button *Browse for sessions*. How you can create process lists easily using the function *mk_list*, is described in Chapter 3.3.6.

Since we usually estimate one constant zwd per station per session, we change the estimation settings in *Estimation - Troposphere* (see Fig. 5.9). Since we estimate piece-wise linear offsets (at least two) we use tight constraints to get 'one' constant offset. We do not estimate gradients (uncheck the boxes in the GUI). The clock estimation parametrization can be found in *Estimation - Least Squares - Clock*. In total we estimate a linear clock function between the two station clocks; no constraint is needed. Take care that the interval is long enough to cover the session. The clock parametrization is shown in Fig. 5.10.

We estimate one constant $\Delta UT1$ value per session, which means that we fix the other Earth Orientation parameters to their a priori values (see Fig. 5.11).

Station coordinates are also not estimated but fixed to their a priori values (Fig. 5.12).

The last options one has to change can be found in *Run - VieVS estimation settings*. There you can (de-)select the first solution (more details about the first solution can be found in Chapter 3.5). You could skip the first solution, but if you apply it, do not estimate more parameters than a linear clock function between the stations. An outlier test is not needed. Fig. 5.13 shows the final options chosen in the exercise. Optionally one can specify a subdirectory where the final output is saved into. The according GUI can be found in *Run - Run options* and is shown in Fig. 5.14. Click the *Save + Run* button to start the processing.

To check the obtained results, one can check the residuals plot, the number of scans as well as the χ^2. The plotting tool (see Chapter 3.10) could be used for visualizing the estimated parameters.

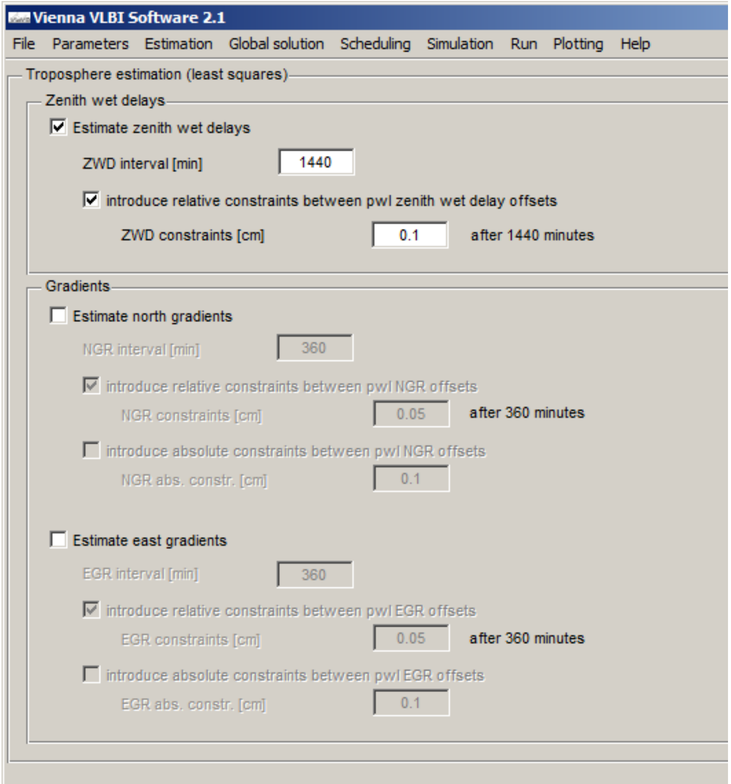

Figure 5.9: Troposphere parameters when processing Intensive sessions

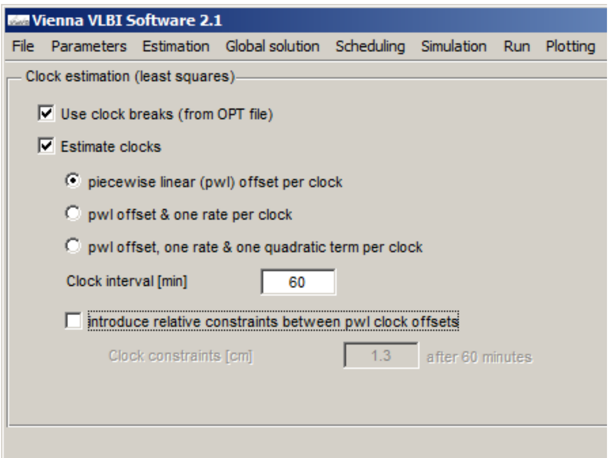

Figure 5.10: Clock parameterization when processing Intensive sessions

An example residuals plot of an intensive session is shown in Fig. 5.15. The residuals could be smaller but are ok.

If you check the command window output (more details in Chapter 3.11.1) you find the number of scans in the current session. In this example we have 15 scans which is not that much. A χ^2 of 1.6 is ok. In the parametrization given above the actual number of estimated parameters is five (one linear clock, two zenith wet delay offsets and one $\Delta UT1$ offset). The number shown in the command window output (eight) is due to the fact that we estimate

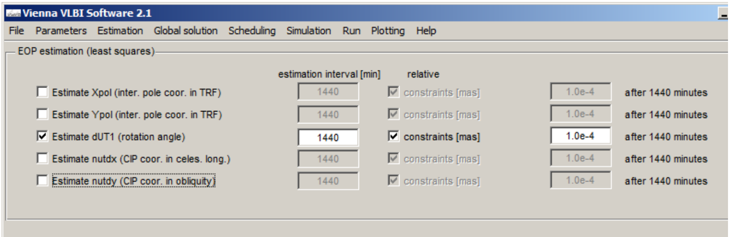

Figure 5.11: EOP estimation settings for Intensive sessions

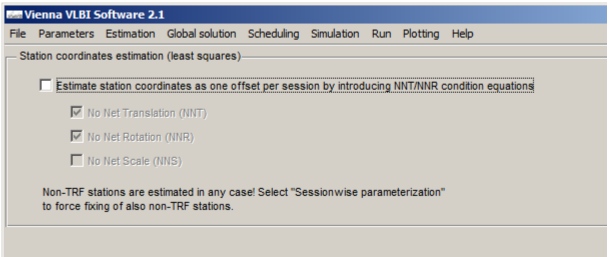

Figure 5.12: Station coordinate estimation settings for Intensive sessions

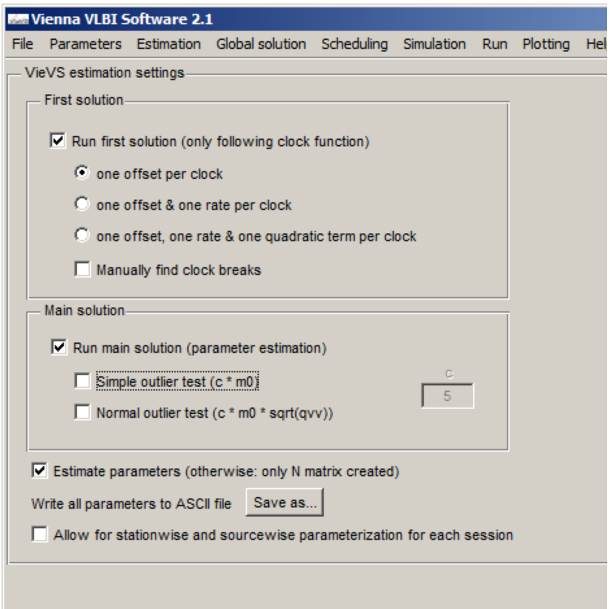

Figure 5.13: Estimation settings-GUI for Intensive sessions

piece-wise linear offsets. The standard deviation of the estimated parameters can be found in the $x\_$ files. For an example session, this file can be loaded and the σ value displayed using the following commands (a more convenient way to visualize parameters is shown in Section 5.4):

```
load('D:/VieVS/DATA/LEVEL3/INT/x_11APR02XK_N003.mat')
x_.dut1.mx(1)
ans = 0.0154
```

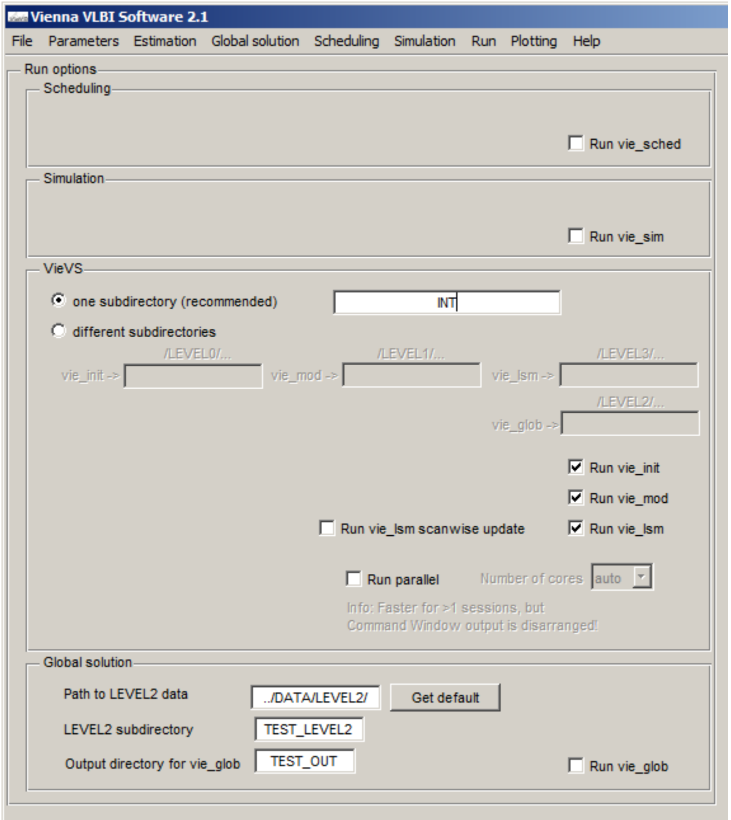

Figure 5.14: Run options for Intensive sessions

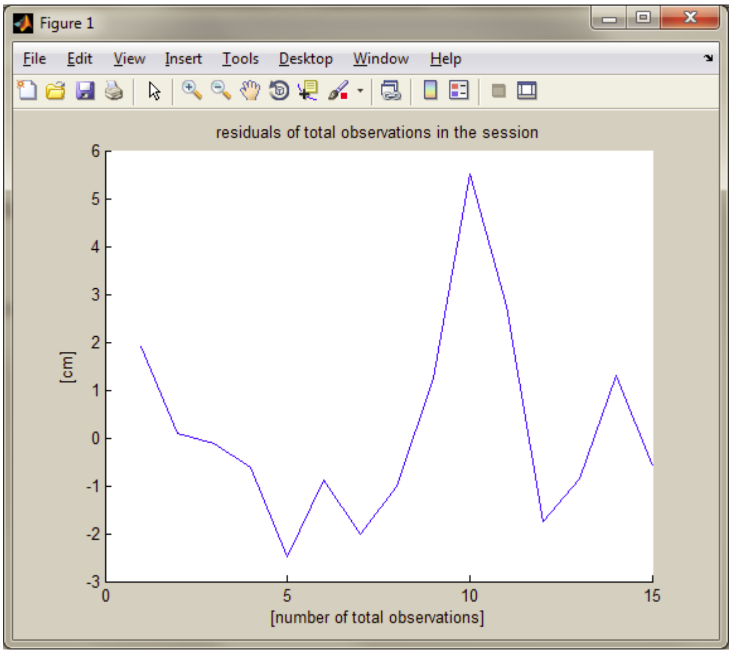

Figure 5.15: Residuals of observations for Intensive sessions

The formal error is 15.4 μs.

5.4 Get results

Estimated parameters can be visualized in *Plotting - Parameters*. The user has to select the output subfolder which is chosen by the user in *Run - Run options* next to 'one subdirectory'. If no output subfolder was given, chose '/' as subfolder. Clicking the button *Load* loads all relevant information from that subfolder to the Matlab workspace.

If more than one session is available in the output subfolder, the user can select if the parameters from only one or all sessions are to be shown. If only one session is available, there is no difference between *One session* and *All sessions*. Up to three solutions ca be visualized as shown in Figure 5.16.

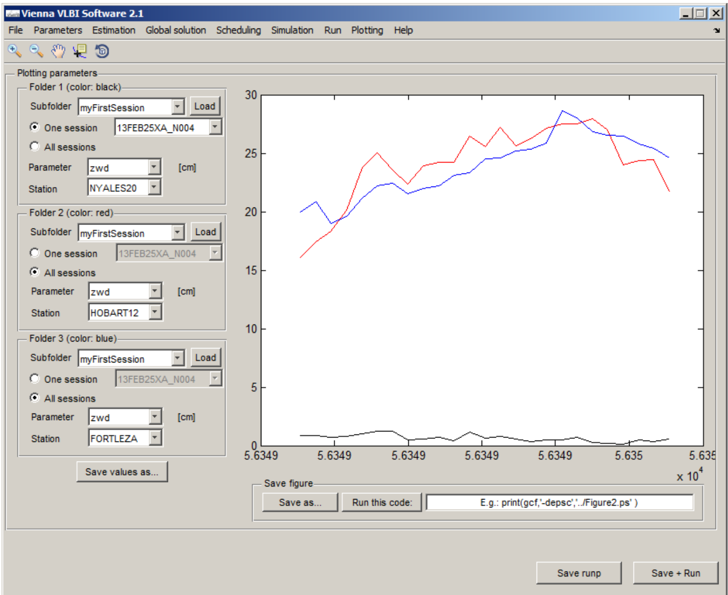

Figure 5.16: Visualized parameters: Zenith wet delays for three stations on February 25^{th} 2013

The values shown in the plot window can also be written to an ASCII file by clicking the button *Save values as...*. A screenshot of such a textfile is shown in Figure 5.17.

5.5 Scheduling, simulating and global solution

Tasks:

- Create observation schedules for given stations for two consecutive days in September 2011.
- According to these schedules simulate the time delays which would be measured in such a network and create in this way NGS files with artificial observations.
- Take these two NGS files as input for an analysis of VLBI observations with VieVS. Plot the calculated baseline length repeatabilities with the VieVS plotting tool.
- In a global solution (of both sessions) compute the station coordinates.

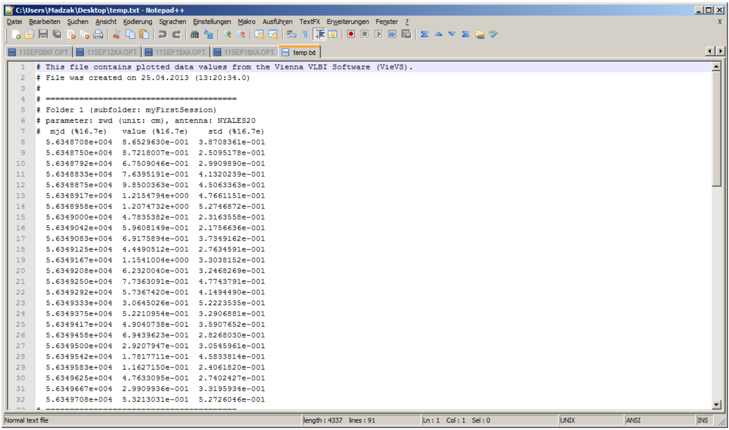

```
# This file contains plotted data values from the Vienna VLBI Software (VieVS).
# File was created on 25.04.2013 (13:20:34.0)
#
# ========================================
# Folder 1 (subfolder: myFirstSession)
# parameter: zwd (unit: cm), antenna: NYALES20
#  mjd (%16.7e)   value (%16.7e)    std (%16.7e)
  5.6348708e+004  8.6529630e-001  3.8708361e-001
  5.6348750e+004  8.7218007e-001  2.5095178e-001
  5.6348792e+004  6.7509046e-001  2.9909890e-001
  5.6348833e+004  7.6395191e-001  4.1320239e-001
  5.6348875e+004  9.8500363e-001  4.5063363e-001
  5.6348917e+004  1.2154794e+000  4.7661151e-001
  5.6348958e+004  1.2074732e+000  5.2746872e-001
  5.6349000e+004  4.7835382e-001  2.3163558e-001
  5.6349042e+004  5.9608149e-001  2.1756636e-001
  5.6349083e+004  6.9175894e-001  3.7349162e-001
  5.6349125e+004  4.4490512e-001  2.7634591e-001
  5.6349167e+004  1.1541004e+000  3.3038152e-001
  5.6349208e+004  6.2320040e-001  3.2468269e-001
  5.6349250e+004  7.7363091e-001  4.7743791e-001
  5.6349292e+004  5.7367420e-001  4.1494490e-001
  5.6349333e+004  3.0645026e-001  5.2223535e-001
  5.6349375e+004  5.2210954e-001  3.2906881e-001
  5.6349417e+004  4.9040738e-001  3.5907652e-001
  5.6349458e+004  6.9439623e-001  2.8268030e-001
  5.6349500e+004  2.9207947e-001  3.0545961e-001
  5.6349542e+004  1.7817711e-001  4.5833814e-001
  5.6349583e+004  1.1627150e-001  2.4061820e-001
  5.6349625e+004  4.7633095e-001  2.7402427e-001
  5.6349667e+004  2.9909936e-001  3.3195934e-001
  5.6349708e+004  5.3213031e-001  5.2726046e-001
```

Figure 5.17: Screenshot of ASCII output of parameter values

5.5.1 Scheduling

A Continuous VLBI Campaign CONT11 was scheduled with the NASA sked program to be observed in the second half of September 2011. The plan for the CONT11 campaign was to acquire state-of-the-art VLBI data over a time period of about two weeks to demonstrate the highest accuracy of which the current VLBI system is capable. The stations participated in the CONT11 are shown in Figure 5.18 (except of WARK12M which had to cancel participation due to technical problems).

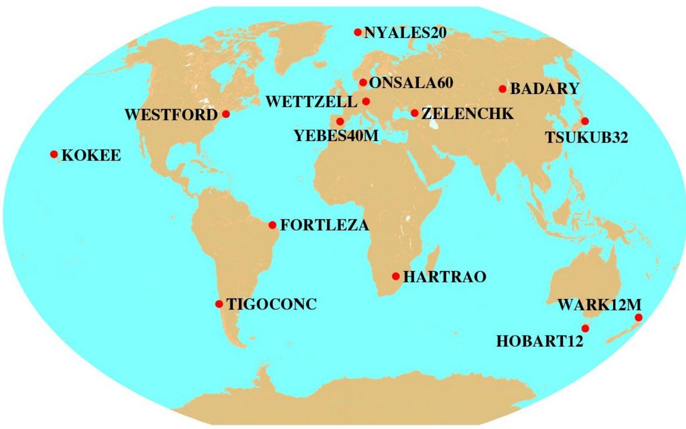

Figure 5.18: Stations of the original CONT11 campaign

Scheduling with VieVS:

In our exercise you should make 24-hour schedules for the first two days of the original CONT11 campaign, i.e. **September 15 and 16, 2011 starting at 5pm**. In the scheduled network following 10 stations should be included (we take fewer stations to speed up the processing):

BADARY, **FORTLEZA**, **HOBART12**, **HARTRAO**, **KOKEE**, **NYALES20**, **TIGOCONC**, **TSUKUB32**, **WESTFORD**, and **WETTZELL**.

Signal-to-Noise Ratio:

All baselines (except the baselines with station TIGOCONC) should have the minimum Signal-to-Noise Ratio 20 in the X-band and 15 for the S-band. For station **TIGOCONC** which is a small 6 meter transportable telescope decreases the desirable **SNR target to 15 for X-**

band and 12 for S-band. This exception for station TIGOCONC has to be set in an external file: ***snrmin.txt*** stored in ***VieVS/CATALOGS/***.

When the *snrmin.txt* is changed and stored according to our demands, the VieVS software can be started.

1. Open Matlab, change the current folder to *VieVS/WORK* and type *vievs*
2. In the GUI go to *Scheduling - Parameters*
   (a) Select the 10 stations which will participate in the session (Fig. 5.19).
   (b) Choose the start of the session (15.9.2011, 5 pm) and the duration (24 hours). (Each session has to be planned separately.) (Fig. 5.19).
   (c) Check the settings for the minimum SNR for the X-Band und S-Band (20, 15) (Fig. 5.19).
   (d) You can change the number of radio sources which will be observed simultaneously (1, 2 or 4) (Fig. 5.19).
   (e) In the GUI menu bar change to *Run* and choose the module VIE_SCHED. The scheduling software can be now started with the *Save + Run* button (Fig. 5.20).

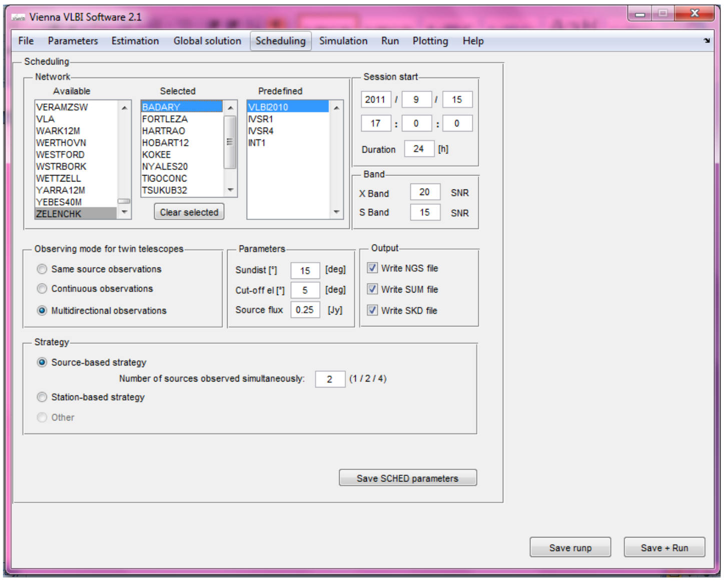

Figure 5.19: VieVS *Scheduling* GUI

Repeat the scheduling for the second session taking place on September 16, 2011. You have to change only the datum in the menu bar *Scheduling* (Fig. 5.19).

The created schedules and the scheduling protocol can be found in *VIEVS/DATA/SCHED/2011/*.

5.5.2 Simulation of the VLBI observations

You have now created two schedules - instructions for the radio telescopes which source will be observed at which time. Because there do not exist any real observations which would follow your instructions, we will simulate artificial time delays.

In VieVS the simulated VLBI observables are generated taking into account the three most important stochastic error sources in VLBI, i.e. tropospheric wet delay, station clock, and measurement error.

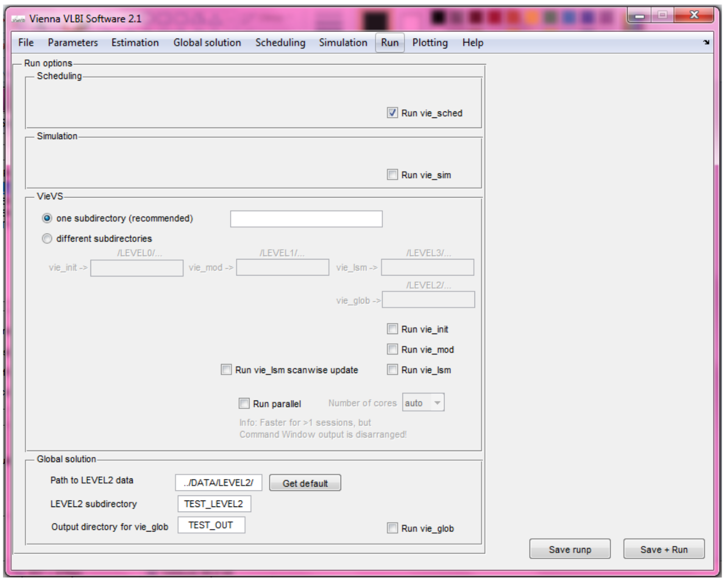

Figure 5.20: VieVS *Run* GUI scheduling options

1. With the simulation tool we want to simulate all observations which were scheduled. Therefore do not choose any directory with outliers (GUI menu bar *File*) and as the directory with specific session options choose an empty directory. If you do not have it in your computer, create an empty directory in *VIEVS/DATA/OPT/* and name it e.g. EMPTY (Fig. 5.21).

2. 2. In the menu bar *File* select sessions (i.e. the prepared schedules in NGS format) which you want to simulate. You find them in *VIEVS/DATA/SCHED/2011/* (Fig. 5.21).

3. In the menu bar *Simulation* you can choose the error sources which will be taken into account. They can be defined for all stations identically in the GUI by the click on *specify now*. You do not need to change the default values (Fig. 5.22).

4. The simulation software can be started in the menu bar *Run*. For the creation of the simulated time delays the modules VIE_INIT, VIE_MOD and VIE_SIM have to be run. You can specify a name of the subdirectory where the interim results and data will be stored in *VIEVS/DATA/LEVEL0/* and *LEVEL1* directories. For the run press the button *Save +Run* (Fig. 5.23).

The simulated NGS files will be stored in *VIEVS/DATA/SIM/2011/*.

5.5.3 Analysis of the artificial VLBI observations

The analysis of the artificial observations will be done in the same way as it would be done for the real time delays. It is only recommended not to use any outliers and option directories.

In the analysis of a 24 hour session we usually estimated: clock parameters, zenith wet delays, troposphere gradients, EOP and station coordinates. For the parameterization of these parameters use the default settings of the GUI.

1. In the menu bar *File* select the NGS files with observations which you want to analyze. The simulated files can be found in *VIEVS/DATA/SIM/2011/* (Fig. 5.24).

2. Do not select any outlier and OPT-directories (Fig. 5.24).

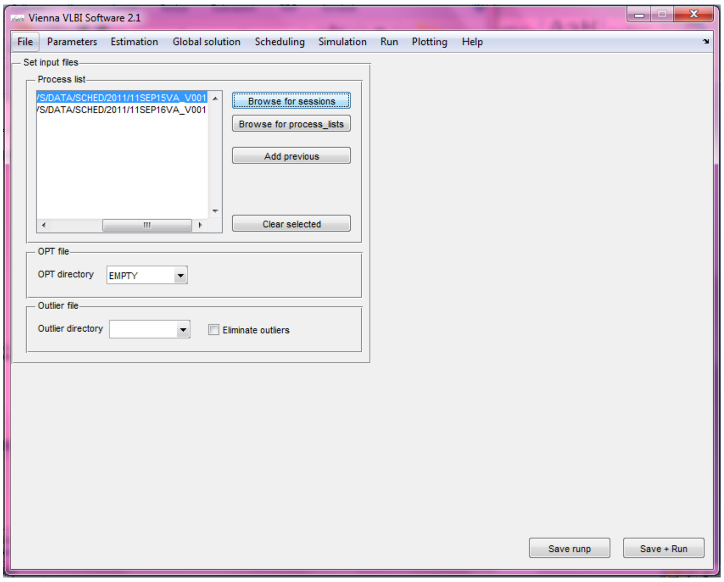

Figure 5.21: VieVS *File* GUI selection for simulation

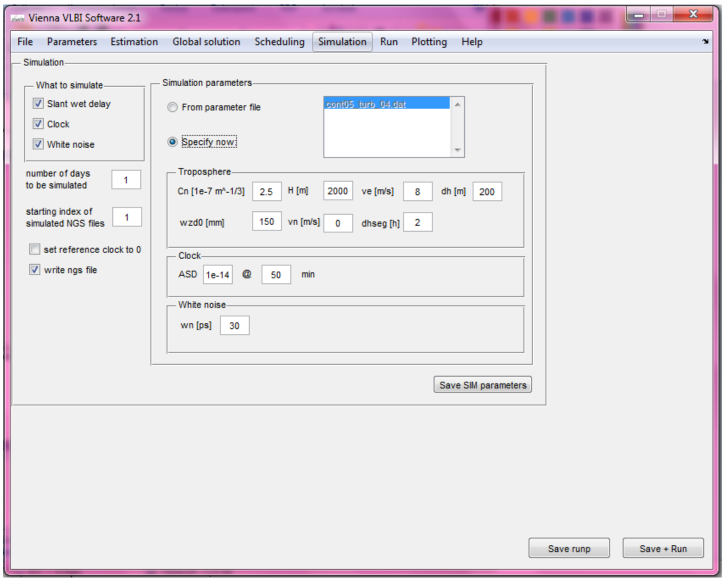

Figure 5.22: VieVS *Simulation* GUI

3. For a further processing of the data with VIE_GLOB click on the button for preparation of the normal equation matrices which will be used as input for VIE_GLOB. This has to be done in the menu bar *Estimation - Global parameters*. You can also add partial derivatives of source coordinates into the NEQ system (Fig. 5.25).

4. In the menu bar *Run* select the modules VIE_INIT, VIE_MOD and VIE_LSM. Choose a name for the subdirectory where the results will be saved (*VIEVS/DATA/LEVEL3/* subfolder). The analysis can be started with the *Save +Run* button (Fig. 5.26).

Use the GUI plotting tool and plot the baseline length repeatabilities computed from these two sessions.

In the menu bar *Plotting - Session analysis* load your subfolder with the results and click

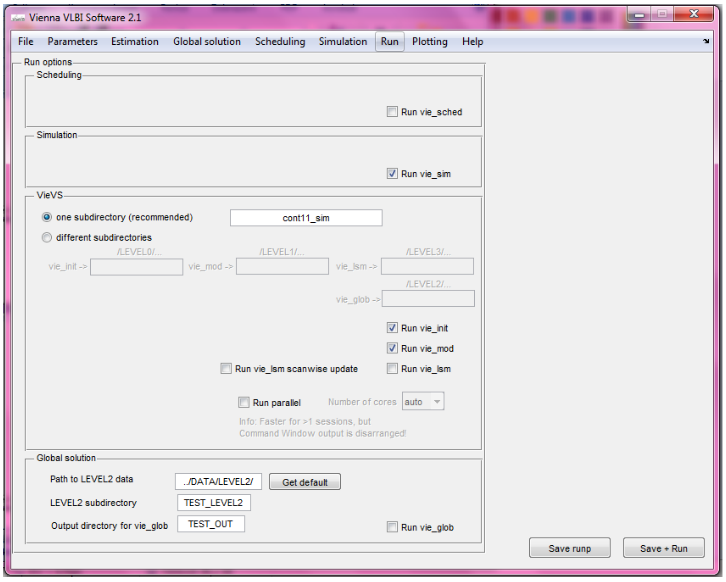

Figure 5.23: VieVS *Run* GUI simulation option

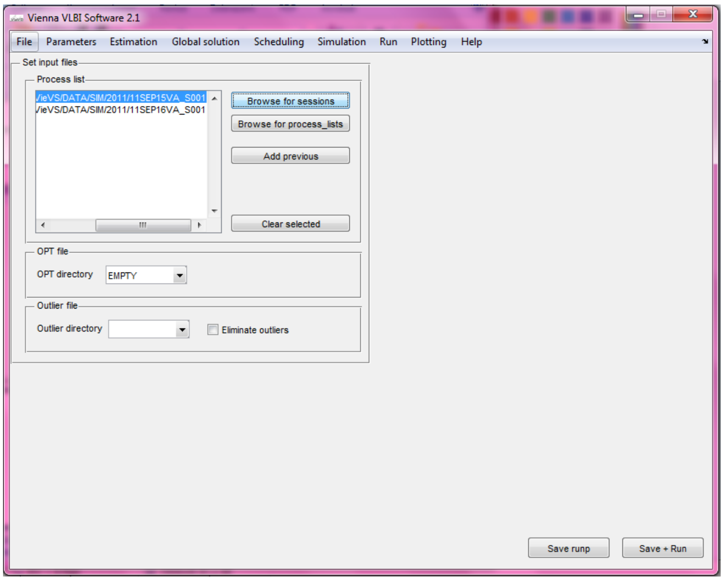

Figure 5.24: VieVS *File* GUI selection for analysis

on *basel. len. rep.* (Figure 5.27).

5.5.4 Global solution

With the module VIE_GLOB one can estimate station coordinates from both sessions in a common adjustment.

Before selecting the options in the GUI, an external .txt file with names of the stations which will be used for datum definition (NNT+NNR) has to be created. The recommended stations for datum definition are listed in Figure 5.28. Save this file in *VIEVS/DATA/GLOB/TRF/DATUM/*. (In case you want to estimate the source coordinates, another datum file for the sources has to be created.)

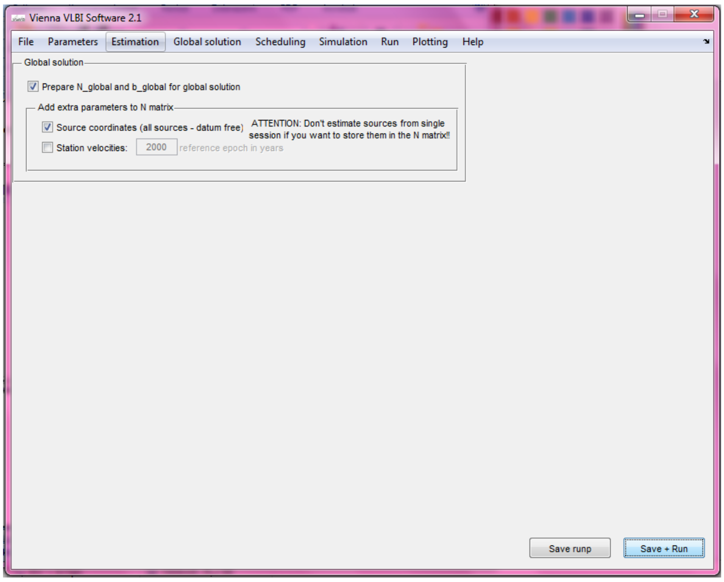

Figure 5.25: VieVS *Estimation* GUI selection for analysis

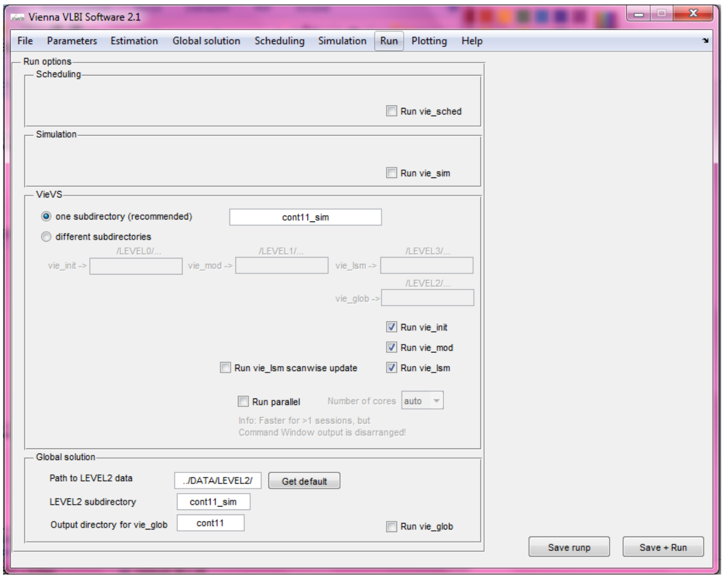

Figure 5.26: VieVS *Run* GUI analysis option

1. Parameters which will be estimated in the global solution can be selected in the menu bar *Global solution - Select parameters*. In this exercise we will estimate the station coordinates (Figure 5.29).

2. In *Global solution - TRF/CRF parameterization* select for the NNT/NNR condition the file with the names of the stations which you have already created (Figure 5.30).

3. In the menu bar *Run* select only the module VIE_GLOB. In the window *LEVEL2 subdirectory* the name of your subfolder (for the global solution) where you stored the NEQ has to be written. In the window *Output directory for vie_glob* you can write an arbitrary name of a folder, where the results from VIE_GLOB will be saved.

4. Start the global solution with the *Save + Run* button (Figure 5.31).

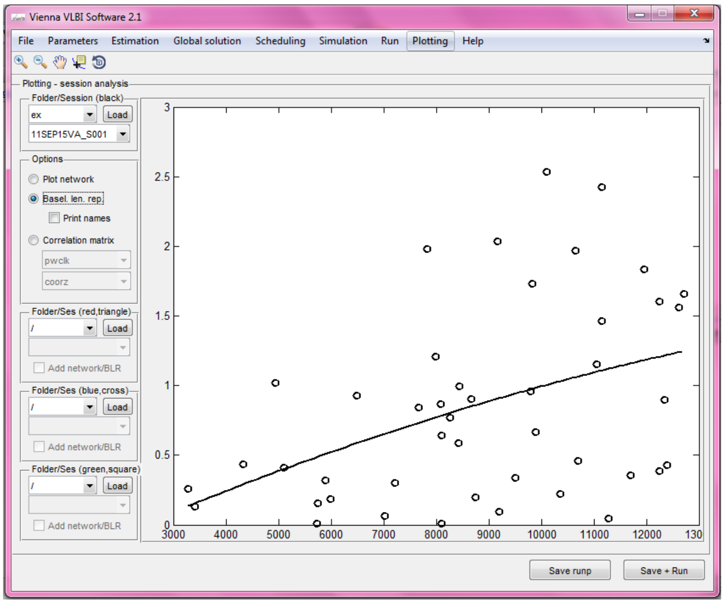

Figure 5.27: VieVS *Plotting* GUI baseline length repeatability

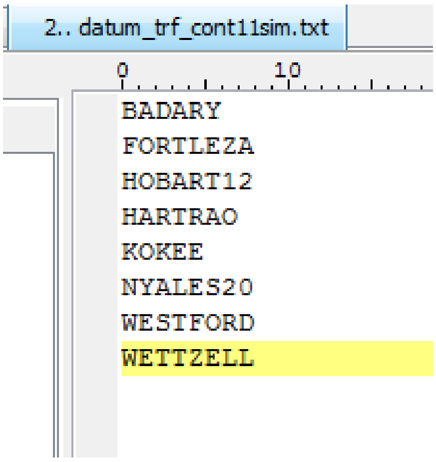

Figure 5.28: List of stations suitable for datum definition

The results are stored in a .txt file in *VIEVS/OUT/GLOB/_ESTIMATES/* subfolder and the plots in *VIEVS/OUT/GLOB/_PLOTS/subfolder*.

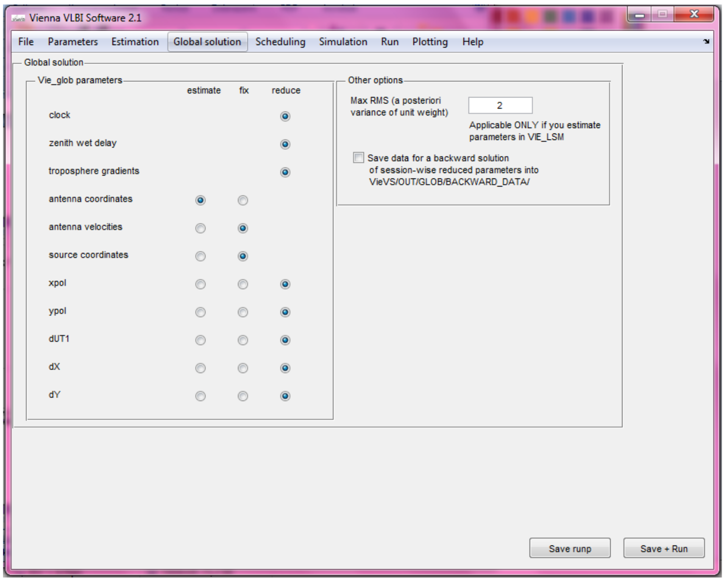

Figure 5.29: VieVS *Global solution* - *Select parameters* GUI

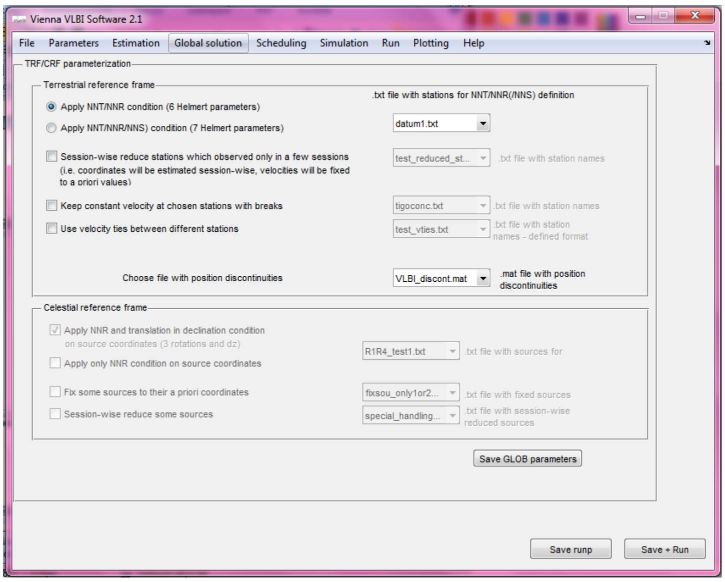

Figure 5.30: VieVS *Global solution* - *TRF/CRF parameterization* GUI

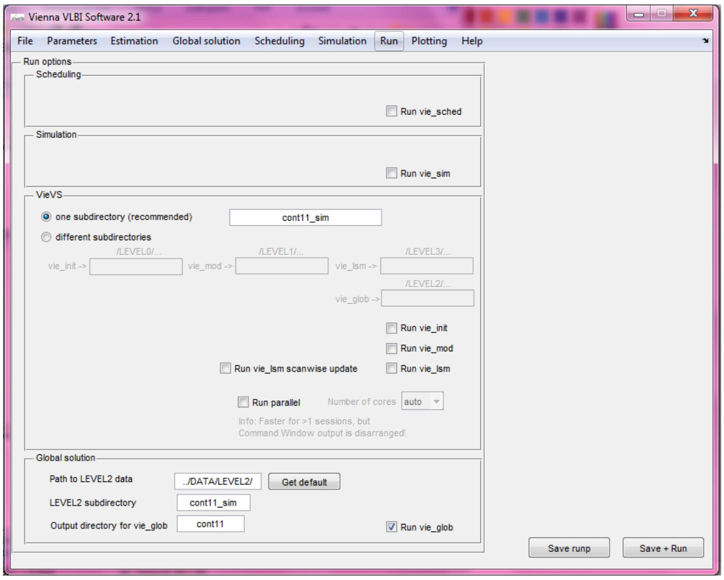

Figure 5.31: VieVS *Run* GUI global solution option

Chapter 6

Matlab crash course

The matlab window is shown in Figure 6.1. The different windows can be moved and resized as desired - they can even be separate windows. There is the window *Current Folder* where the content of the current directory (selectable in the dropdown menu above) is shown, similar to the Microsoft Explorer. In the *Workspace* there are all variables available right now. So when you assign the value 5 to a, it appears in that window. All those commands are written in the *Command window*. The *Editor* is used for all kinds of programming. The code in there can be run by pressing *F5* or clicking on the *Save and run (F5)* button.

Some important example commands are shown in Table 6.1.

6.1 Interface (GUIDE)

The Matlab GUIDE is a drag-and-drop program for creating graphical user interfaces. It can be opened by typing `guide` in the command window and hit Return; a screenshot of an empty GUI is shown in Figure 6.2.

This interface consists of all arranged objects (buttons, textboxes, popupmenues, sliders, checkboxes, ...) saved in a .fig files (e.g. myProgram.fig) and a corresponding .m files (same filename, e.g. myProgram.m) containing all callback functions.

Each object (e.g. button) has an unique identifiable name (Tag) which can be seen in the Property Inspector (double click on the object) under 'Tag'. If a button is called 'button1', there exists (automatically created) a function in *myProgram.m* called *button1_Callback*. This function is called when the button is clicked.

There exist also other functions than callback functions, depending on what has been done in the interface (e.g. button release, delete, resize function, selection change in a button group, ...).

The state of the interface is stored in one matlab structure, called *handles*. The fields of this structure are object handles, one for each object (e.g. handles.button1). This field contains all properties (e.g. size, values, functions) which can be changed or retrieved by *set* and *get*.

In this structure also user data can be stored since this variable is available in all functions (*handles* is an input argument to all callback functions). Example: User wants to load a number from a textfile. This number can be saved in *handles.userNumber*. The handles structure has to be updated at the end of each function when content of it has been changed: `guidata(hObject, handles);`.

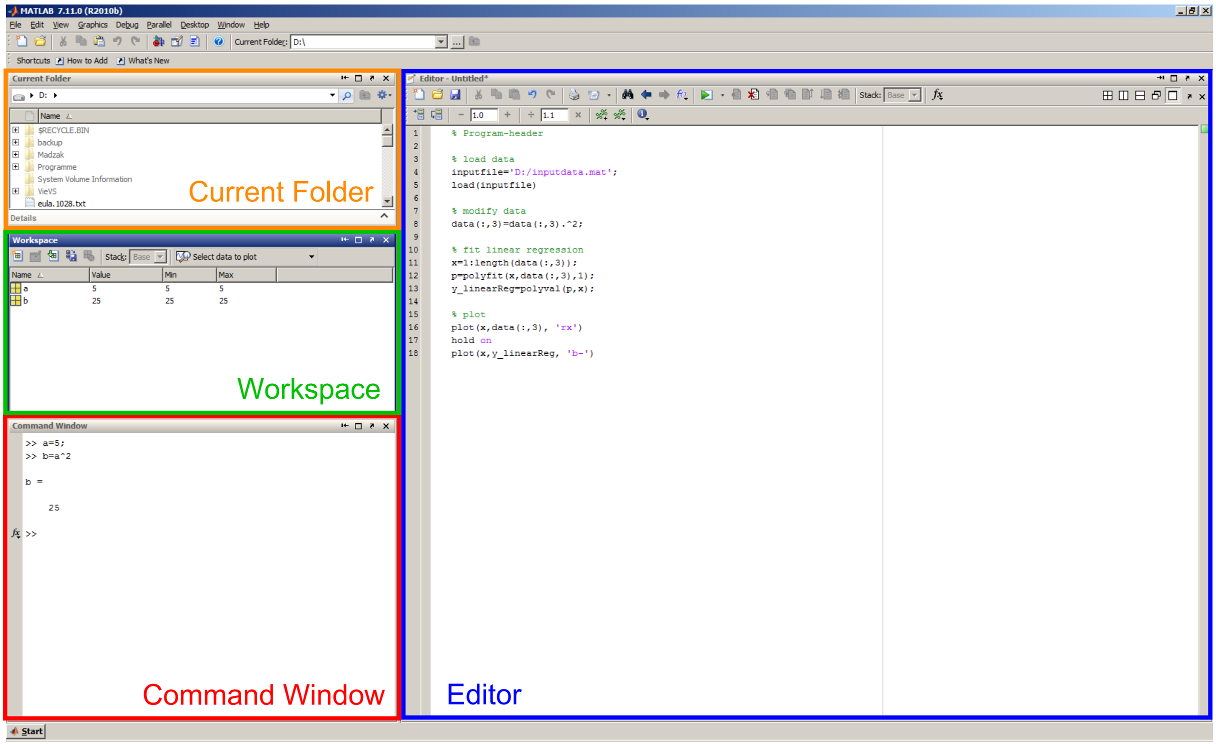

Figure 6.1: Matlab window overview

Command	Explanation
`a=5;`	Assign 5 to the variable a (semicolon supresses command window output)
`a=[1,2,3,4,5];`	Define a row vector (equal: `a=1:5;`)
`a=[1,2,3,4,5]';`	Define a column vector (' transposes a matrix)
`b=rand(20,30);`	Define 20x30 matrix with random numbers between 0 and 1
`a=b(3:5,4:10);`	Take row 3,4,5 and columns 4 to 10 from matrix b and assign it to a (a will be a 3x7 matrix)

`for k=1:size(a,2)`
`   c(k)=a(1,k)*4;`
`end`
	For-loop from 1 to 7 where values of a (row 1) are multiplied by 4 and assigned to c

`c=a(1,:)*4;`	The same operation as above but more efficient
`x=0:0.01:4*pi; y=sin(x);`	Create vector x from 0 to 4π with increment 0.01 and a vector y containing the corresponding sine values
`plot(x,y,'-.bx');`	Plots x versus y with a blue (b), dash-dot (-.) line and crosses (x) as markers
`save('../vars/myVars.mat', 'a', 'b', 'c')`	Saves the variables a, b and c to a .mat file in ../vars/
`load('../vars/myVars.mat')`	Restores variables a, b and c to Workspace

Table 6.1: Some important matlab commands

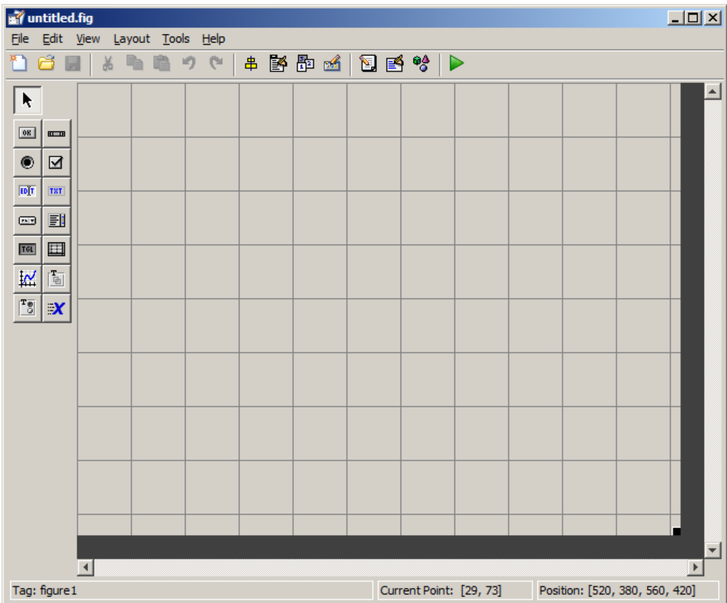

Figure 6.2: Empty graphical user intarface using Matlab GUIDE

Appendix A

Problems

In this appendix some errors are described which might occur when using VieVS. If those do not help or if you find any other bugs or have comments, do not hesitate to contact us on `http://vievs.geo.tuwien.ac.at/` or any of the developers per e-mail.

A.1 GUI cannot close

This problem usually occurs when the user changes the matlab work directory while the VieVS interface is still open. *Solution:* Change matlab work directory to */VieVS/WORK/* and close the GUI. If this still does not close the GUI in windows, go to Task manager and kill the matlab task.

A.2 GUI buttons remain unselectable

This problem can occur when the code does not successfully run until the enabling of the button is reached. In this case there might be a bug in the code (please, report it to the developers in Vienna), the matlab path has been changed (should always be */VieVS/WORK/*), or the software was used a way it should not be. In the latter case, simply restart VieVS.

A.3 EOP limit

If you process a session and get an EOP limit information on the command window, there are probably no a priori EOP values of the chosen EOP series available (default EOP time series is C04 08). A solution might be either downloading the newest file from the vievs server (if your file is not up-to-date, or (usually when a very recent session is to be analysed) you might chose a different a priori model (e.g. 'finals' in *Parameters - EOP*).

A.4 Check for new leap second

```
+++ please check for new leap second TAI-UTC tai_utc.m +++
```

The treatment of leap second is controlled in the subroutine /VIEVS/VIE_MOD/tai_utc.m. Following the latest Bulletin C from the IERS, where the announce for a leap second is published, the *mjdmax* set with the announced date. If a session after *mjdmax* is processed, the warning above appears. If you are sure that there was no new leap second since then, this warning can be ignored.

To solve the warning, check for an update of this routine on the VieVS server or update yourself. Therefore, check the latest Bulletin C from the IERS website. If there is no leap second announced, modify *mjdmax* to the given date of the announcement. In the case of a leap second, add the corresponding date in mjd and the new value for the difference between TAI and UTC.

A.5 Station not in superstation file

If there is a station not in the superstation file but taking part in a session, the program will crash with this information in the command window. One solution is to add the station to the superstation file (see section 4.6). The other solution is to use your own ASCII catalog containing the station coordinates of all stations of the session.

A.6 Source not in supersource file

If a source is not found in supersource file, it should be added there (see section 4.7 for details). Or the user may provide an ASCII file containing all source coordinates and select this one in *Parameters - Reference frames*.

Bibliography

Abbondanza, C. and Sarti, P. (2010). Effects of illumination functions on the computation of gravity-dependent signal path variation models in primary focus and Cassegrainian VLBI telescopes. *J. Geod.*, 84, 515–525.

Altamimi, Z., Collilieux, X. and Métivier, L. (2011). ITRF2008: an improved solution of the international terrestrial reference frame. *J. Geod.*, 85, 457–473.

Andersen, O.B. (2006). www.spacecenter.dk/data/global-ocean-tide-model-1/.

Bare, C.C., Clark, B.G., Kellerman, K.I., Cohen, M.H. and Jauncey, D.L. (1967). Interferometry experiment with independent local oscillators. *Science*, 157.

Bierman, G. (1977). *Factorization Methods for Discrete Sequential Estimation*. Academic, New York.

Bizouard, C. and Gambis, D. (2009). The combined solution C04 for Earth orientation parameters consistent with International Terrestrial Reference Frame. In H. Drewes, ed., *Geodetic Reference Frames*, Vol. 134, 265–270, IAG Symposium, Munich, Germany, 9-14 October 2006.

Böckmann, S., Artz, T. and Nothnagel, A. (2010). VLBI terrestrial reference frame contributions to ITRF2008. *J. Geod.*, 84, 201–219.

Böhm, J. (2004). Troposphärische Laufzeitverzögerungen in der VLBI. *Geowissenschaftliche Mitteilungen*, 68, Schriftenreihe der Studienrichtung Vermessung und Geoinformation, Technische Universität Wien, ISSN 1811-8380 (in German).

Böhm, J. and Schuh, H. (2007). Troposphere gradients from the ECMWF in VLBI analysis. *J. Geod.*, 81, 403–408.

Böhm, J., Werl, B. and Schuh, H. (2006). Troposphere mapping functions for GPS and very long baseline interferometry from European Centre for Medium-Range Weather Forecasts operational analysis data. *J. Geophys. Res.*, 111, doi:10.1029/2005JB003629.

Böhm, J., Heinkelmann, R. and Schuh, H. (2007). Short note: A global model of pressure and temperature for geodetic applications. *J. Geod.*, 81, 679–683.

Böhm, J., Heinkelmann, R., Mendes Cerveira, P.J., Pany, A. and Schuh, H. (2009a). Atmospheric loading corrections at the observation level in VLBI analysis. *J. Geod.*, 83, 1107–1113.

Böhm, J., Kouba, J. and Schuh, H. (2009b). Forecast vienna mapping functions 1 for real-time analysis of space geodetic observations. *J. Geod.*, 86, 397–401.

Böhm, J., Hobiger, T., Ichikawa, R., Kondo, T., Koyama, Y., Pany, A., Schuh, H. and Teke, K. (2010). Asymmetric tropospheric delays from numerical weather models for UT1 determination from VLBI Intensive sessions on the baseline Wettzell-Tsukuba. *J. Geod.*, 84, 319–325.

Böhm, J., Böhm, S., Nilsson, T., Pany, A., Plank, L., Spicakova, H., Teke, K. and Schuh, H. (2011). The new Vienna VLBI Software VieVS. In *Proceedings of the 2009 IAG Symposium, Buenos Aires, Argentina*, Vol. 136, International Association of Geodesy Symposia, 31 August - 4 September 2009.

Broten, N.W., Legg, T.H., Locke, J.L., McLeish, C.W., Richards, R.S., Chisholm, R.M., Gush, R.M., Yen, J.L. and Galt, J. (1967). Long baseline interferometry: A new technique. *Science*, 156.

Brown, G.W., Carr, T.D. and Block, W.F. (1968). Long Baseline Interferometry of S-Bursts from Jupiter. *Astrophys. Lett.*, 1, 89–94.

Campbell, J. (2000). From Quasars to Benchmarks: VLBI Links Heaven and Earth. In *IVS 2000 General Meeting Proceedings*, 19–34, NASA/CP-2000-209893.

Capitaine, N. (2000). Definition of the celestial ephemeris pole and the celestial ephemeris origin. In *Towards Models and Constants for Sub-Microarcsecond Astrometry*, 153–163, U.S. Naval Observatory.

Chen, G. and Herring, T.A. (1997). Effects of atmospheric azimuthal asymmetry on the analysis of space geodetic data. *J. Geophys. Res.*, 102, 20489–20502.

Cohen, M.H., .L., J.D., Kellerman, K.I. and Clark, B.G. (1968). Radio interferometry at one-thousandth second of arc. *Science*, 162, 88–94.

Collioud, A. and Charlot, P. (2009). The Bordeaux VLBI Image database. In *Proceedings of the 19th European VLBI for Geodesy and Astrometry Working Meeting, 24-25 March 2009, Bordeaux*, 19–22.

Davis, J.L., Herring, T.A., Shapiro, I.I., Rogers, A.E.E. and Elgered, G. (1985). Geodesy by radio interferometry: Effects of atmospheric modeling errors on estimates of baseline length. *Radio Science*, 20, 1593–1607.

Davis, J.L., Elgered, G., Niell, A.E. and Kuehn, C.E. (1993). Ground-based measurement of gradients in the "wet" radio refractivity of air. *Radio Science*, 28, 1003–1018.

Dehant, V. and Mathews, P.M. (2009). Earth rotation variations. In T.A. Herring, ed., *Treatise on Geophysics, Volume 3 Geodesy*, Elsevier.

Desai, S.D. (2002). Observing the pole tide with satellite altimetry. *J. Geophys. Res.*, 107.

Egbert, G.D. and Erofeeva, S.Y. (2002). Efficient inverse modeling of barotropic ocean tides. *J. Atmos. Oceanic Technol.*, 19, 183–204.

Englich, S., Heinkelmann, R. and Schuh, H. (2008). Re-assessment of ocean tidal terms in high-frequency Earth rotation variations observed by VLBI. In A. Finkelstein and D. Behrend, eds., *Measuring the future. Proceedings of the 5th IVS general meeting*, 314–318, ISBN 978-5-02-025332-2.

Eriksson, D. and MacMillan, D. (2012). Continental Hydrology Loading Observed by VLBI Measurements. In D. Behrend and K.D. Baver, eds., *IVS 2012 General Meeting Proceedings*, 415–419.

Eubanks, T.M., ed. (1991). Proceedings of the U.S. Naval Observatory Workshop on Relativistic Models for Use in Space Geodesy. U.S. Naval Observatory Washington D.C. 20392-5100, U.S.A.

Fey, A., Gordon, D. and Jacobs, C.S., eds. (2009). The second realization of the international celestial reference frame by very long baseline interferometry. Frankfurt am Main: Verlag des Bundesamts für Kartographie und Geodäsie, Presented on behalf of the IERS / IVS Working Group.

Folkner, W.M., Williams, J.G. and Boggs, D.H. (2008). The Planetary and Lunar Ephemeris DE 421. *IPN Progress Report 42-178 August 15, 2009*, 31, `http://ipnpr.jpl.nasa.gov/progress_report/42-178/178C.pdf`.

Gipson, J. and MacMillan, D.S. (2009). Recent modeling improvements in solve analysis. In G. Bourda, P. Charlot and A. Collioud, eds., *Proceedings of the 19th European VLBI for Geodesy and Astrometry Working Meeting, 24-25 March 2009, Bordeaux*, 54–57.

Gold, T. (1967). Radio method for the precise measurement of the rotation period of the earth. *Science*, 157, 302–304.

Haas, R. (1999). Explanatory Supplement to the Section "Antenna Deformation" of the IERS Conventions (1996). In H. Schuh, ed., *DGFI Report No. 71*, 26–29.

Hawarey, M., Hobiger., T. and Schuh, H. (2005). Effects on the 2nd order ionospheric terms on VLBI measurements. *Geoph. Res. Lett.*, 32, doi:10.1029/2005GL022729.

Heinkelmann, R. (2008). Bestimmung des atmosphärischen Wasserdampfes mittels VLBI als Beitrag zur Klimaforschung. *Geowissenschaftliche Mitteilungen*, 82, Schriftenreihe der Studienrichtung Vermessung und Geoinformation, Technische Universität Wien, ISSN 1811-8380 (in German).

Heinkelmann, R. and Schuh, H. (2010). Very long baseline interferometry: accuracy limits and relativistic tests. In *Relativity in Fundamental Astronomy. Proceedings IAU Symposium*, Vol. 261, 286–290.

Hellings, R.W. (1986). Relativistic effects in astronomical timing measurements. *Astron. J.*, 91, 650–659, erratum, ibid. p. 1446.

Herring, T.A. (1992). Modeling atmospheric delays in the analysis of space geodetic data. In D.. Spoelstra, ed., *Refraction of Transatmospheric Signals in Geodesy*, 157–164, Netherlands Geodetic Commission, publications on Geodesy No. 36.

Herring, T.A., Shapiro, I.I., Clark, T.A., Ma, C., Ryan, J.W., Schupler, B.R., Knight, C.A., Lundquist, G., Shaffer, D.B., Vandenberg, N.R., Corey, B.E., Hinteregger, H.F., Rogers, A.E.E., Webber, J.C., Whitney, A.R., Elgered, G., Rönnäng, B.O. and Davis, J.L. (1986). Geodesy by radio interferometry: evidence for contemporary plate motion. *J. Geophys. Res.*, 91, 8341–8347.

Herring, T.A., Davis, J.L. and Shapiro, I.I. (1990). Geodesy by radio interferometry: The application of kalman filtering to the analysis of very long baseline interferometry data. *J. Geophys. Res.*, 95, 12561–12581.

Herring, T.A., Mathews, P.M. and Buffett, B.A. (2002). Modeling of nutation-precession: Very long baseline interferometry results. *J. Geoph. Res.*, 107, 2069.

Hinteregger, H.F., Shapiro, I.I., Robertson, D.S., Knight, C.A., Ergas, R.A., Whitney, A.R., Rogers, A.E.E., Moran, J.M., Clark, T.A. and Burke, B.F. (1972). Precision geodesy via radio interferometry. *Science*, 178, 396–398.

Hobiger, T. (2006). VLBI as a tool to probe the ionosphere. *Geowissenschaftliche Mitteilungen*, 75, Schriftenreihe der Studienrichtung Vermessung und Geoinformation, Technische Universität Wien, ISSN 1811-8380.

Hobiger, T., Ichikawa, R., Koyama, Y. and Kondo, T. (2008). Fast and accurate ray-tracing algorithms for real-time space geodetic applications using numerical weather models. *J. Geoph. Res.*, 113, doi:10.1029/2008JD010503.

Kellermann, K.I. and Moran, J.M. (2001). The development of high-resolution imaging in radio astronomy. *Annual Review of Astronomy and Astrophysics*, 39, 457–509.

Klioner, S.A. (1991). General relativistic model of VLBI observables. In W.E. Carter, ed., *Proc. AGU Chapman Conf. on Geodetic VLBI: Monitoring Global Change*, 188–202, American Geophysical Union, Washington D.C, NOAA Technical Report NOS 137 NGS 49.

Kondo, T., Kimura, M., Koyama, Y. and Osaki, H. (2004). Current Status of Software Correlators Developed at Kashima Space Research Center. In N.R. Vandenberg and K.D. Baver, eds., *International VLBI Service for Geodesy and Astrometry 2004 General Meeting Proceedings*, 186–190, NASA/CP-2004-212255.

Lambert, S.B. and Le Poncin-Lafitte, C. (2009). Determining the relativistic parameter γ using very long baseline interferometry. *Astron. Astrophys.*, 499, 031–335.

Lambert, S.B. and Le Poncin-Lafitte, C. (2011). Improved determination of γ by VLBI (Research Note). *Astron. Astrophys.*, 529, doi: 10.1051/0004–6361/201016370.

Letellier, T. (2004). *Etude des ondes de marée sur les plateaux continentaux*. Université de Toulouse III.

Ma, C., Arias, E.F., Eubanks, T.M., Fey, A.L., Gontier, A.M., Jacobs, C.S., Sovers, O.J., Archinal, B.A. and Charlot, P. (1998). The international celestial reference frame as realized by very long baseline interferometry. *The Astronomical Journal*, 116, 516–546.

MacMillan, D.S. (1995). Atmospheric gradients from very long baseline interferometry observations. *Geoph. Res. Letters*, 22, 1041–1044.

MacMillan, D.S. and Ma, C. (1994). Evaluation of very long baseline interferometry atmospheric modeling improvements. *J. Geophys. Res.*, 99, 637–651.

Mathews, P.M., Dehant, V. and Gipson, J.M. (1997). Tidal station displacement. *J. Geophys. Res.*, 102, 20469–20477.

Moran, J.M., Crowther, P.P., Burke, B.F., Barrett, A.H., Rogers, A.E.E., Ball, J.A., Carter, J.C. and Bare, C.C. (1967). Spectral line interferometry with independent time standards at stations separated by 845 kilometers. *Science*, 157, 676–677.

Niell, A.E., Whitney, A., Petrachenko, B., Schlüter, Vandenberg, N., Hase, H., Koyama, Y., Ma, C., Schuh, H. and Tuccari, G. (2006). VLBI2010: Current and Future Requirements for Geodetic VLBI Systems. *IVS Memorandum 2006-008v01*, ftp://ivscc.gsfc.nasa.gov/pub/memos/ivs–2006–008v01.pdf.

Nothnagel, A. (2009). Conventions on thermal expansion modelling of radio telescopes for geodetic and astrometric VLBI. *J. Geod.*, 83, 787–792.

Nothnagel, A., Vennebusch, M. and Campbell, J. (2002). On Correlations Between Parameters in Geodetic VLBI Data Analysis. In N.R. Vandenberg and K.D. Baver, eds., *IVS 2002 General Meeting Proceedings*, 260–264.

Pany, A., Böhm, J., MacMillan, D.S., Schuh, H., Nilsson, T. and Wresnik, J. (2010). Monte Carlo simulations of the impact of troposphere, clock and measurement errors on the repeatability of VLBI positions. *J. Geod.*, 85, 39–50.

Petit, G. (2000). Importance of a common framework for the realization of space-time reference systems. In *Proc. IAG Symposium IGGOS*, 3–7, Springer-Verlag.

Petit, G. and Luzum, B., eds. (2010). IERS Conventions 2010. Frankfurt am Main: Verlag des Bundesamts für Kartographie und Geodäsie, IERS Technical Note No. 36.

Petrachenko, B.a. (2009). Progress Report of the IVS VLBI2010 Committee: Desing Aspects of the VLBI2010 System. Tech. rep., NASA/TM-2009-214180, ftp://ivscc.gsfc.nasa.gov/pub/misc/V2C/TM-2009-214180.pdf.

Petrov, L. (1999). Steps towards phase delay VLBI. In W. Schlüter and H. Hase, eds., *Proceedings of the 13th Working Meeting on European VLBI for Geodesy and Astrometry*, 144–151, Viechtach/Wettzell Feb. 12-13, 1999.

Petrov, L. and Boy, J.P. (2004). Study of the atmospheric pressure loading signal in very long baseline interferometry observations. *J. Geophys. Res.*, 109.

Petrov, L., Gordon, D., Gipson, J., MacMillan, D., Ma, C., Fomalont, E., Walker, R.C. and Carabajal, C. (2009). Precise geodesy with the Very Long Baseline Array. *J. Geod.*, 83, 859–876.

Plag, H.P. and Pearlman, M., eds. (2009). Global geodetic observing system: Meeting the requirements of a global society on a changing planet in 2020. Springer-Verlag Berlin Heidelberg.

Rabbel, W. and Schuh, H. (1986). The Influence of Atmospheric Loading on VLBI-Experiments. *J. Geoph.*, 59, 164–170.

Ray, R.D. (1999). A global ocean tide model From TOPEX/Poseidon altimetry: GOT99.2. *NASA Technical Memorandum TM-209478*, 58.

Richter, G.W. and Matzner, R.A. (1983). Second-order contributions to relativistic time delay in the parameterized post-newtonian formalism. *Phys. Rev. D*, 28, 3007–3012.

Rius, A., Rodriguez, J. and Campbell, J. (1987). Geodetic VLBI with Large Antennas. In J. Campbell and H. Schuh, eds., *Mitt. Geod. Inst. Univ. Bonn, No. 72*, 59–67.

Robertson, D.S., Carter, W.E. and Dillinger, W.H. (1991). New measurement of solar gravitational deflection of radio signals using VLBI. *Nature*, 349, 768–770.

Rogers, A.E.E. (1970). Very long baseline interferometry with large effective bandwidth for phase delay measurements. *Radio Science*, 5, 1239–1247.

Rogers, A.E.E. (1975). A receiver phase and group delay calibrator for use in very long baseline interferometry. *Haystack Observatory Technical Note*, Haystack Observatory, Westford, MA.

Saastamoinen, J. (1972). Atmospheric correction for the troposphere and stratosphere in radio ranging of satellites. In *The use of artificial satellites for geodesy, Geophys. Monogr. Ser. 15*, 274–251, Amer. Geophys. Union.

Sarti, P., Abbondanza, C., Petrov, L. and Negusini, M. (2011). Height bias and scale effect induced by antenna gravitational deformations in geodetic VLBI data analysis. *J. Geod.*, 85, 1–8.

Savcenko, R. and Bosch, W. (2008). Eot08a - empirical ocean tide model from multi-mission satellite altimetry. Deutsches Geodätisches Forschungsinstitut (DGFI), München, report No. 81.

Scherneck, H.G. (1991). A parameterized solid earth tide model and ocean tide loading effects for global geodetic baseline measurements. *Geophys. J. Int.*, 106, 677–694.

Schlüter, W. and Behrend, D. (2007). The International VLBI Service for Geodesy and Astrometry (IVS): current capabilities and future prospects. *J. Geod.*, 81, 379–387, doi: 10.1007/s00190–006–0131–z.

Schuh, H. (1987). Die Radiointerferometrie auf langen Basen zur Bestimmung von Punktverschiebungen und Erdrotationsparametern. *DGK Reihe C, Dissertationen*, Heft Nr. 328.

Schuh, H. (2000). Geodetic Analysis Overview. In *IVS 2000 General Meeting Proceedings*, 219–229, NASA/CP-2000-209893.

Sekido, M., Takiguchi, H., Koyama, Y., Kondo, T., Haas, R., Wagner, J., Ritakari, J., Kurihara, S. and Kokado, K. (2008). Ultra-rapid UT1 measurement by e-VLBI. *Earth Planets Space*, 60, 865–870.

Shapiro, I.I. and Knight, C.A. (1970). Geophysical applications of long baseline radio interferometry. In L. Mansinha, D. Smylie and A. Beck, eds., *Earthquake Displacement Fields and the Rotation of the Earth*, 285–301, Reidel, Dordrecht.

Sillard, P. and Boucher, C. (2001). A review of algebraic constraints in terrestrial reference frame definition. *J. Geod.*, 75, 63–73.

Skurikhina, E. (2001). On Computation of Antenna Thermal Deformation in VLBI Data Processing. In D. Behrend and A. Rius, eds., *15th Workshop Meeting on European VLBI for Geodesy and Astrometry*, 124.

Snajdrova, K., Böhm, J., Willis, P., Haas, R. and Schuh, H. (2005). Multi-technique comparison of tropospheric zenith delays derived during the CONT02 campaign. *J. Geod.*, 79, 613–623.

Sovers, O.J., Fanselow, J.L. and Jacobs, C.S. (1998). Astrometry and geodesy with radio interferometry: experiments, models, results. *Reviews of Modern Physics*, 70, 1393–1454.

Spicakova, H., Böhm, J., Böhm, S., Nilsson, T., Pany, A., Plank, L., Teke, K. and Schuh, H. (2010). Estimation of geodetic and geodynamical parameters with VieVS. In D. Behrend and K. Baver, eds., *IVS 2010 General Meeting Proceedings*, 202–206, NASA/TP-2010-215864.

Steigenberger, P., Böhm, J. and Tesmer, V. (2009). Comparison of GMF/GPT with VMF1/ECMWF and Implications for Atmospheric Loading. *J. Geod.*, 83, 943–951.

Takahashi, F., Kondo, T., Takahashi, Y. and Koyama, Y. (2000). *Wave Summit Course: Very Long Baseline Interferometer*. IOS Press, ISBN 1-58603-076-0.

Teke, K. (2011). *Subdaily parameter estimation in VLBI data anlysis*. Geowissenschaftliche Mitteilungen, Heft 87, Geowissenschaftliche Mitteilungen Heft 87, Wien.

Teke, K., Heinkelmann, R., Böhm, J. and Schuh, H. (2008). VLBI Baseline Length Repeatability Tests of IVS-R1 and -R4 Session Types. In A. Finkelstein and D. Behrend, eds., *'Measuring the Future', Proceedings of the 5th IVS General Meeting*, 173–177, ISBN 978-5-02-025332-2.

Teke, K., Böhm, J., Nilsson, T., Schuh, H., Steigenberger, P., Dach, R., Heinkelmann, R., Willis, P., Haas, R., García-Espada, S., Hobiger, T., Ichikawa, R. and Shimizu, S. (2011). Multi-technique comparison of troposphere zenith delays and gradients during CONT08. *J. Geod.*, 85, 395–413.

Thompson, A.R., Moran, J.M. and Swenson, G.W.J. (1986). *Interferometry and Synthesis in Radio Astronomy.*. Wiley, New York.

Tingay, S., Alef, W., Graham, D. and Deller, A.T. (2009). Geodetic VLBI correlation in software. *J. Geod.*, 83, 1061–1069.

Titov, O. (2010). VLBI2020 from Reality to Vision. In D. Behrend and K.D. Baver, eds., *IVS 2010 General Meeting Proceedings*, 60–64, NASA/CP-2010-215864.

Titov, O. and Schuh, H. (2000). Short Periods in Earth Rotation seen in VLBI Data analysed by least-squares collocation technique. In B. Kolaczek, H. Schuh and D. Gambis, eds., *IERS Technical Note 28*, 11–14, Paris Observatory.

van Dam, T. (2010). Ncep derived 6-hourly, global surface displacements at 2.5 x 2.5 degree spacing. *Data set at http://geophy.uni.lu/ncep-loading.html*.

vanDam, T.M. and Herring, T.A. (1994). Detection of atmospheric pressure loading using very long baseline interferometry measurements. *J. Geophys. Res.*, 99, 4505–4517.

Vandenberg, N.R. (1999). Interactive/Automatic Scheduling Program. Program Reference Manual, NASA Goddard Space Flight Center / NVI Inc.

Whitney, A.R., Rogers, A.E.E., Hinteregger, H.F., Knight, C.A., Lippincott, S., Levine, J.I., Clark, T.A., Shapiro, I.I. and Robertson, D.S. (1976). A very-long-baseline interferometer system for geodetic applications. *Radio Science*, 11, 421–432.

Wresnik, J., Haas, R., Böhm, J. and Schuh, H. (2007). Modeling thermal deformation of VLBI antennas with a new temperature model. *J. Geod.*, 81, 423–431.